CHARACTERIZATION AND APPLICATION OF ANALYSIS METHODS FOR ECG AND TIME INTERVAL VARIABILITY DATA

PAULI TIKKANEN

Department of Physical Sciences,
Division of Biophysics, and
Biomedical Engineering Program

OULU 1999

PAULI TIKKANEN

CHARACTERIZATION AND APPLICATION OF ANALYSIS METHODS FOR ECG AND TIME INTERVAL VARIABILITY DATA

Academic Dissertation to be presented with the assent of the Faculty of Science, University of Oulu, for public discussion in Raahensali (Auditorium L 10), Linnanmaa, on May 24th, 1999, at 12 noon.

OULUN YLIOPISTO, OULU 1999

Manuscript received 30.3.1999
Accepted 9.4.1999

Communicated by
Professor Metin Akay
Docent Kari-Pekka Estola

ISBN 951-42-5214-4
(URL: http://herkules.oulu.fi/isbn9514252144/)

ALSO AVAILABLE IN PRINTED FORMAT

ISBN 951-42-5213-6
ISSN 0355-3191 (URL: http://herkules.oulu.fi/issn03553191/)

OULU UNIVERSITY LIBRARY
OULU 1999

To my family

Tikkanen, Pauli, **Characterization and Application of Analysis Methods for ECG and Time Interval Variability Data**
Department of Physical Sciences, Division of Biophysics, and Biomedical Engineering Program, University of Oulu,
FIN-90571, Oulu, Finland.
1999
Oulu, Finland
(Manuscript received 30 March 1999)

Abstract

The quantitation of the variability in cardiovascular signals provides information about the autonomic neural regulation of the heart and the circulatory system. Several factors have an indirect effect on these signals as well as artifacts and several types of noise are contained in the recorded signal. The dynamics of RR and QT interval time series have also been analyzed in order to predict a risk of adverse cardiac events and to diagnose them.

An ambulatory measurement setting is an important and demanding condition for the recording and analysis of these signals. Sophisticated and robust signal analysis schemes are thus increasingly needed. In this thesis, essential points related to ambulatory data acquisition and analysis of cardiovascular signals are discussed including the accuracy and reproducibility of the variability measurement. The origin of artifacts in RR interval time series is discussed, and consequently their effects and possible correction procedures are concidered. The time series including intervals differing from a normal sinus rhythm which sometimes carry important information, but may not be as such suitable for an analysis performed by all approaches. A significant variation in the results in either intra- or intersubject analysis is unavoidable and should be kept in mind when interpreting the results.

In addition to heart rate variability (HRV) measurement using RR intervals, the dynamics of ventricular repolarization duration (VRD) is considered using the invasively obtained action potential duration (APD) and different estimates for a QT interval taken from a surface electrocardiogram (ECG). Estimating the low quantity of the VRD variability involves obviously potential errors and more strict requirements. In this study, the accuracy of VRD measurement was improved by a better time resolution obtained through interpolating the ECG. Furthermore, RT_{max} interval was chosen as the best QT interval estimate using simulated noise tests. A computer program was developed for the time interval measurement from ambulatory ECGs.

This thesis reviews the most commonly used analysis methods for cardiovascular variability signals including time and frequency domain approaches. The estimation of the power spectrum is presented on the approach using an autoregressive model (AR) of time series, and a method for estimating the powers and the spectra of components is also presented. Time-frequency and time-variant spectral analysis schemes with applications to HRV analysis are presented. As a novel approach, wavelet and wavelet packet transforms and the theory of signal denoising with several principles for the threshold selection is examined. The wavelet packet based noise removal approach made use of an optimized signal decomposition scheme called best tree structure. Wavelet and wavelet packet transforms are further used to test their efficiency in removing simulated noise from the ECG. The power spectrum analysis is examined by means of wavelet transforms, which are then applied to estimate the nonstationary RR interval variability. Chaotic modelling is discussed with important questions related to HRV analysis.

Keywords: Autonomic regulation, heart rate variability, RR interval, ventricular repolarization duration, ambulatory data, time and frequency domain, wavelet transforms, denoising

Acknowledgements

The research reported in this thesis was carried out in the Division of Biophysics at the Department of Physical Sciences, University of Oulu, Finland, during the years 1994-98.

I would like to express my gratitude to Professor Martti Mela for the opportunity to do this work and for his supervision and advice during the course of the study.

I am deeply grateful to Docent Lawrence C. Sellin for patient guidance and supervision of the research projects. Without his expert support carrying through this study would have been much harder and taken longer. I am indebted to him for effective team-work, help in writing the reports, and revising the language of the thesis.

I wish to thank Professor Heikki Huikuri for expert guidance and collaboration regarding the medical aspects of this work.

I would like to thank Professor Matti Weckström for the cooperation within the last few months spent in finishing the thesis. I would also like to express my gratitude to Professor Rauno Anttila, the former head of the department, for his useful collaboration. Stimulating discussions with Professor Matti Karras in the course of the work are also greatly appreciated.

I am indebted to Dr. Seppo Nissilä and Ilkka Heikkilä for their expertise within these years. I wish to thank Hannu Kinnunen and Jan-Erik Palmgren for the pleasant teamwork in the subprojects involved in this work. I also appreciate much the expert knowledge of Medical Physicist Markku Linnaluoto which was needed in the study.

I am grateful to Professor Metin Akay, Darthmouth College, Thayer School of Engineering, USA, and Docent Kari-Pekka Estola, Nokia Research Center, Helsinki, Finland, the official reviewers of the thesis, for their comments and suggestions to the manuscript. I would like to thank Docent Tapio Rantala for reading and commenting the manuscript.

The financial support granted by Astra Finland, Instrumentariumin tiedesäätiö, Division of Biophysics and Biomedical Engineering Program, University of Oulu is gratefully acknowledged. The computational facilities provided by the Center for Scientific Computing, Espoo, Finland, were an important component in performing the study.

I thank the rest of the staff at the Department of Physical Sciences, especially in the Division of Biophysics for help and cooperation within the course of the work.

Finally, I would like to thank my wife Virpi and daughter Venla for their support and patience during these years. They have given a great deal of welcome change during the sometimes lonely work.

Oulu, March 1999 Pauli Tikkanen

List of original papers

This thesis is based on the following papers, which are referred to in the text by their Roman numerals:

I Tikkanen P, Kinnunen H, Nissilä S, Heikkilä I & Mela M (1999) Ambulatory heart rate variability analysis methods. Automedica 17(4): 237-267.

II Tikkanen PE, Sellin LC, Kinnunen HO & Huikuri HV (1999) Using simulated noise to define optimal QT intervals for computer analysis of ambulatory ECG. Medical Engineering & Physics 21(1): 15-25.

III Tikkanen PE (1999) Nonlinear wavelet and wavelet packet denoising of ECG signal. Biological Cybernetics 80(4): 259-267.

IV Huikuri HV, Airaksinen KEJ, Koistinen MJ, Palmgren J-E, Linnaluoto MK, Tikkanen P & Sellin LC (1997) Two-dimensional vector analysis of beat-to-beat dynamics of ventricular repolarization. Annals of Noninvasive Electrocardiology 2(2): 121-125.

Paper I deals with the data analysis methods for heart rate variability time series and discusses also several aspects related to data recorded in ambulatory settings. The author has been mainly responsible for organizing and writing the text, only the part dealing with artifacts, their effects and correction was written by Hannu Kinnunen, M.Sc. Derivation of the data analysis methods, research and discussion on the characterization of the presented methods was performed by the author. The examples of data analysis were produced also by the author. This long paper could have been published also in two separate papers, but it was more convenient to bind these together due to clarity of the presentation. In QT interval study (paper II) the author was in charge of writing the manuscript, solely planned the simulation scheme and performed the data analysis. The computer program was developed and written by the author, except the first versions of

the waveform detection algorithms, which were coded by Hannu Kinnunen, M.Sc., under supervision of the author. Developing signal processing settings e.g. for interpolation, interpreting and reporting the results were done by the author. Paper III has been produced solely by the author. Therefore, the development of the signal analysis schemes, performing the simulations and reporting the results were carried out by the author. In paper IV, the author was responsible for the signal analysis methods in the course of the study. Developing a computer program for the analysis of MAP signals was done by Jan-Erik Palmgren, M.Sc., under supervision of the author. The author was also responsible for the technical aspects of the paper. The results reported in section 5.4 are not presented in any of the original papers. Theoretical research linked to that section as well the data analysis were completely performed by the author. Further, the thesis includes some theoretical considerations which are not given in the original papers. These were created by the author alone.

Abbreviations

AIC	Akaike information criterion
AGC	Automatic gain control
AMI	Acute myocardial infarction
ANS	Autonomic nervous system
APD	Action potential duration
AR	Autoregressive
AV	Atrioventricular
CHF	Congestive heart failure
CO	Cardiac output
CSA	Compressed spectral arrays
CTM	Measure of central tendency
CWT	Continuous wavelet transform
CV	Coefficient of variation
DWD	Discrete Wigner distribution
DWT	Discrete wavelet transform
ECG	Electrocardiogram
FIR	Finite impulse response
FFT	Fast Fourier Transform
FHRV	Fetal heart rate variability
FPE	Final prediction error
HF	High frequency
HR	Heart rate
HRV	Heart rate variability
LF	Low frequency
LF/HF	The ratio of the power estimates for the LF and HF components
LMS	Least mean square
MAP	Monophasic action potential

MI	Myocardial infraction
MP	Matching pursuit
pNN50	The percentage of difference between adjacent normal RR intervals greater than 50 ms computed over the entire 24 hour ECG recording
QMF	Quadrature mirror filter
QRS	Q-, R-, and S-waves in electrocardiogram
QT	QT time interval
RLS	Recursive least square
RMSSD	Root mean square of successive differences
RR	RR time interval
RT	RT time interval
RWED	Running windowed exponential distribution
SA	Sinoatrial
SD	Standard deviation
SDA	Selective discrete Fourier transform algorithm
SDNNIDX	The mean of the standard deviations of all normal RR intervals for all five minutes segments of a 24 hour ECG recording
SPWD	Smoothed pseudo Wigner distribution
STFT	Short-time Fourier transform
SV	Stroke volume
SURE	Stein's unbiased risk estimate
TFR	Time frequency representation
TI NN	Triangular interpolation of the normal-to-normal histogram
ULF	Ultra low frequency
WD	Wigner distribution
WP	Wavelet packet
WT	Wavelet transform
VLF	Very low frequency
VRD	Ventricular repolarization duration

Contents

1. Introduction

1.1. Background

Variabilities in cardiovascular activity, such as RR interval and ventricular repolarization duration (VRD), have been widely used as a measure of cardiovascular function. It is typical for these signals that they fluctuate on a beat-to-beat basis around their mean value and the fluctuation are associated with autonomic neural regulation of the heart. Monitoring the fluctuations observed in heart rate and VRD thus provides information concerning their autonomic regulation and disturbances. For example, heart rate fluctuates due to factors such as age, respiration, cardiovascular and neurologic diseases, medication, as well as physical and mental stress (Malliani *et al.* 1991, VanRavenswaaij-Arts *et al.* 1993, Pagani *et al.* 1995).

To predict a risk of adverse cardiac events the primary analytical measurements have been heart rate variability (Moser *et al.* 1994, Tsuji *et al.* 1994) and QT analysis (Decker *et al.* 1994). Abnormalities in heart rate fluctuation have been shown to precede the spontaneous onset of ventricular tachyarrhythmias (Huikuri *et al.* 1996). For example, low heart rate variability predicts increased mortality after acute myocardial infarction (AMI) (Malik *et al.* 1990). Clinical and experimental data have shown that prolongation of the QT interval measured from the standard 12-lead ECG is a risk factor for ventricular arrhythmia and sudden cardiac death in patients with or without previous AMI. The increased risk due to QT prolongation is independent of age, history of AMI, heart rate and drug use. The variability of successive RR intervals traditionally has been used to access the risk in patients in terms of future mortality. Recently, emphasis has been directed towards understanding the dynamic changes in the repolarization phase of the heart (Extramiana *et al.* 1997, Huikuri 1997). It is probable that there are dynamic changes in the ventricular repolarization duration (QT interval) throughout the 24-hour period (Merri *et al.* 1993).

The autonomic nervous system (ANS) regulates the functioning of the heart through its sympathetic and parasympathetic parts. It is of interest to quantify the amounts of signal fluctuation related to these two parts of the ANS separately and also their balance in the neural regulation of the heart. For instance, heart

rate is affected by factors such as respiration, the thermoregulatory system and mechanisms regulating blood pressure (Hainsworth 1995).

Autonomic regulation of the heart and the cardiovascular system has been investigated widely, but no uniform concept exists regarding the function of neural mechanisms. Furthermore, there is a lack of standardization of the parameters and their meaning in signal variability analysis. For example, the analysis of the frequency spectrum is made using several approaches such as Fourier transform and AR-modelling based methods with several variations.

The quantification of neural regulation is a demanding task, because interpretation relies on an indirect measurement, i.e. the observed fluctuation in cardiovascular variability signals. The heart rate signal includes noise from various sources and information not related to autonomic regulation of the heart summed with the relevant information. There are technical and methodological limitations in the measurement of the QT interval, for example, due to artifacts, low sampling frequency, and inaccuracies in the definition of the end of the T wave in the ambulatory ECG recordings. Measurement of monophasic action potential (MAP) with a contact electrode have been confirmed as an accurate method for analysis of local ventricular repolarization duration (Franz 1991).

Heart rate variability (HRV) has been studied extensively during the last few years. The analysis of the frequency spectrum of the heart rate signal has attracted attention mainly due to its ability to expose different sources of fluctuations (Baselli *et al.* 1987, Bianchi *et al.* 1993, Kamath & Fallen 1993, Malliani *et al.* 1991) and its power to illustrate the balance of the autonomic neural regulation. There also exist several widely used time-domain parameters representing fluctuations in heart rate (Kleiger *et al.* 1992). Lately, more emphasis has been placed on the non-linear analysis of heart rate variability (Huikuri *et al.* 1996, Signorini *et al.* 1994).

The analysis of variability in cardiovascular signals is applied widely and there are thus many differences in experimental setups. In addition, the parameters used for quantifying variability vary from one area of research to another. The meaning of some parameters may remain unclear, and the understanding of the applications of novel methods can also be imperfect. Sometimes, these factors can make it relatively difficult to interpret the results and compare them among the projects. Data are commonly recorded in a laboratory, where the conditions are strictly controlled and the effects of disturbing factors are minimized. The recording of ambulatory data is affected by many outside disturbances, and therefore, special interest must be taken in the quality of the recorded data and the characteristics of the analytical methods. Neglect of such matters can lead to serious errors in interpreting the results.

1.2. Aims and the outline of the thesis

This study is a methodological approach to deal with the analysis of short term fluctuations in the cardiovascular variability signals. In this context, the periods of the oscillations observed in signals vary from a few seconds to tens of seconds.

The thesis includes the development of analysis schemes and studies of the dynamics of RR interval, ventricular repolarization duration (VRD) and action potential duration (APD) time series. Some emphasis will be on the ambulatory data with discussion of the accuracy and the reproducibility of the measurement as well as the effects of artifacts. A computer program for the measurement of RR and QT intervals from the ambulatory electrocardiogram (ECG) is described. Furthermore, the accuracy of the different QT interval estimates will be obtained through simulated noise tests. The invasive measurement of APD variability is used to emphasize the requirements needed for the VRD variability estimation and to study the factors determining the VRD dynamics. The novel wavelet transform approaches are proposed to remove noise from ECG and the denoising performances are quantified by simulations. The spectral estimation using wavelet transforms will be presented for RR interval data obtained from healthy subjects during a drug injection and from ordinary cardiology patients prior to the onset of ventricular fibrillation. Overall, the stress is more on the demonstration of the signal analysis schemes than the larger data analysis settings.

A review of the signal analysis methods applied to cardiovascular variability signals is provided. Furthermore, the limits and advantages of the methods are discussed. An important point is to present the mathematical background of the methods and demonstrate their application using some experimental data. It is worth noting that there often exist a correlation between the results and some phenomena, but the analysis method may not be a suitable one to describe these phenomena. To obtain relevant results and a correct diagnosis, a deeper understanding of the nature of applied methods would be necessary. There are often some basic assumptions and rules for the methods and signals, which should be taken account in order to make the analysis more useful. As the evaluation of the results is made with deeper understanding of the methodological aspects, one can better say "what is actually possible to show by our results".

First the physiological and medical background is briefly reviewed in order to give some basis for the application of the analytical methods. Extraction of the cardiovascular variability signals is presented and important aspects of measurement techniques are pointed out. The mathematical and methodological background is presented for time and frequency domain analysis methods. The estimation of the power spectrum is considered important especially the parametric methods and the autoregressive (AR) approach. Time-frequency and time-variant spectral analysis methods are reviewed and a novel wavelet approach is introduced. The wavelet section includes discussions of the continuous and discrete wavelet transform with a subband filtering scheme as well as a more recent application of the wavelet packet transform using an optimized signal decomposition. The use of chaotic modelling is also considered and important issues related to HRV analyses are presented.

2. Cardiovascular variability signals

2.1. Physiological background

The sinus rhythm fluctuates around the mean heart rate, which is due to continuous alteration in the autonomic neural regulation, i.e. sympathetic-parasympathetic balance. Periodic fluctuations found in heart rate originate from regulation related to respiration, blood pressure (baroreflex) and thermoregulation.

Parasympathetic (vagal) regulation to the heart is inhibited simultaneously with inspiration, and the breathing frequency coincides with fluctuations observed in heart rate (Eckberg 1983). Furthermore, thoracic stretch receptors and peripheral hemodynamic reflexes also result in respiratory arrhythmia (Akselrod *et al.* 1985). Respiratory arrhythmia are consequently due to parasympathetic regulation and can be excluded by atropine or vagotomy (Akselrod *et al.* 1985). The maximal amplitude of respiratory related heart rate fluctuation is found at breathing rate of 6 cycles per minute, because the fluctuation increases as respiration rate achieves the frequency of the intrinsic baroreflex-related heart rate fluctuations (VanRavenswaaij-Arts *et al.* 1993).

The fluctuations due to blood pressure regulating mechanisms originate from self-oscillation in the vasomotor part of the baroreflex loop (VanRavenswaaij-Arts *et al.* 1993). These fluctuations coincide with synchronous oscillations in blood pressure called Meyer waves (Kitney & Rompelman 1987). Increase of sympathetic nerve impulses strengthen (Pagani *et al.* 1984, Pomeranz *et al.* 1985) and sympathetic or parasymphatetic blockade weaken these fluctuations in heart rate (Pomeranz *et al.* 1985).

Changes in peripheral resistance produce low frequency oscillations in heart rate and, for example, in systolic blood pressure. Thermal stimulation given on the skin can be used to stimulate the oscillations, which are originally due to thermoregulatory adjustment of peripheral blood flow (VanRavenswaaij-Arts *et al.* 1993). These fluctuations are controlled by the sympathetic part of the autonomic nervous system.

The overall autonomic function is controlled by a central command from the brain. However, the autonomic nervous system operates as a feedback system, and heart rate is thus regulated by many reflexes which may increase or decrease the

sympathetic or parasympathetic activity or both of them (Hainsworth 1995). Reflexes can act simultaneously and their interactions may be complex. The arterial baroreceptor reflex originates from receptors located in the arteries such as carotid sinuses and aortic arch. The increase in blood pressure excites baroreceptors producing an augmented efferent vagal and reduced sympathetic activity. Peripheral arterial chemoreceptors located in the carotid and aortic bodies produce, most often, an increase in the rate and depth of respiration. Because this reflex influence on heart rate through respiration, the effects may be covered by other respiratory responses. The coronary chemoreflex (Bezold-Jarisch reflex) can cause bradycardia and is significant in pathological states such as myocardial ischemia and infarction. Atrial receptors streched by the increase in atrial volume and some of them by atrial contraction, the response being linked directly to atrial pressure. These volume receptors cause an increase in heart rate and operate through the sympathetic nerves producing their response very slowly. There exist also other cardiovascular reflexes coming from receptors located e.g. in pulmonary arteries, lungs and muscles.

The physiological importance of heart rate can be demonstrated by an axiomatic relation in which cardiac output (CO) can be defined by a product between heart rate and stroke volume (SV) as $\mathrm{CO} = \mathrm{HR} \cdot \mathrm{SV}$. Because heart rate and stroke volume are not independent of each other, the definition of cardiac output is not always so straightforward in terms of physiological adjustment.

The rate of depolarization of the cardiac pacemaker defines heart rate. The sinoatrial (SA) node, the atrioventricular (AV) node and the Purkinje tissue can be regarded as potential pacemaker tissues in a heart. As the fastest depolarization rate is found in the sinoatrial node and the depolarization impulse spreads through the conduction system to other pacemakers before they spontaneously depolarize, the sinoatrial node usually defines the heart rate. However, failing to produce a normal pacemaker impulse, other pacemaker tissues can act as a cardiac pacemaker.

Autonomic neural regulation of the heart is determined by its sympathetic and parasympathetic parts. The parasympathetic nerves are connected to the sinoatrial node, the AV conducting pathways and the atrial and ventricular muscles as well as coronary vessels (Kamath & Fallen 1993). Sympathetic nerve fibers innervate the SA node, the AV conducting pathways, coronary vessels and the atrial and ventricular myocardium (Kamath & Fallen 1993, Hainsworth 1995). Both divisions of the autonomic nervous system always have some activity which continuously regulates the function of the heart. Heart rate response therefore presents a balance between sympathetic and parasympathetic (vagal) regulation which can be considered also as an antagonist function.

Heart rate has a major effect on ventricular repolarization duration (VRD), but the autonomic nervous system also regulates directly the repolarization of the ventricles. In addition, electrolytic factors, age and gender have an effect on it. It has been shown that when the autonomic nervous system regulates VRD there are similar periodic fluctuations as seen in heart rate (Merri *et al.* 1993).

2.2. Changes of signal variability connected to specific diseases

A decrease in vagal neural activity into the heart may result in diminished HRV after myocardial infarct (MI) leading to the prevalence of symphatetic neural regulation and to electrical instability (Task Force of ESC & NASPE 1996). Reduced heart rate variability is also associated with an increased risk for ventricular fibrillation and sudden cardiac death (Farrell *et al.* 1991, Casolo *et al.* 1992). Huikuri *et al.* (1996) concluded that changes in long term RR interval dynamics with beat-to-beat RR interval alternans is likely to precede the spontaneuous onset of sustained ventricular tachyarrhythmias. Results obtained using spectral analysis of HRV suggest a change of sympatho-vagal balance toward a symphatetic dominance and a diminished vagal tone in patients surviving an acute myocardial infarction (Lombardi *et al.* 1992, Task Force of ESC & NASPE 1996). Cardiac diseases such as congestive heart failure, coronary artery disease and essential hypertension are also associated with a reduced vagal and an enhanced sympathetic tone, which change heart rate varibility dynamics (VanRavenswaaij-Arts *et al.* 1993, Malliani *et al.* 1991). Because HRV analysis can be regarded as a noninvasive, reproducible and an easy to use method reflecting the degree of autonomic control of the heart (Bellavere 1995), it has been widely used to diagnose the autonomic dysfunction due to diabetic neuropathy (Pagani *et al.* 1988a, Freeman *et al.* 1991, Bernardi *et al.* 1992). It has been generally observed, that overall HRV is reduced and sympatho-vagal balance may be altered during tilt maneuver or standing in diabetic patients (Malliani *et al.* 1991, Kamath & Fallen 1993).

Although HRV is used in a wide range of clinical applications, diminished HRV has only been generally accepted as a predictor of risk after acute myocardial infarction and as an early warning of diabetic neuropathy. Diminished HRV can predict mortality and arrhythmic events independently of other risk factors after acute myocardial infaction, and long-term HRV analysis have proven to be a more definite predictor compared to a short-term analysis (Task Force of ESC & NASPE 1996). Heart rate variability analysis should also be joined with other risk factors so as to improve the predictive use.

Any heart disease (left ventricular hyperthrophy, heart failure, etc.) can modify repolarization duration (Coumel *et al.* 1994). Anomalies in repolarization duration are signs of electrical instability in the heart and can lead to malignant arrhythmias such as ventricular fibrillation and Torsades de Pointes. Analysis of ventricular repolarization duration dynamics provides essential information on a propensity for ventricular arrhythmias, because some life-threatening arrhythmias arise in myocardial tissue (Huikuri 1997). Altered dynamics of the VRD, and the events of the alternating T wave amplitude particularly in patients with the long QT syndrome as well as with structural heart disease at fast heart rates, suggest that the analysis of the ventricular repolarization dynamics may provide an important clinical tool (Huikuri 1997).

2.3. Other events modifying signal variability

Several pharmaceutical interventions can be used to modify heart rate dynamics as shown by human (Selman *et al.* 1982) and animal (Adamson *et al.* 1994) studies. Atropine administration has been used to prove the connection between vagal neural activity and high frequency (respiratory related) fluctuation in RR interval time series (Pomeranz *et al.* 1985). Scopolamine significantly augments heart rate variability (Ferrari *et al.* 1993) which suggest an increasing coincident vagal activity into the heart. The effect of β-adrenergic receptor blockades has been studied after myocardial infarction (Molgaard *et al.* 1993, Sandrone *et al.* 1994). There are also studies on the effect of antiarrhythmic drugs such as flecainide (Zuanetti *et al.* 1991, Bigger *et al.* 1994) and propafenone (Zuanetti *et al.* 1991, Lombardi *et al.* 1992), as well as encainide and moricizine (Bigger *et al.* 1994) on the heart rate dynamics. Merri *et al.* (1993) studied the effect of β-adrenergic blocker (nadolol) on ventricular repolarization duration and its dynamics. Their finding was that the length of repolarization duration was shorter, the signal variance was greater and the spectral pattern was shifted to higher frequencies due to this medication. A change of the dynamic relationship between ventricular repolarization duration and heart rate has been observed as a consequence of nadolol administration with normal patients (Merri *et al.* 1992).

Heart rate variability has been employed to investigate the short and long term autonomic responses to physical and mental exercise. It has been observed that the increase in respiratory related fluctuation, the total HRV reduction and the recorded signal become more nonstationary as the intensity of the dynamic physical exercise increases (Malliani *et al.* 1991). Heavy physical exercise has been shown to augment low-frequency (LF) fluctuations in heart rate, and the recovery of the spectral pattern may last even 48 hours after finishing exercise (Furlan *et al.* 1993). The sympatho-vagal balance seems to change towards sympathetic dominance e.g. in hypertensive patients (Pagani *et al.* 1988b). Long term physical exercise has positive effects on hemodynamics and neural control mechanisms, for example, by lowering the arterial pressure in hypertensive patients (Pagani *et al.* 1988b) and increasing baroreflex gain in patients with ischemic heart disease (Rovere *et al.* 1988). An overall observation, also related to dynamic mental stress, is an increase of the sympathetically- and a decrease of vagally-mediated fluctuations in heart rate (Pagani *et al.* 1995).

2.4. RR interval time series

The basic procedure used for determing the heart rate and its fluctuations is described below. An electrocardiogram (ECG) is measured, using appropriate data acquisition equipment. The time elapsing between consecutive heart beats is defined as that between two P waves, when a P wave describes the phase of atrial depolarization. In practice, it is the QRS complex that is used to obtain the time period between heart beats. This complex is detected in the R wave, because it

has a very clear amplitude and better frequency resolution than the P wave, and a much better signal-to-noise ratio. The time interval between the P and R waves can be assumed and has been shown to be constant (Kitney & Rompelman 1987).

Defining the times of occurrence of two concecutive R waves as $s(t)$ and $s(t+1)$, $t = 1, \ldots, N$, the expression $x(t) = s(t+1) - s(t)$ is obtained for a time period in milliseconds. This $x(t)$ is called the *RR interval time series* or else the times to which it refers are simply called *RR intervals*. A *heart rate time series* $[\mathrm{min}^{-1}]$ can be obtained by $y(t) = 1000 \cdot (60/x(t))$ and the *mean heart rate* is simply $\mathrm{HR} = N^{-1} \sum_{t=1}^{N} y(t)$. These formulae indicate a nonlinear relationship between the values in a given time series, which should be taken into account when comparing the results obtained by time and frequency domain approaches (Sapoznikov *et al.* 1993). At the moment, RR intervals seem to be the more frequently used time series in heart rate variability (HRV) analysis. For a discussion of the choice between different time series (tachograms), see Janssen *et al.* (1993).

2.5. VRD time series

QT time interval in electrocardiographic signals has been used to perform both static and dynamic analyses of the duration of the ventricular repolarization. There exist difficulties in the detection of the onset of Q wave and the offset of T wave due to poor signal-to-noise ratio and varying ECG morphology. For these reasons other estimates, such as $\mathrm{RT}_{\mathrm{max}}$ interval, has been widely used. Moreover, this provided a motivation to investigate and compare the noise sensitivity of different QT interval estimates. Because Q-S time interval is a result of the depolarization period of the ventricles, it is actually more correct to measure the time interval between the R and T waves as one is interested in the changes occurring within the ventricular repolarization period (Merri *et al.* 1989). R wave has been used to estimate the start of the repolarization period because searching for the offset of S wave can be difficult. The maximum (apex) of T wave has been often regarded as a more reliable estimate for the end of the repolarization period than the T wave offset. The total repolarization duration, i.e. time interval between the offsets of S and T waves, can further be analysed with respect to early and late repolarization duration as well as repolarization area (Merri *et al.* 1989, Merri 1989). In this work the objective will be on the measurement of the repolarization duration in the ambulatory ECG.

The 24-hour ambulatory ECG has certain problems and drawbacks because the signal is corrupted by noise from various sources and also several conditions may alter the ECG morphology. The ambulatory ECG is usually acquired with a sampling frequency of 128 Hz giving a time resolution of 7.81 ms for each sample, which is too low for QT interval variability measurement. It has been suggested that the QT interval should be determined at least with resolution of 1 ms (Speranza *et al.* 1993), which would require 1 kHz sampling frequency for ECG signal. In an ambulatory measurement setting, with data acquisition times lasting up to 24 hours, the sampling frequency can not be that high, because then the amount

of the stored data rises rapidly. In present ambulatory ECG analysis systems the possibility of exporting a beat-to-beat QT time series extracted with high time resolution is also lacking. These problems have been solved by exporting raw ECG data and, by oversampling ECG signal (Speranza *et al.* 1993) or by interpolating waveforms (Merri *et al.* 1991) a better time resolution for the time interval measurement results.

2.6. APD time series

The local ventricular repolarization duration can be measured by placing a contact electrode in a ventricular muscle. Rate-dependent dynamics of VRD obtained from the right ventricular apex provides an example. This approach can solve the above mentioned problems related to the ambulatory QT measurement. However, measuring monophasic action potentials (MAP) is an invasive procedure. The duration of repolarization phase, which is termed as action potential duration (APD), is estimated as a time interval between the onset and offset of the action potential. The offset is defined as the maximal positive derivative of the upstroke phase of the action potential waveform. The offset can be defined at time points where the waveform has come down 15, 30, 50 and 90 % from the maximal amplitude of the MAP. Most often used definitions are 50 and 90 % points. The APD time series are extracted from the consecutive waveforms and the beat-to-beat analysis is performed.

2.7. ECG waveform detection

The RR and QT interval measurement (paper II) was based on an implementation of an algorithm described previously (Laguna *et al.* 1990) and the detection scheme will be briefly reviewed here. The basic concept of the algorithm is to look for the zero crossing points, the crossings of certain experimentaly-determined threshold values, as well as the local maximum or minimum values of the differentiated ECG signal $d(t)$ and its low-pass filtered version $f(t)$.

The differentiator and the low-pass filter described by Laguna *et al.* (1990) were modified according to the sampling rate in order to obtain an optimal frequency response. The sampling rate of the analysed ECG was one parameter of the waveform detection procedure, and in this way, the preprocessing filters and the algorithm itself can adapt to the different sampling rates.

The flowchart of the implemented waveform detection procedure is shown in Figure 1 in paper II. The first step is to calculate the signals $d(t)$ and $f(t)$, which is done for the whole period of the ECG selected for analysis. The waveform detection procedure continues by determining the initial value of the threshold value H_n used to search the maximum absolute value of the QRS in the signal $f(t)$. The threshold value H_{n+1} is continuously updated (Laguna *et al.* 1990)

during the waveform detection using the equation

$$H_{n+1} = 0.8 \cdot H_n + (0.16 \cdot |f(PK_n)|) \quad , \tag{2.1}$$

where $|f(PK_n)|$ is the absolute value of the signal $f(t)$ at the detected fiducial R wave position of the beat n.

The initialisation of the average of RR intervals RR_{av} and the first RR interval value are then obtained. The RR_{av} value is later used to check the calculated value of a new RR interval and thus provides a basis for identifying the QRS complex.

The initial position of a QRS complex is detected using an adaptive threshold method determined by the RR interval average value, as shown in Figure 1 in paper II. After that, the algorithm continues to search the position of the R wave. In the present approach, the fiducial point of the R wave was detected using three methods: at the maximum amplitude upwards or downwards from the baseline, or at the zero crossing point of the signal $f(t)$ during the QRS complex. The last technique was implemented in the original algorithm by Laguna *et al.* (1990). It was found that, in some cases, a more accurate definition can be obtained, if the fiducial point of the R wave is defined at the maximal upward amplitude of QRS. With this algorithm, an accurate determination of the R wave is an absolutely necessary condition for a reliable Q wave detection.

After detecting the R wave position and updating the threshold H_n and RR_{av}, the onset of Q wave is searched keeping the R wave position as a reference point. Here it should be mentioned, that examining the pattern of the Q wave is made by analysing the differentiated signal $d(t)$ and not the signal $f(t)$, because the signal $d(t)$ includes the high frequency components of the Q wave.

Next the T wave maximum and T wave end are detected from the signal $f(t)$. The following definition for the limits of a search window calculated from the R wave position was used:

$$(bwind, ewind) = (a \cdot RR_{av}, b \cdot RR_{av}) \quad , \tag{2.2}$$

where a and b are parameter values in the procedure. This definition is a slightly different one from the given by Laguna et al. As the threshold for T wave end was used the value $H_s = f(T_i)/2$, T_i denoting the position of the maximal downward or upward slope after the T wave maximum.

Finally, a value of QT interval is calculated using the relation $QT(n) = T_{end}(n) - QT_{onset}(n)$, where $T_{end}(n)$ and $QT_{onset}(n)$ are the positions of T wave end and the onset of the QT time interval during the beat n. The analysis of the next cardiac beat is started 150 ms after the last T wave end is defined.

The effects of the four alternative definitions of the QT interval onset on the analysis of QT interval dynamics were compared: true QRS onset, R wave maximum, ascending or descending maximal slopes of the R wave. One reason for this was quite practical: in some circumstances dealing with ambulatory ECG, the determination of the QRS onset seems to be uncertain e.g. because of a missing Q wave and the relatively low sampling rate. In the original implementation of this algorithm, the Q wave onset found is rejected if the difference between Q wave and R wave fiducial points is larger than 80 ms (Laguna *et al.* 1990). In that case, QRS onset is defined in the onset of R wave.

2.8. Ambulatory HRV data

The aim of recording RR intervals has been to gain information about the neural regulation of the heart and the circulatory system. Observing the changes occuring over long periods of time (i.e. several hours) requires ambulatory recording, which is usually performed using standard commercial equipment (Holter devices). This provides procedures for ECG signal acquisition and analysis, extracting the RR interval time series from the ECG signal and analysing them. The sampling frequency typically used for an ECG signal with Holter devices is 128 Hz, which means a timing accuracy of 7.81 ms for R wave detection. Thus a low sampling frequency produces inaccuracies in RR interval measurement and bias in the analysis. A timing accuracy of the order of 1 ms would be desirable for the assessment of chaos, for example.

One factor affecting ambulatory HRV measurement is circumstances that vary with time, i.e. the fact that external conditions can be far from stable. This may produce nonstationary changes in a time series and make the assessment of the physiological events more difficult, or even impossible, than under stable laboratory conditions. A method for separating non-periodic (nonstationary) changes from periodic ones has been proposed by Sapoznikov *et al.* (1994). Variable conditions may also produce periodic fluctuations which become summed in the time series, making it difficult to distinguish the regulatory processes from each other. This can obviously lead to misinterpretations in some circumstances.

2.8.1. Accuracy of HRV measurement

The accuracy of spectral estimates performed on RR intervals obtained from ambulatory Holter systems has been studied by Pinna *et al.* (1994). It has been observed that the centre and dispersion of the estimation error changes from one Holter system to another. There are large inter-recorder differences and variable spectral distortion among selected spectral bands. Use of the Fourier spectral estimate gave more stable results than did the AR spectral estimate in ten minute ECG sequences. The main factor limiting the accuracy of the RR interval measurement was the low frequency with which the ECG signal was sampled, a topic discussed theoretically by Merri *et al.* (1990). Pinna *et al.* (1994) concluded that spectral analysis of RR interval time series with very low variability may be seriously altered when performed on an ECG signal acquired using a Holter system.

The accuracy of spectral estimates of HRV was investigated by generating a simulated RR interval time series of variable length (180-540 seconds) using an autoregressive model from a set of recordings and adding Gaussian noise (Pinna *et al.* 1996). The accuracy of Fourier (Blackman-Tukey) and AR spectral estimates could then be evaluated in terms of the normalized bias and variance. The results showed that the bias (systematic error) of the estimate was a less important factor than the variance (random error). Both decreased as the length of the time series increased, but the variance decreased more rapidly. The power estimate was most

stable in the HF band, while that in the VLF band had the highest variance. No minimum length was proposed for a time series, but it was concluded that even with the shortest record the bias made a less significant contribution to the estimates. It was pointed out that a relative high variability in spectral parameters is typical of RR interval time series, and that this should be noted in the analysis of the short time series.

2.8.2. Reproducibility of HRV measurements

There are a number of factors that affect HRV measurements, and obtaining precisely controlled conditions is problematic. Furthermore, variability is always seen between repeated measurements. From this point of view, it is essential to study both short-term (over several days or couple of weeks) and long-term (over 6-7 months) reproducibility of the analyses, even though this can be a tedious task. A few published investigations on the reproducibility of HRV exist, e.g. references Dimier-David *et al.* (1994), Kamalesh *et al.* (1995), Pitzalis *et al.* (1996), Pomeranz *et al.* (1985) and Ziegler *et al.* (1992).

Kamalesh *et al.* (1995) investigated the short-term reproducibility of HRV measurements in patients with chronic stable angina and found no significant changes in the time or frequency domain parameters between two 24 hour ambulatory ECG recordings. The short-term and mid-term (over one month) stability of spectral parameters was studied in healthy young subjects by Dimier-David *et al.* (1994), who observed that the intra-observer and inter-observer reproducibility of spectral analyses are high under controlled conditions. They did not employ any standardization for breathing frequency or volume.

Pitzalis *et al.* (1996) studied the short and long-term reproducibility of HRV measurements in normal subjects. They concluded that time domain parameters, as evaluated over the whole 24 hour recording, can be expected to be reproducible during relatively stable conditions but frequency domain parameters calculated for ten minute ECG sequences were reproducible only under known stable conditions, as factors of other than neural origin can greatly alter the spectrum. The measurement of total power needed resting conditions to produce reproducible results. Respiratory oscillations in the spectrum (high frequency component) can be measured reproducibly during controlled breathing. The low frequency component was reproducible, particularly at rest and during tilt, which indicates that these fluctuations are quite stable. The reproducibility of the power estimates when normalized by reference to the total power seemed to be no better than that of the real values. It should be noted that the time domain parameters were not reproducible if they were evaluated from ten minutes sequences instead of the whole 24 hour period.

The results of analyses performed on signals of short (e.g. five to ten minutes) and long (possibly 24 hours) duration seem to differ. Pitzalis *et al.* (1996) suggest that analyses of long signals may homogenize the results and give better reproducibility of the frequency domain parameters. In analyses performed on 24 hour

recordings, the results have often been calculated for short sequences and then averaged over the whole recording. The authors also conclude that frequency domain parameters should be evaluated from short signals and under controlled conditions to minimize the effects of disturbing factors (Pitzalis *et al.* 1996). Recording the respiratory activity would probably help to explain the RR interval fluctuations.

It should be mentioned that the amount of heart rate variability depends on the subjects. Thus, the reproducibility observed in the case of normal subjects, for example, cannot be assumed to occur in patients with cardiac diseases (Pitzalis *et al.* 1996).

2.8.3. Artifacts in RR interval time series

When the activity of the autonomic nervous system (ANS) is evaluated in terms of HRV, variations in the sinus rhythm of the heart and the RR interval time series analyzed should contain only normal RR intervals. The RR intervals obtained from ambulatory recordings, however, often include abnormal intervals, which do not represent the sinus rhythm and differ in length from normal RR intervals. These can arise from rhythm disturbances (ectopic beats) or errors in the detection of QRS complexes of technical or physiological origin. These artifacts lead to spurious transient spikes in the resulting RR interval time series. The computation of HRV indices can be unfavourably affected by the presence of even a small number of such transients. In addition to high-frequency transient spikes, non-periodic low-frequency changes in the sinus rhythm, i.e. normal physiological or emotional responses of the heart, which are easily encountered in long-term recordings, can have adverse effects on some HRV indices.

As the interest in HRV increases, more efforts are being made to understand the effects of artifacts and artifact processing techniques on HRV measurements (Lippman *et al.* 1994, Malik *et al.* 1989b, Sapoznikov *et al.* 1992). If the number of transient spikes in a RR interval time series is small, it is possible to reject them or correct for them, and thus to obtain a smooth signal consistent with normal RR intervals. Data segments containing frequent artifacts, however, should be rejected from further analysis. Detrending can be used to remove the effects of non-periodic low-frequency changes in RR intervals. The amount of rejected data and the artifact detection criteria and correction techniques used should be taken into consideration when discussing the reliability and reproducibility of different HRV approaches.

2.8.3.1. Errors in the detection and classification of QRS complexes

The detection of QRS complexes (R waves) always precedes the further processing of a RR interval time series. Achieving an accurate, artifact-free RR interval time series requires optimal electrode positioning. Ambulatory ECG recording

is exposed to many technical and physiological disturbances which are not easily prevented or controlled, and consequently errors in the automatic detection of QRS complexes cannot always be avoided. That is, the accuracy of QRS detection can be affected, the detector can miss normal QRS complexes or spuriously detect additional events within normal RR intervals. A missed R wave will lead to an interval, which is approximately twice as long as the average interval, while a detection of an additional event within a normal interval will lead to two shorter intervals, the sum of which equals the real interval. Unfortunately combinations of missed and false detections exist, resulting in difficulties in artifact identification.

It can be impossible to tell on the basis of RR interval data alone whether the cause of an artifact is physiological or technical. In addition, information is needed on the underlying shape of the ECG signal. Considering the activity of the ANS system, however, the origin of the artifact is not important, since all abnormal RR intervals are not useful for further analysis. A review of software QRS detection in ambulatory monitoring has been published by Pahlm & Sörnmo (1984).

Along with detecting QRS complexes, most algorithms used with commercial long-term ECG devices attempt to classify them according to type, as "normal" (i.e. originating from sinus rhythm) or "abnormal" (ectopic). Randomly occurring ectopic (extra) beats are frequently encountered in normal subjects; but if an ectopic beat is mistakenly analyzed as normal, an artifact is induced into the time series, since the RR intervals connected with an abnormal beat differ in length from normal intervals. Thus the role of this classification can be very important. Errors in QRS classification are not rare, however, as noted in Malik *et al.* (1993) and Sapoznikov *et al.* (1992). Therefore systems including QRS classification may require effective artifact correction in the same way as systems without this classification. While single ectopic beats can be corrected to allow further analysis, segments containing pathological rhythm disturbances are usually rejected. The classification of ectopic beats can, according to their occurrence in time relative to surrounding beats, form the basis for the selection of the correction method (Mulder 1992). Ectopic beats can be interposed extra-systoles, compensated extra-systoles, or phase-shifted extra-systoles.

Disturbances of physiological origin

Errors in QRS detection arise from disturbances and extraordinary waveforms in the measured ECG signal (Pahlm & Sörnmo 1984, Thomas *et al.* 1979). Abnormal initiations of the heart beat (ectopic beats) can lead to a variety of morphologies of QRS complexes and cause difficulties in both their classification and their detection. Potential physiological sources of errors also include: abnormally large P or T waves, and myopotentials similar enough to QRS complexes in amplitude and frequency content to cause spurious detection. Variations in the position of the heart with respect to the measuring electrodes and changes in the propagation medium between the heart and the electrodes, both being dependent on the position and breathing of the patient, can cause: sudden changes in the amplitude

of the ECG signal and morphology of the QRS complex, leading to missed QRS complexes, as well as low frequency baseline shift. The ability of the QRS detector to tolerate variations in ECG waveforms depends on the recognition criteria themselves and the pre-processing of the raw ECG data, of which the most essential part is filtering (Friesen *et al.* 1990, Hamilton & Tompkins 1986).

Disturbances of technical origin

Like physiological changes in the ECG signal, the tolerance of different QRS detection procedures can vary with respect to technical disturbances (Friesen *et al.* 1990, Hamilton & Tompkins 1986). These include movement of electrodes (relative to the skin and heart) or other changes in conductivity between the electrodes and the skin, which can result in rapid baseline shift. Capacitively or inductively coupled disturbances, e.g. power line interference and extra peaks originating from the movement of wires or discharges of static electricity when clothes, skin, electrodes and wires chafe against each other in the presence of dry air and skin can also cause disturbances.

Problems at the electrode-skin interface

Most of the disturbances in automatic QRS detection are connected with electrode-skin impedance, since poor conductivity between the electrodes and the skin both reduces the amplitude of the ECG signal and increases the probability of disturbances. Along with pathological arrhythmias, problems at the electrode-skin interface are the most common reasons for having to reject large segments of RR interval data in HRV analyses. The need to take account of the interaction of the skin with the electrodes is commonly described in the literature dealing with the non-invasive recording of surface potentials, but the mechanism of the disturbances caused by rapid impedance changes has been not described. The reason may lie in the fact that problems with electrode contacts can be avoided if the electrodes are correctly attached, electrode paste is used and the tests are performed at rest. Even at normal activity levels, electrode paste usually improves conductivity between the skin and the electrodes enough to prevent problems. Movement of the electrodes relative to the skin and the heart, caused by rapid motion on the part of the subject, can give rise to sudden changes in electrode-skin impedance and consequently a baseline shift in the measured ECG signal. These problems due to unavoidable movement of the electrodes are especially frequent in exercise tests, and are accentuated further if the electrodes are loose or the subject has an unusually high skin impedance.

The larger the electrode-skin impedance, the smaller the relative impedance change needed to cause a major shift in the baseline of the ECG signal, and if the skin impedance is extraordinarily high, it may be impossible to detect the

QRS complexes reliably in the presence of body movement. In such cases the sudden baseline shifts may be of such an amplitude that they lead to the saturation of the voltage amplifier or confuse the automatic gain control (AGC). The exact electrode-skin impedance depends largely on the electrode and the type of electrolyte used, the properties of the subject's skin and the measurement frequency. If the skin is dry, the electrode-skin impedance can be as high as several hundred kilo-ohms at frequencies below 100 Hz. Three-electrode leads are usually better than two-electrode ones, since a separate ground electrode is available.

If the electrode-skin impedance is high, a distribution of charges and subsequent potential difference can be generated on both sides of the interface or between the electrodes. The origin of such a potential difference can be electrode offset potential or an unequal local distribution of charges on the skin surface generated, for example, by static electricity. When an impedance change takes place at the electrode-skin interface, the potential differences drive a current over the electrode-skin-tissue-skin-electrode circuit, or parts of it, and a shift in voltage is measured by the differential amplifier. Due to the transient form of the current and the high-pass property of the ECG amplifier, the baseline returns to normal after some time. Once the skin impedance becomes lower due to sweat gland activity, baseline shifts are no longer generated. Besides eliminating these impedance changes, the improved conductance puts an end to the unfavourable effects of static electricity, because the charges are rapidly equalized over the body surface and on the electrodes. When the sweat glands are filled with conducting sweat (sweat can be considered the equivalent of 0.3 % saline), many low-resistance parallel pathways result, thus significantly reducing the electrode-skin impedance and alleviating the problems (Malmivuo & Plonsey 1995). A further lowering of the impedance takes place due to hydration of the skin.

2.8.3.2. Non-periodic changes in RR intervals

Conventional mathematical analysis methods such as standard deviation, correlation and power spectrum analysis presuppose that the data are stationary in the wide sense. This means that in the case of HRV analysis the sinus rhythm of the heart can be approximated as stable. This approximation holds best over a short period and under steady-state conditions. In addition to the transient spikes mentioned earlier, non-periodic changes in the heart rhythm can impair the stationarity of the signal and have adverse effects on HRV indices. Non-periodic changes can be induced in a RR interval time series by normal responses of the heart to physical activity, emotional stimuli or reflexes of various kinds.

The question might arise as to whether it is permissible to correct an RR interval time series for abnormalities if their background is physiological. As discussed earlier, a correction procedure should be employed for ectopic beats, since they do not carry information on the sinus rhythm, but the need to correct for non-periodic changes in the sinus rhythm, e.g. by removing the changes in the HR trend, depends largely on the application and on the mathematical HRV indices

used. When day-to-day variation is to be studied in a single subject, for example, it is important to detrend the data series so that the statistics regarding frequently-occurring parameters can be compared. If conventional methods are used, the correction of non-periodic changes in heart rhythm should be preferred, since rough nonstationary sequences in the RR interval data can bias the results of the analysis. Detrending is usually applied to cut down on the effects of non-periodic low-frequency changes in RR intervals.

2.8.4. Limitations and effects of artifacts

In view of the non-periodic nature of the artifacts in RR interval time series, it is clear that spectral domain methods in general and time domain methods based on the calculation of standard deviations and mean values are sensitive to artifacts in the automatic measurement of RR intervals. Malik *et al.* (1993) have shown experimentally that pNN50 and indices based on the calculation of standard deviation are more sensitive to artifacts than the HRV index (the number of normal-to-normal intervals of modal duration) or TI NN (triangular interpolation of the normal-to-normal histogram). A comparison of methods for the removal of ectopy is presented by Lippman *et al.* (1994).

Mulder (1992) describes the effect of artifacts in considerable breadth, placing emphasis on spectral methods. The impulse-like deviation in RR interval time series caused by errors in QRS detection, both missed R waves and additional triggers, and also interposed ectopic beats have a similar effect on the power spectrum in that power is increased at all frequencies. The effect of a phase-shifted ectopic beat is similar in form but smaller in amplitude. As the number of corrupted beats (not consecutive) increases, the total spectral variability grows linearly, while in the case of more consecutive artifacts, e.g. intervals of twice the normal length the Fourier transform of an artifact complex is no longer flat but follows the form of a sinc-function, adding more power to the lower frequencies. As can be observed in Figure 2.1, the effect of compensated ectopic beats is markedly different, i.e. their contribution is large at higher frequencies and small at lower frequencies.

Responses of the heart to physical activity or emotional stimuli clearly affect the mean values, standard deviation and low frequencies of the RR spectrum (see Figure 2.2). Detrending is usually used to remove low frequency baseline shifts by subtracting a fitted polynomial. Another method, based on the ratio between the peak power and bandwidth of the LF range in the power spectrum, is described by Sapoznikov *et al.* (1994). A wavelet filtering approach is used to remove very slowly oscillating components from RR interval data (Wiklund *et al.* 1997). In long term measurements, stationarity can be achieved better if the data are first divided into shorter segments which are analyzed one by one and then averaged. When using Fourier transform-based approaches, however, compromises must be made between the requirements of stationarity and good frequency resolution, since the frequency resolution of the FFT algorithm is better if longer segments are analyzed at a time.

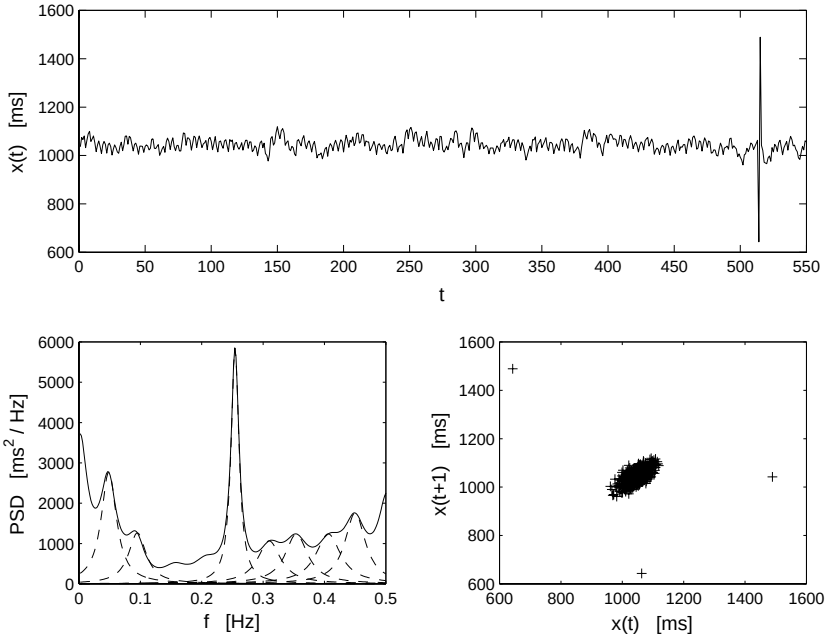

Fig. 2.1. **RR time series obtained from a healthy young subject when asleep (top). The ECG signal includes a compensated ectopic beat, producing the sequence *normal-short-long-normal* in the RR intervals. Power spectrum estimated by the modified covariance method with a model of order 20 (bottom left). The estimate include the sum spectrum (solid line) and the spectra of the separate components (dashed lines). First-order difference plot of the RR intervals (bottom right).**

2.8.5. Correction of abnormal RR intervals

The decision as to whether a deviating interval should be corrected or not usually forms the most difficult step in the removal of abnormal intervals. A segment of an RR interval time series is accepted for further analysis if the number of qualified intervals exceeds a preset acceptance percentage which varies widely according to the application and the patient group, a typical figure being around 95 % as in Mulder (1992) and Pitzalis *et al.* (1996). There are no specific recommendations in the literature as to the maximum number of artifacts one can interpolate or accept.

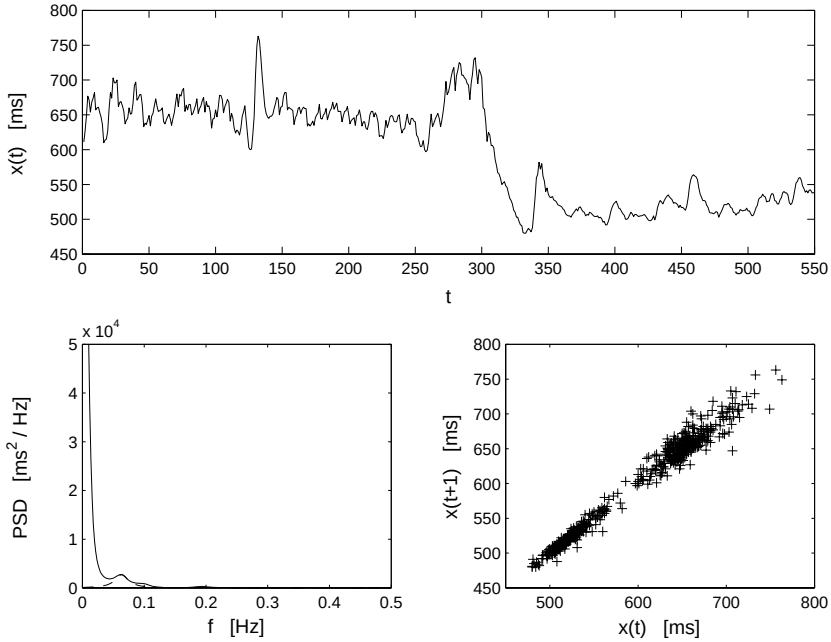

Fig. 2.2. **RR time series obtained from a healthy young subject, including an abrupt change in RR intervals due to physical activity (top). Power spectrum estimated by the modified covariance method with a model of order 20 (bottom left). First-order difference plot of the RR intervals (bottom right).**

2.8.5.1. Detection of artifacts

Error detection algorithms attempt to distinguish normal intervals from abnormal ones. The optimum would be for the algorithm to adapt to the data and derive the error detection criteria from the distribution indices of the normal-to-normal intervals. An algorithm which automatically identifies artifacts and corrects them in a RR interval time series is presented by Berntson *et al.* (1990). It can be noticed from the literature, however, that relatively simple detection criteria supported by additional visual verification are still being used in computerized artifact detection in connection with HRV measurement. This is explained by the fact that results obtained with simple procedures are not distinctively poorer than those arising from more complex solutions (Mulder 1992). As the normal intra-subject and inter-subject variability in heart rhythm is large, automatic adjustment of the criteria can be difficult. Short and sudden surges are usually treated successfully by most methods, but the decision on whether deviating intervals resulting from non-periodic physiological fluctuations should be corrected is more problematic. So far, researchers have wanted to solve the most critical questions during the visual verification after computerized detection.

The simple artifact detection criteria described in the literature include absolute upper and lower limits for acceptable intervals (e.g. 300 - 1500 ms), absolute or relative differences from the previous RR interval (e.g. 20 - 40 %), from the following RR interval, from the previous accepted interval, from the mean, from the mean updated by previously accepted intervals or from a fitted polynomial representing the baseline. Malik *et al.* (1989b) used four simple detection criteria and found none of them to be significantly better than the others. As a single detection criterion always has its particular weaknesses, a combination of criteria should be preferred (Sapoznikov *et al.* 1992).

2.8.5.2. Correction of artifacts

There are two basic methods for removing individual artifacts from an analysis: total exclusion of abnormal intervals or substitution of a better matching value. The exclusion approach is widely used, suits well for time domain analysis, and can also be used with frequency domain analysis if only a few beats are to be excluded, where as the substitution approach is used relative widely with both time domain and frequency domain analysis. The substitution can take the form of simply replacing the abnormal value with a local mean or median value, but more sophisticated procedures include linear, non-linear or cubic spline interpolation methods or more complicated predictive modelling (Lippman *et al.* 1994).

The substitution approach can be used with good justification in a physiogical sense if the artifact is known to be of technical origin, while if it is due to a physiological or mental factor, both approaches can be used with success. The comparison, by Lippman *et al.* (1994), of methods for removing ectopy from 5-minute RR sequences showed that the simple deletion method and the more complex non-linear predictive interpolation method gave the best results. In general, the removal of abnormal intervals tends to increase the low frequency component of the spectrum and reduce the standard deviation, but it should be noted that the sum of the intervals after correction does not always equal the sum of the original intervals. A correction procedure, presented by Mulder (1992), attempts to retain the total time, and this approach can be successful if the sinus rhythm is not disturbed during a period of disturbances; however, short intervals connected with phase-shifted extra systoles can make it impossible to preserve the sum of the intervals.

3. Analysis of signal variability

3.1. Interpolation of the ECG signal

In paper II, the ECG was interpolated in order to increase the sampling rate of the measured signal. That is important because of the relatively low sampling rate (often 128 Hz) of the ambulatory ECG. The objective is to increase sampling rate to obtain, for example, a more accurate measurement of the end of the T wave. Speranza *et al.* (1993) utilized this technique in order to gain an improved resolution of the RT interval variability measurement. They checked the performance of the technique and showed that the interpolation caused a distortion in the QRS complex, but did not affect the T wave. The difference was less than 3 % of the peak-to-peak amplitude of the original signal, when the ECG was sampled at 250 Hz and interpolated to 1 kHz, and was comparable to the signal digitized at 1 kHz (Speranza *et al.* 1993).

Interpolation is the process of increasing sampling rate by an integer factor M, that is, upsampling by M. First, the time base of the signal is changed so that $M-1$ zero valued samples are placed between each sample pair of the original signal $x(t)$ $(t = 1, 2, \ldots, N)$. This new sequence is defined by

$$\nu(t) = \begin{cases} x(\frac{t}{M}), & t = 0, \pm M, \pm 2M, \ldots \\ 0, & \text{otherwise} \end{cases} . \tag{3.1}$$

For instance, when having a signal sampled at 128 Hz and interpolating it to 1024 Hz sampling rate (interpolation by factor 8), 7 zeros are placed between each sample pair. Thus, the time interval between each sample pair changes from 7.81 ms to 0.98 ms.

A symmetric, linear phase, FIR digital filter was used. This filter resamples data at a higher rate using low-pass interpolation. This allows the original data $x(t)$ to pass through the filter unchanged and interpolates $M-1$ values between data samples such that the mean square error between them and their ideal values is minimized (Oetken *et al.* 1979). The length of the designed filter is $2ML+1$, where M is an integer factor used to increase sampling rate and L is an integer factor determining the degree of the filter. The cutoff frequency α was given in

radians ($0 < \alpha \leq 1.0$), so that the input data is assumed to be band-limited with the frequency $\alpha\pi/M$.

The increase in sampling-rate obtained by the addition of $M-1$ zeros between successive values of $x(t)$ results in a signal $y(t)$ whose spectrum $Y(\omega_y)$ is a M-fold periodic repetition of the input signal spectrum $X(\omega_x)$ (Proakis *et al.* 1992). Since only the frequency components of $x(t)$ in the range $0 \leq \omega_y \leq \pi M$ are unique, the images of $X(\omega)$ above $\omega_y = \pi/M$ should be rejected by passing the sequence $\nu(t)$ through a lowpass filter. The frequency response of the filter can be ideally given as

$$H_M(\omega_y) = \begin{cases} C, & 0 \leq |\omega_y| \leq \pi/M \\ 0, & \text{otherwise} \end{cases} , \tag{3.2}$$

where C is a factor required to normalize the sequence $y(t)$.

3.2. Time domain analysis

Time domain analysis of RR interval time series covers histogram and scattergram analysis, and the calculation of several common statistical indices. In many studies, these indices are compared with frequency domain parameters, and the correlations between these parameters are also calculated.

When dealing with the interpretation of parameters such as histograms, it should be pointed out that they do not in general contain any information on periodic fluctuations in RR intervals. Respiration frequency, for example, cannot be observed on the basis of these parameters, nor can the variance related to a specific frequency band (i.e. spectral component) be measured by these indices if RR intervals without any band-pass filtering are concidered. Time domain indices tend instead to rather measure the average variability in time series or maximum amplitude of the variability, depending on the nature of the index considered. See Kleiger *et al.* (1992) and references therein, for a more detailed discussion on the use of time domain parameters.

3.2.1. Time domain indices

There are several statistical indices which have been used to describe heart rate variability, e.g. average, median, deviation between maximum and minimum values (range), standard deviation (SD) and root mean square of successive differences (RMSSD). The formulation of these is well known and they do not require complex calculations.

The statistical properties of a time series $x(t)$ are often described using basic indices such as the mean $\overline{x}$ and standard deviation s_x, which can be obtained from

the given data as follows:

$$\overline{x} = \sum_{t=1}^{N} x(t)/N \quad , \qquad s_x = \sqrt{\sum_{t=1}^{N} (x(t) - \overline{x})^2/N} \quad . \tag{3.3}$$

The variance is the square of the standard deviation, $\mathrm{var}(x(t)) = s_x^2$. The coefficient of variation and the range, i.e. the deviation between the maximum and minimum values in a time series, are formulated as

$$\mathrm{CV}_x = 100 \cdot s_x/\overline{x} \quad , \tag{3.4}$$

$$d_x = \max_t(x(t)) - \min_t(x(t)) \quad . \tag{3.5}$$

The mean square of successive differences (RMSSD) is calculated for the purposes of HRV analysis by

$$\mathrm{RMSSD}_x = \sqrt{\sum_{t=1}^{N-1} (x(t) - x(t+1))^2/N} \quad . \tag{3.6}$$

Certain "modified" indices also exist, such as "the percentage of difference between adjacent normal RR intervals greater than 50 ms computed over the entire 24 hour ECG recording" (pNN50) or "the mean of the standard deviations of all normal RR intervals for all 5 minutes segments of a 24 hour ECG recording" (SDNNIDX) (Stein *et al.* 1994, Öri *et al.* 1992).

3.2.2. Analysis of distribution

The distribution of RR intervals can be analysed in terms of a histogram of the time series (Baselli & Cerutti 1985, Hoopen & Bongaarts 1969), in which the "frequencies" in the histogram bins may be expressed in absolute numbers or as relative "frequencies" of the time series values. The histogram has also been presented either by drawing a line between the bins or by giving the portions of the time series values numerically (Baevskij *et al.* 1984).

A few parameters generated for the analysis of RR interval histograms are introduced in Baevskij *et al.* (1984). The bin having the largest "frequency" is termed the mode of histogram and the "amplitude" of this mode has also been observed. The width of the histogram base, i.e. the maximal deviation in time series values, has been proposed as another basic measure of RR interval variability. Several parameters may be constructed from these three elementary measures.

Casolo *et al.* (1989) used the width of the histogram base as a measure of total variability, and defined the width at levels of 10% and 50% of the maximum height of the histogram. Odemuyiwa *et al.* (1991) approximated the shape of the histogram as a triangle in order to reduce the effect of less marked variabilities.

The results produced by the histogram naturally depend on the bin width used. If a large bin width is chosen, the histogram will be vague in shape, while a small

bin width will accentuate unimportant details. It is worth noting that the bin width of a histogram should remain constant in order to allow rational comparison of the absolute results. A simple estimate for bin width is given by Scott (1979)

$$h_N = 3.49 \cdot \frac{s_x}{N^3} \quad , \tag{3.7}$$

where s_x is the standard deviation of N time series values. The estimate takes the variability in time series into account by using the standard deviation. This expression can be used successfully with approximately Gaussian data (Scott 1979). In practice, the bin width can be selected to be near the estimate h_N. The estimation of frequency distributions has been studied in Willard & Connelly (1992), where different non-parametric methods using both simulated and real data are compared and improvements to the histogram are proposed.

3.3. Frequency domain analysis

3.3.1. Interpretation of spectral estimates

Spectral estimates can be studied by integrating over a given frequency band or by decomposing the spectrum into components. The first approach can be performed with Fourier and autoregressive (AR) techniques, but the latter is possible only with AR techniques.

One problem affecting integration of the spectrum is definition of the frequency bands. Doing this signal by signal would be quite a laborious task, because it would mean checking all the estimates manually. Frequency ranges can be defined by an experimental procedure or obtained from the literature and kept constant, but problems will arise when the locations of components vary between signals. The definition of frequency ranges has been studied experimentally by Jaffe *et al.* (1993), where the aim is to optimize the ranges to some extent.

Use of the spectrum decomposition procedure gives estimates for the component spectrum and powers. In addition, the central frequencies as well as the power estimates can be utilized to search for the appropriate components. Use of the maximum of component spectrum and the band width of the component to detect periodic fluctuations is discussed in Sapoznikov *et al.* (1994). The mean, median and central frequency has been used to obtain the characteristic frequency of a specific band in Korhonen (1997). Several definitions exist for the frequencies of the components in a RR interval time series spectrum, as summarized in the following short description:

- The *very low frequency* (VLF) component is found at frequencies $f < 0.04$ Hz (Kamath & Fallen 1993). These fluctuations in RR intervals are due to thermoregulation mechanisms (VanRavenswaaij-Arts *et al.* 1993). Some low frequency trends or nonstationarities may also exist, which can be observed in the form of increased power at low frequencies in the spectrum.

- The *low frequency* (LF) component is usually observed around $f = 0.1$ Hz. This is mainly due to the systems regulating blood pressure (Kamath & Fallen 1993, Kitney *et al.* 1985) and reflects the autonomic sympathetic tone in heart rate regulation (Malliani *et al.* 1991, Pagani *et al.* 1986), although it has also been suggested that parasympathetic regulation plays some role in it (Akselrod *et al.* 1985, Pomeranz *et al.* 1985).

- The *high frequency* (HF) component will be often found in the frequency band $0.15 < f < 0.40$ Hz, which is related to the frequency of respiration (e.g. cycle length T = 4 *s*, $f = 0.25$ Hz) (Baselli *et al.* 1987, Kitney *et al.* 1985) and is often called *respiratory sinus arrhythmia (RSA)*. The amplitude and frequency of this component are closely related to the respiration volume and frequency (Novak & Novak 1993, Novak *et al.* 1993). The HF component has been considered a measure of parasympathetic neural regulation of heart rate (Katona & Jih 1975, Pagani *et al.* 1986, Pomeranz *et al.* 1985).

Sometimes an *ultra low frequency* (ULF) component is defined with a frequency band of $f < 0.0033$ Hz (Kamath & Fallen 1993). The balance between sympathetic and parasympathetic neural regulation is often measured by the ratio of the power estimates for the LF and HF components (LF/HF ratio) (Malliani *et al.* 1991, Pagani *et al.* 1986). An RR time series for a healthy young subject is shown in Figure 3.1, together with a spectrum estimated using an AR model, showing the components of spontaneous RR fluctuation described above and a pole diagram representing the locations of the poles of the parametric model on the complex z-plane. In this example, the model order was selected by visually examining the spectrum when the order 16 gave a reasonable result. The power spectrum estimate represent the sum spectrum (solid line) and the spectra of the separate components related to respective pole pairs (dashed lines).

3.3.2. On the use of spectral analysis

The use of frequency domain analysis in different clinical circumstances has been extensively reviewed in Rienzo *et al.* (1993), Malliani *et al.* (1991), Kamath & Fallen (1993) and Öri *et al.* (1992). Spectral analysis has been often performed for RR interval time series including 256 or 512 values, the recording lasting several minutes depending on the heart rate. Analyses of this kind can provide information on *short term* fluctuations in RR intervals.

Short term fluctuations and their changes over several hours can be studied with ambulatory recordings (24 hour Holter recordings), a long recording being segmented into shorter RR interval time series of 512 values, as for instance described in Cerutti *et al.* (1989) and Furlan *et al.* (1990). Such a short time series can be assumed to conform better with the stationarity requirement for the relevant spectrum estimation. Circadian variation in spectral parameters has been studied in Guzzetti *et al.* (1991) and Huikuri *et al.* (1992), and long term RR interval recordings in Bianchi *et al.* (1993), Rienzo *et al.* (1989), Malik *et al.* (1989a)

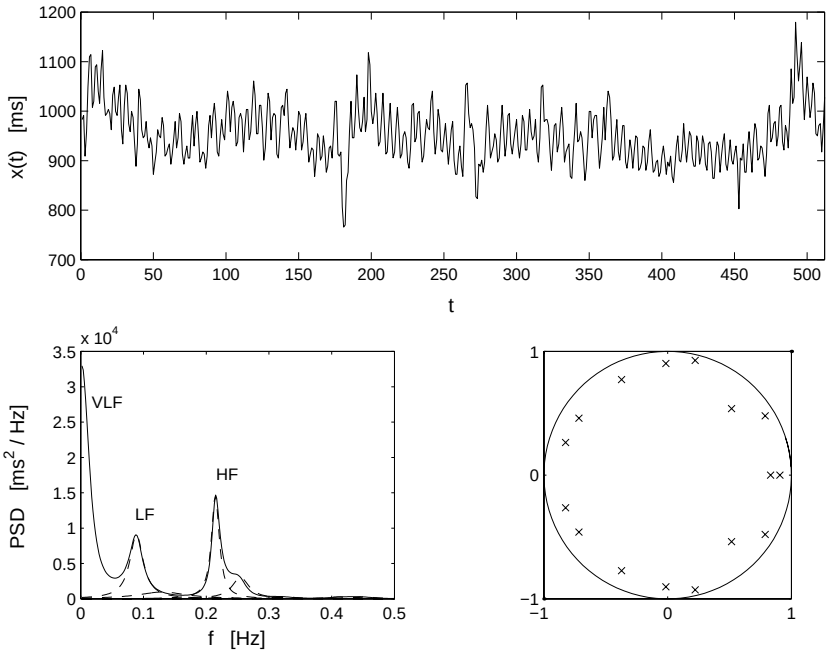

Fig. 3.1. **RR time series obtained from a healthy young subject under resting conditions (top). Power spectrum estimated by the modified covariance method with a model of order 16 (bottom left). The corresponding pole diagram (bottom right).**

and Saul *et al.* (1987).

Long term variation in autonomic neural regulation has been studied using the VLF and ULF components mentioned above, and the spectrum has been calculated from the whole 24 hour recording. The spectrum has been reported to have the shape $1/f$ (Kobayashi & Musha 1982, Saul *et al.* 1987).

3.3.3. Mathematical background to spectral analysis

The RR interval time series includes information of wide origin and its nature will hardly allow an assumption of wide sense stationarity in the strict statistical sense under any conditions. The RR intervals should rather be understood as being approximately stationary at most, whereupon the analysis would give relevant results in a medical sense. There may exist sections which can very well be assumed to be (almost) stationary, and also sections that are far from allowing such an assumption. It is often necessary to divide a recording into shorter

stationary sequences. Nonstationarities include transient phenomena and slowly varying changes (trends), the identification of which is more difficult. The theory of many approaches is nevertheless based on the assumption of signal stationarity. In this context a calculated spectrum for a RR interval time series, for example, is understood as a "model" for periodic fluctuations rather than as a "true" spectrum.

Let $x(t)$ be a stationary process defined at discrete values $t = 0, \pm 1, \pm 2, \ldots$. The autocovariance function will be written as (Priestley 1981)

$$r(k) = E\{(x(t) - \mu)(x(t+k) - \mu)\} \quad , \qquad k = 0, \pm 1, \pm 2, \ldots \tag{3.8}$$

and the autocorrelation function will then be $\rho(k) = r(k)/r(0)$. Here the mean value of the process $x(t)$ is defined, using the expectation operator $\mu = E\{x(t)\}$. For a wide-sense stationary process, the mean value is constant and the autocorrelation satisfies the property $\rho(n_1, n_2) = \rho(n_1 - n_2) = \rho(k)$.

Let us then assume that $x(t)$ is a zero mean stationary process. There must then exist an orthogonal process $Z(\omega)$ such that (Priestley 1981)

$$x(t) = \int_{-\pi}^{\pi} \exp(i\omega t)\, dZ(\omega) \tag{3.9}$$

and $E\{|dZ(\omega)|^2\} = dH(\omega)$, where $dH(\omega) = h(\omega)d\omega$, $-\pi \leq \omega \leq \pi$ and $\omega = 2\pi f$. This is called the *spectral presentation of a discrete stationary process.*
The autocovariance sequence is

$$r(k) = \int_{-\pi}^{\pi} \exp(i\omega k)\, h(\omega)\, d\omega \tag{3.10}$$

and the power spectral density is

$$h(\omega) = \frac{1}{2\pi} \sum_{k=-\infty}^{\infty} r(k) \exp(-i\omega k) \quad , \qquad -\pi \leq \omega \leq \pi \quad . \tag{3.11}$$

3.3.4. Spectrum estimation using a periodogram

Let us divide the N-point process $x(t)$ into K non-overlapping segments, each having M points. The Fourier transform of the p:th segment can be written as

$$X^p(\omega) = \sum_{t=1}^{M} x(t) \exp(-i\omega t) \quad , \qquad -\pi \leq \omega \leq \pi \quad . \tag{3.12}$$

The periodogram estimate of the spectral density function of a single data segment is given by

$$\hat{P}_x^p(\omega) = M^{-1} |X^p(\omega)|^2 \quad , \qquad p = 1, \ldots, K \quad . \tag{3.13}$$

If the periodograms of K segments are averaged, the estimate is called a Bartlett averaged periodogram. It should be noted here that the periodogram is only one way of estimating the spectrum of the process, and is by no means a "definition" of the spectrum.

Modifications of the averaged periodogram also exist, among which the Welch periodogram is introduced. In this method, data segments are allowed to overlap by 50% or 70%, for example, and each data segment will be weighted with a window function before calculating the periodogram. As a result, one has for the periodogram of each segment

$$\tilde{P}_x^p(\omega) = \frac{1}{MU} |\sum_{t=1}^{M} x(t)w(t) \exp(-i\omega t)|^2 \quad . \tag{3.14}$$

The factor $U = M^{-1} \sum_{t=1}^{M} w(t)^2$ is a normalization factor for the power in the window function $w(t)$. The Welch periodogram estimate will be then an average of these periodograms:

$$\hat{P}_x^w(\omega) = \frac{1}{L} \sum_{p=1}^{L} \tilde{P}_x^p(f) \quad . \tag{3.15}$$

The statistical properties of periodograms are discussed by Priestley (1981) and Kay (1988).

Sometimes one may need to approximate a periodogram more closely, which can be done by using the *zero padding* procedure (Kay 1988). This is performed by extending the data set with zeros, and taking the Fourier transform of the whole data set. This operation does not achieve any better resolution in the spectrum, however, although the frequency spacing will be denser. Zero padding actually interpolates the values of the measured spectrum at more frequencies, producing a smoother spectrum.

3.3.5. Parametric modelling of time series

Parametric modelling of time series has some advantages over non-parametric (Fourier) methods. Here only autoregressive (AR) models are examined and the focus is on spectral estimation, which has been the main object of interest in HRV analysis. There are many algorithms for obtaining estimates for AR parameters, e.g. methods based on estimation of the autocorrelation sequence (Yule-Walker), the Burg algorithm, and least squares linear prediction algorithms (including the modified covariance method) (Kay 1988, Marple 1987). There are also adaptive algorithms such as least mean square (LMS) and recursive least square (RLS), which update the parameter estimates as a new data sample becomes available (Marple 1987).

3.3.5.1. AR spectrum estimate

Estimation of the signal spectrum with AR models enables the frequencies of spectral components to be determined more exactly than by non-parametric estimation. The frequency estimates can be calculated after determining the poles of the parametric model. Tracking of the pole locations in the complex z-plane can be utilized when monitoring spectral changes in time series, for example. Furthermore, the powers of the spectral components and their balance can be estimated more accurately. Estimation of the AR spectrum does not need windowing of the time series as can be the case with the Fourier spectrum.

Let us define an autoregressive model for a stationary time series $x(t)$ as follows:

$$\sum_{k=0}^{p} a_k x(t-k) = e(t) \quad , \qquad a_0 \equiv 1 \quad , \tag{3.16}$$

where a_k are the model parameters to be estimated, $e(t)$ is the residual time series or error process, and p is the model order. The estimates for the model parameters, $\hat{a}_k$, can now be regarded as the "components" observed in the power spectrum estimate, which are to be fitted into the time series $x(t)$ in order to minimize the process $e(t)$ in some sense.

The power spectrum of the process $x(t)$ is given as $P_x(z) = H(z)H(1/z)P_e(z)$, which can be written

$$P_x(z) = \frac{\sigma_e^2}{A(z)A(1/z)} \quad , \tag{3.17}$$

where the Z transform of the above recursion is

$$H(z) = \frac{1}{1 + \sum_{k=1}^{p} a_k z^{-k}} = \frac{1}{A(z)} \tag{3.18}$$

and $P_e(z) = \sigma_e^2$ denotes the spectrum of the residual time series.

Let us estimate the power spectrum of $x(t)$. Assuming an AR process of order p, it can be written:

$$\hat{P}_{AR}(z) = \frac{\hat{\sigma}_e^2}{\prod_{k=1}^{P}(z - p_k)(z^{-1} - p_k^*)} \quad , \tag{3.19}$$

where $\hat{\sigma}_e^2$ is the estimated variance of $e(t)$, and p_k are the poles of the model. This can also be given by using the estimates $\hat{a}_k$ and denoting $z = \exp(i\omega)$:

$$\hat{P}_{AR}(\omega) = \frac{\hat{\sigma}_e^2}{|1 + \sum_{k=1}^{p} \hat{a}_k \exp(-i\omega k)|^2} \quad . \tag{3.20}$$

The spectrum of the single component can be estimated by the following expression:

$$\hat{P}_k(z) \approx \frac{c_k}{(z - p_k)(z^{-1} - p_k^*)} \quad , \tag{3.21}$$

assuming that $\omega \approx \omega_k$ and $z = \exp(i\omega)$. For the constant c_k can be written

$$c_k \approx \frac{\hat{\sigma}_e^2}{\prod_{j \neq k}(z - p_k)(z^{-1} - p_k^*)} \quad , \qquad z_k = \exp(i\omega_k) \quad . \tag{3.22}$$

Now the frequency ω_k is related to the pole p_k. It is assumed that a part of the estimate $\hat{P}_{AR}(z)$, c_k, will be constant when $\omega \approx \omega_k$. The AR spectrum estimate should follow the relation $\hat{P}_{AR}(z) \approx \sum_k \hat{P}_k(z)$, i.e. the spectrum is the sum of the spectrum estimates of the components.

3.3.5.2. Estimation of the powers related to components

It was defined, above, the spectrum estimate of a single component related to the pole p_k. It may sometimes also be useful to estimate the power associated with a component. In HRV analysis, powers are estimated in order to evaluate the strength and balance of autonomic regulation.

The power of a component observed at frequency ω_k can be estimated by utilizing the residue of the function analyzed (Johnsen & Andersen 1978, Marple 1987)

$$\hat{P}(\omega_k) = q\,\Re\{\operatorname*{Res}_{p_k}\{\frac{\hat{P}_{AR}(z)}{z}\}\} \quad , \tag{3.23}$$

where the residue of $\hat{P}_{AR}(z)/z$ is determined for the pole p_k. The operation $\Re\{\cdot\}$ denotes the real part of the function. The total power associated with the spectrum and the residues of the function are related as follows:

$$\frac{1}{2\pi j}\oint f(z)dz = \sum_{k=1}^{n} \operatorname*{Res}_{p_k} f(z) \quad . \tag{3.24}$$

Furthermore, the total power of the signal should be equal to the sum of the power estimates of the components, $P_{tot} \approx \sum_k \hat{P}(\omega_k)$. Finally, the estimated power of a single component is calculated by

$$\hat{P}(\omega_k) = q\,\Re\{\frac{(z - p_k)\hat{\sigma}_e^2}{z\hat{A}(z)\hat{A}(\frac{1}{z})}\} \quad , \tag{3.25}$$

where $z = p_k$ and $\hat{A}(z) = \prod_{k=1}^{P}(1 - p_k z^{-1})$. Now $q = 1$ for a real pole and $q = 2$ for a complex pole. $\hat{\sigma}_e^2$ is the estimate for the prediction error variance at the given model order.

In HRV analysis, the power estimates are sometimes presented in *normalized units* [n.u.] instead of *absolute units* [ms^2]. The power estimate in normalized units will be (Pagani *et al.* 1986)

$$\hat{P}(\omega_k)_{\text{n.u.}} = 100 \cdot \frac{\hat{P}(\omega_k)}{P_{tot} - \hat{P}_0} \quad , \tag{3.26}$$

where $\hat{P}_0$ represents the power estimate of very low fluctuations in a signal ($f <$ 0.03Hz) and P_{tot} the total power of the signal. It is obvious that $0 < \hat{P}(\omega_k)_{n.u.} \leq 100$.

3.3.5.3. Model order selection

It is essential to choose an appropriate model order, but the task can be a problematic one. The order of the AR model has a major effect on the spectral estimate for a time series. Too low an order will result in a smoothed spectrum, and too high an order will increase the resolution of the spectrum and may introduce spurious peaks. The estimate for the power associated with a single component is also dependent on the order that is selected. The orders $p = 15 - 20$ are often satisfactory with RR interval time series, giving a meaningful spectrum.

Minimization of the prediction error variance is alone not a sufficient method for model order selection in the case of AR models, since $\hat{\sigma}_e^2$ decreases as the order increases (Choi 1992), but this decrease should smooth out after a certain order, indicating that the optimum has been reached. The autocorrelation function of a residual time series can also be studied, and if the model order is correct the residuals should be uncorrelated. The locations of the poles in the complex z-plane should then be quite stable.

Several *penalty function methods* for model order selection exist that utilize the prediction error variance, e.g. FPE (final prediction error) and AIC (the Akaike information criterion) (Choi 1992). It is expected that these criteria may fail in real world time series. They provide a basis for model order selection, but the final decission has to be made by a subjective inspection. If one can assume that the properties of time series do not change significantly from one such series to another, one probably will not make a serious mistake by choosing a relatively high model order and keeping it constant.

3.3.6. Bispectrum estimation

A potential tool for future RR interval variability analysis may be the estimation of the bispectrum. The power spectrum is based on the second order statistics of the time series, but the bispectrum make use of third order statistics. By definition, a gaussian random process has a zero higher-order spectrum of order two (bispectrum) (Nikias & Petropulu 1993), which allows the study of the deviation from the gaussianity or to suppress gaussian noise. The method also contains information about the phase character of the signal, which is failed with the methods based on the second order statistics. Moreover, the bispectrum estimation can be used in detection and characterization of the nonlinearities by analysis of quadratic phase coupling in the frequency domain. A preliminary study on quadratic phase locking in HRV can be found in Calcagnini *et al.* (1996).

3.4. Time frequency analysis

3.4.1. Time frequency representations

There may be a need for monitoring the spectral properties of the signal as time elapses, especially, when "long" time periods are under consideration. The temporal location of the spectral components may give more information than one single spectrum. The short-time Fourier transform (STFT) is a linear Time Frequency Representation (TFR) used to present changes in the signal that vary with time. The Fourier transform does not explicitly show the time location of the frequency components, but some form of time location can be obtained by using a suitable pre-windowing window (Hlawatsch & Boudreaux-Bartels 1992). The STFT can be defined for $x(t)$ as

$$S_x^g(t,\omega) = \int x(s)\, g^*(s-t) \exp(-i\omega s)\, ds \quad . \tag{3.27}$$

$S_x^g(t,\omega)$ is a local spectrum of the signal $x(s)$ around the analysis time s, because multiplying by the short window $g^*(s-t)$ suppresses the signal outside the neighbourhood around the time $s = t$. The properties of the window $g^*(s)$ also have an effect on the calculated STFT (Hlawatsch & Boudreaux-Bartels 1992, Rioul & Vetterli 1991).

The time-frequency resolution of the STFT is limited by the time-frequency product, i.e. having a small time resolution means poor frequency resolution, or vice versa. The resolution is also constant as a function of the frequency, which is due to the window chosen for the STFT (Rioul & Vetterli 1991).

As an example of quadratic TFRs, the Wigner distribution (WD) is given:

$$W_x(t,\omega) = \int x(t+v)\, x^*(t-v) \exp(-i\omega\tau)\, d\tau \quad , \qquad v = \tau/2 \quad . \tag{3.28}$$

Detailed reviews of several types of time frequency representation and their application can be found in Cohen (1989), Hlawatsch & Boudreaux-Bartels (1992) and Loughlin (1996), for instance.

3.4.2. Time-variant spectral analysis

Techniques have recently been developed and demonstrated that allow the tracking of spectral parameters as time elapses. Approaches of this type have also been called time-variant spectral analysis or time-frequency analysis. For a detailed description of the algorithms and methodologies proposed and for some experimental studies, see references Basano *et al.* (1995), Bianchi *et al.* (1993), Cerutti *et al.* (1989), Keselbrener & Akselrod (1996), Lee & Nehorai (1992), Mainardi *et al.* (1994, 1995), Novak & Novak (1993) and Novak *et al.* (1993). The advantages of these methodologies are associated mainly with reducing the influence of

nonstationarities and monitoring transient cardiac events occuring in long-term recordings.

In Cerutti *et al.* (1989), a procedure of compressed spectral arrays (CSA) was implemented which can reduce the spectral data obtained from 24 hour ambulatory ECG recordings. The method was based on the calculation of AR spectral estimates for successive RR interval segments, and checking whether a new spectrum differs significantly from the preceding one.

Time-variant spectral analysis was introduced into HRV analysis by Lee & Nehorai (1992), and particularly for the analysis of 24 hour ambulatory recordings by Bianchi *et al.* (1993). Here the AR parameters are estimated by the recursive least square (RLS) approach, and the time-variant power spectrum is given as

$$\hat{P}_{AR}(\omega, t) = \frac{\hat{\sigma}_e^2(t)}{\hat{A}(z,t)\hat{A}(z^{-1},t)} \quad , \qquad z = \exp(i\omega) \quad , \tag{3.29}$$

with $\hat{A}(z,t) = 1 + \sum_{k=1}^{p} \hat{a}_k(t) z^{-k}$ and t denoting the time index.

Mainardi *et al.* (1994) introduced two algorithms for recursive tracking of the pole displacements of an estimated AR model. The procedure was formulated and tested in more detail in Mainardi *et al.* (1995). The algorithms were based on the classical linearization approach and recursive calculation of the roots of a polynomial (Bairstow method).

The discrete Wigner distribution (DWD) was applied to heart rate variability analysis in Novak & Novak (1993), and a modified algorithm was proposed for auto- and cross-DWD. The cross-terms were suppressed by means of a smoothing data window and a Gauss frequency window (Novak & Novak 1993). This approach has been employed further in a study of the influence of respiration on heart rate (Novak *et al.* 1993), showing its ability to estimate spectral changes in nonstationary RR interval time series.

Keselbrener & Akselrod (1996) proposed a selective discrete Fourier transform algorithm (SDA) for time-frequency presentation of cardiovascular time series. This approach is very close to the STFT, and involves calculating the spectra with short time windows, but SDA utilizes a shorter window for high frequencies in the spectrum and a wider window for low frequencies.

Fourier transform-, autoregressive and time-frequency representation (TFR)-based power spectral estimators applied to nonstationary time series are compared in Pola *et al.* (1996), the results of which show that TFRs such as SPWD (smoothed pseudo Wigner distribution) and RWED (running windowed exponential distribution) should be utilized when good time resolution or the preservation of instantaneous power is essential. RWED has proved to be efficient in reducing the cross-term amplitudes, but SPWD is more capable of evaluating the mean power in the time-frequency plane. It can also be concluded that one problem entailed in the classical estimators is the dependence of the time resolution on the observation window, which often means a poor time resolution for the oscillations observed in cardiovascular time series.

On the whole, increased interest is being shown in time-variant spectral analysis or the monitoring of spectral parameters as a function of time. These techniques seem to offer approaches for overcoming the requirement for signal stationarity.

3.5. Wavelet analysis

The wavelet transform (WT) is a fairly new approach in the field of biomedical time series analysis, and only a few published articles exist on its use in HRV analysis, although it seems to possess some obvious advantages over classical time-frequency analysis methods, see Akay *et al.* (1993) and Tsuji & Mori (1994). The motivation for applying the wavelet transform to the analysis of ECG signal and RR interval time series lies mainly in the monitoring of nonstationary signals and the long-term evolution of the power spectrum.

General and also more detailed theoretical discussions on the wavelet transform and its applications to biomedical signal processing can be found in references Akay (1995), Clouet *et al.* (1995), Cohen & Kovacević (1996), Hess-Nielsen & Wickerhauser (1996), Karrakchou *et al.* (1996), Rioul & Vetterli (1991), Thakor & Sherman (1995) and Unser & Aldroubi (1996). WT as a tool in the time-dependent spectral analysis approach to stochastic processes has been discussed by Priestley (1996), especially the term "frequency" in connection with nonstationary time series.

3.5.1. Continuous wavelet transform

As a starting point, the continuous wavelet transform (CWT) is introduced and then extended to the theory of discrete (multiresolution) wavelet and wavelet packet transform, which are used to decompose the signal. CWT is defined for a signal $x(t)$ by (Daubechies 1992)

$$\mathcal{W}x(a,b) = \int_{-\infty}^{+\infty} x(t)\psi_{a,b}(t)\ dt \quad , \tag{3.30}$$

where a and b is the scaling and translation factor. Different versions of wavelet functions $\psi_{a,b}(t)$ are obtained from the basic wavelet by

$$\psi_{a,b}(t) = |a|^{-\frac{1}{2}}\psi(\frac{t-b}{a}) \quad , \tag{3.31}$$

where a and b are real numbers ($a \neq 0$). The wavelet function $\psi_{a,b}(t)$ has a constant norm in the space $L^2(\mathbb{R})$ of square integrable functions due to the normalizing factor $|a|^{-\frac{1}{2}}$. The continuous wavelet transform is invertible with (Cohen & Kovacević 1996)

$$x(t) = \frac{1}{C_\psi}\int_{-\infty}^{+\infty}\int_{-\infty}^{+\infty} \mathcal{W}x(a,b)\psi_{a,b}(t)\ \frac{da\ db}{a^2} \tag{3.32}$$

if the wavelet function satisfies the admissibility condition

$$C_\psi = \int_{-\infty}^{+\infty} \frac{|\hat{\psi}(\omega)|^2}{|\omega|}\ d\omega < +\infty \quad ,$$

where $\hat{\psi}(\omega)$ is the Fourier transform of the wavelet function $\psi_{a,b}(t)$. The constant C_ψ is finite only if $\hat{\psi}(0) = 0$ or equivalently

$$\int_{-\infty}^{+\infty} \psi(t)\ dt = 0 \quad .$$

To ensure that the wavelet function decays quickly to zero and is thus well localized in the time domain, the following relation should be fulfilled (Daubechies 1992)

$$\int_{-\infty}^{+\infty} (1 + |t|^\alpha)|\psi(t)|\ dt < +\infty \quad , \qquad \alpha > 0 \quad , \tag{3.33}$$

which is a subtly stronger condition than integrability of the function $\psi_{a,b}(t)$. This also satisfies the admissibility condition as $|\hat{\psi}(\omega)| \leq B|\omega|^\beta$ with $\beta = \min(\alpha, 1)$, B being a constant.

By analogy with the Fourier transform, which uses a complex exponential $\exp(i\omega t)$ as its basis function, the wavelet transform utilises the function $\psi_{a,b}(t)$ to represent a signal as a linear superposition of basis functions. The physical term frequency ω is related to complex exponential functions and does not have a direct interpretation when other functions such as wavelets are being considered (Priestley 1996). One can observe from the above formulation that wavelets are indexed with the parameters a and b instead of the variable ω. Actually, wavelet functions are located in time by the parameter b, while a denotes to the width of the wavelet. This leads to the interpretation that the wavelet transform can describe local properties of a time series $x(t)$ in the neighbourhood of each time point rather than global ones as the standard Fourier transform do.

It was shown earlier that the short time Fourier transform $S_x^g(t, \omega)$ is a function of the variables t and ω that has a certain location in time. The width of the window $g(t)$ was constant for all ω, so that all frequencies were evaluated with the same resolution. In the case of wavelet transform, a large value of the scaling factor a stretches the basic wavelet function and allows the analysis of low-frequency components of the signal. The small value of a gives a contracted version of the basic wavelet, and then allows the analysis of high-frequency components, respectively. In other words, the wavelet transform uses a short time interval for evaluating higher frequencies and a long time interval for low frequencies, high frequency components of short duration can be observed successfully. The properties naturally depend strongly on each wavelet function.

The frequency resolution of the wavelet transform is poor at high frequencies and good at low frequencies, which means that the time resolution at high frequencies will be good and that at low frequencies will be poor (Priestley 1996). The time-frequency resolution even in this case cannot be arbitrarily good, but is thus limited by the rules analogous to the well known Heisenberg's uncertainty principle.

Priestley (1996) derived an expression for the time-dependent spectrum of a stochastic process:

$$E\{|a_{m,n}|^2\} \sim 2\pi h_t(\omega_m) \quad , \qquad t = n/2^m, \quad \omega_m = 2\pi 2^m \quad , \tag{3.34}$$

which allows the squared modulus of wavelet coefficients to be interpreted as a time-dependent spectrum. It is assumed here that the mother wavelet has a complex form $\psi(t) = \exp(2\pi i t)$, and its squared Fourier transform $|\hat{\psi}_m(\omega)|^2$ is suitably concentrated around $\omega = \omega_m$. Although the term frequency should be understood with care and in a somewhat heuristic sense, time-frequency analysis is probably one of the most powerful features of the wavelet approach in this context.

3.5.2. Discrete wavelet transform

By choosing fixed values $a = a_0^m$ and $b = nb_0a_0^m$, $m, n = 0, \pm1, \pm2, \ldots$, we get for the discrete wavelet transform (DWT) (Daubechies 1992):

$$\begin{aligned} \mathcal{W}x(m,n) &= \langle x(t), \psi_{m,n}(t)\rangle \\ &= \int_{-\infty}^{+\infty} x(t)\psi_{m,n}(t)\ dt = a_0^{-m/2}\int_{-\infty}^{+\infty} x(t)\psi(a_0^{-m}t - nb_0)\ dt \quad . \end{aligned}$$

Values $a_0 = 2$ and $b_0 = 1$ construct discrete wavelets $\psi_{m,n}(t) = 2^{-m/2}\psi(2^{-m}t - n)$ used in multiresolution analysis constituting an orthonormal basis for $L^2(\mathbb{R})$.

To obtain a complete characterization of $x(t)$ using discretized wavelets $\psi_{m,n}(t)$, and further, to recover $x(t)$ from the discrete transform in a numerically stable manner, wavelet function should constitute a frame. The transform between the signal and the wavelet function should be bounded above and below:

$$A\ ||x(t)||^2 \leq \sum_{m,n} |\langle x(t), \psi_{m,n}(t)\rangle|^2 \leq B\ ||x(t)||^2 \tag{3.35}$$

with $A > 0$, $B < \infty$. If frame bounds A and B are equal, then the frame is called tight.

3.5.3. Multiresolution wavelet analysis

In multiresolution analysis successive approximation subspaces V_j fulfill the property $V_j \subset V_{j+1}$ with

$$\overline{\cup_{j=-\infty}^{+\infty} V_j} = L^2(\mathbb{R}) \quad \text{and} \quad \cap_{j=-\infty}^{+\infty} V_j = 0 \quad .$$

The multiresolution feature follows from the condition that all the spaces are scaled versions of the central space V_0:

$$x(t) \in V_j \Longleftrightarrow x(2^j \cdot) \in V_0 \quad .$$

The space V_0 has to be also invariant under integer translation:

$$x(t) \in V_0 \Rightarrow x(\cdot - n) \in V_0$$

for all $n \in \mathbb{Z}$. A scaling function $\phi_{m,n}(t) \in V_0$ is also required which is an orthonormal basis in V_0, where $\phi_{m,n}(t) = 2^{-m/2}\phi(2^{-m}t - n)$. Under these assumptions, the multiresolution scheme involves an orthonormal wavelet basis of $L^2(\mathbb{R})$, $\psi_{m,n}(t) = 2^{-m/2}\psi(2^{-m}t - n)$, so that

$$P_{m-1}x(t) = P_m x(t) + \sum_{n=-\infty}^{+\infty} \langle x(t), \psi_{m,n}(t)\rangle \psi_{m,n}(t) \quad ,$$

where P_m is the orthogonal projection onto space V_m. The signal $x(t)$ is consequently obtained by

$$x(t) = \sum_{m,n=-\infty}^{+\infty} \langle x(t), \psi_{m,n}(t)\rangle \psi_{m,n}(t) \quad .$$

The decomposition of the signal $x(t)$ using discrete analysis wavelet functions $\psi_{j,k}(t)$ and discrete scaling functions $\phi_{K,k}(t)$ can be given on different scales as follows:

$$x(t) = \sum_{j=1}^{K} \sum_{k=-\infty}^{\infty} d_j(k)\psi_{j,k}(t) + \sum_{k=-\infty}^{\infty} a_K(k)\phi_{K,k}(t) \quad ,$$

where $d_j(k)$ are the wavelet coefficients (detailed signals) at scale 2^j and $a_K(k)$ is the scaling coefficients (approximated signal) at scale 2^K. In Figure 3.2, the idea of discrete wavelet analysis is presented by means of a wavelet decomposition tree. A decomposition onto dyadic scales associates the frequency content of the signal and scales as

$$2^{-j}\,\pi \leq \Delta\omega_j \leq 2^{1-j}\,\pi$$

for $j = 1, 2, \ldots$. The signal spectrum includes the range $0 - \pi$ rad and $\Delta\omega_j$ is the frequency band corresbonding the level j.

3.5.4. Subband filtering

Multiresolution analysis comprises a hierarchical and fast scheme to compute the wavelet coefficients of an analyzed signal. The scheme involves the computation of sequentially coarser approximations of $x(t)$ and the difference in signals between two consecutive levels. In the subband filtering approach the computation consists of the analysis and the synthesis steps which correspond to the decomposition and the reconstruction stages in wavelet analyses (Strang & Nguyen 1996). The discrete wavelet transform can be implemented by the scaling (lowpass) and wavelet (highpass) filters

$$h(n) = \frac{1}{\sqrt{2}} \langle \phi(t), \phi(2t - n)\rangle \tag{3.36}$$

and

$$g(n) = \frac{1}{\sqrt{2}} \langle \psi(t), \phi(2t - n)\rangle = (-1)^n h(1 - n) \tag{3.37}$$

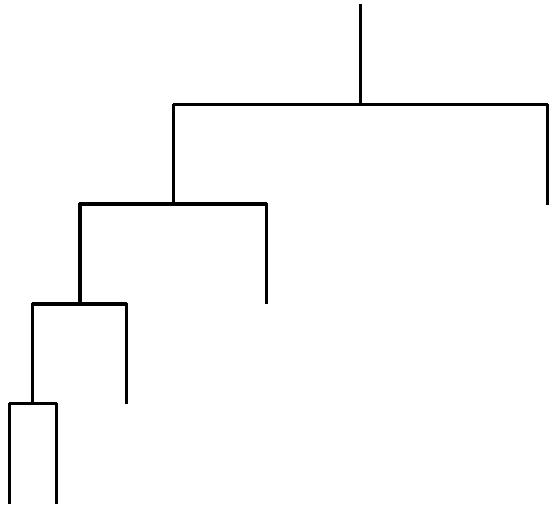

Fig. 3.2. **A wavelet signal decomposition presented by a tree structure.**

being quadrature mirror filters (QMF) (Daubechies 1992). The estimation of the detail signal at level j will be done by convolving the approximate signal at level $j-1$ with the coefficients $g(n)$. Convolving the approximate signal at level $j-1$ with the coefficients $h(n)$ gives an estimate for the approximate signal at level j. The analysis step (decomposition stage) involves filtering the approximate signal and retaining every other sample of the filter output (downsampling). The synthesis step then involves upsampling and filtering to obtain a reconstructed signal. In Figure 3.3, the decomposition and reconstruction stages in a subband filtering scheme establishing a filter bank are presented.

3.5.5. Wavelet packet analysis

If one defines the scaling function $W_0(t) = \phi(t)$ and the wavelet function $W_1(t) = \psi(t)$, then we can write for functions $W_m(t)$, $m = 0, 1, 2, \ldots$, as

$$W_{2m}(t) = 2 \sum_{n=0}^{2N-1} h(n) W_m(2t - n) \tag{3.38}$$

and

$$W_{2m+1}(t) = 2 \sum_{n=0}^{2N-1} g(n) W_m(2t - n) \quad . \tag{3.39}$$

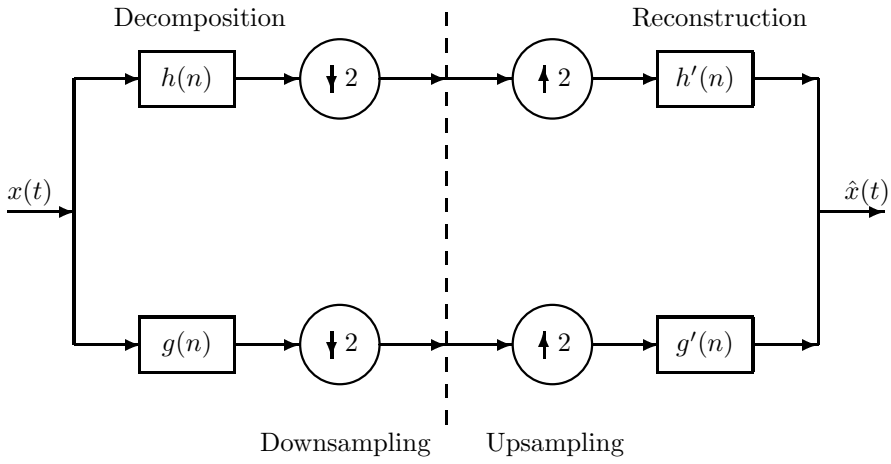

Fig. 3.3. **A schematic presentation of a subband filtering procedure using filter banks. The operations $\downarrow 2$ and $\uparrow 2$ stand for downsampling and upsampling by two.**

The analyzing functions called wavelet packet atoms are given in an orthogonal case as

$$W_{j,m,n}(t) = 2^{-j/2} W_m(2^{-j}t - n) \quad , \tag{3.40}$$

where j is a scale parameter, n is a time-localization parameter and parameter m gives roughly the number of "cycles" included in the oscillating waveform. Wavelet packet can be considered as a waveform whose oscillations persists for many cycles but are still finite. With fixed value of j the function $W_{j,m,n}(t)$ analyzes the signal around the position $2^j \cdot n$ at the scale 2^j. The analyzed frequencies are roughly given by $n/2N$ with $n = 0, 1, \ldots, (2j-1)$.

Wavelet packet analysis is a generalization of wavelet analysis offering a richer decomposition procedure. Both detailed and approximated signals are split at each level into finer components. A set of details and approximations is called the wavelet packet decomposition tree.

3.5.6. Optimization of the wavelet packet decomposition

Wavelet (multiresolution) decomposition allows searching an optimal decomposition among L trees if a signal of length $N = 2^L$ has been decomposed at L levels. Wavelet packet analysis involves the selection of an optimal decomposition tree among at most 2^L different subtrees of depth L. The optimization can be based on e.g. the minimization of the entropy of analyzed signal, where the optimized decomposition is called the best tree. The idea is to look at each node of the decomposition tree and quantify the information to be gained by performing each split.

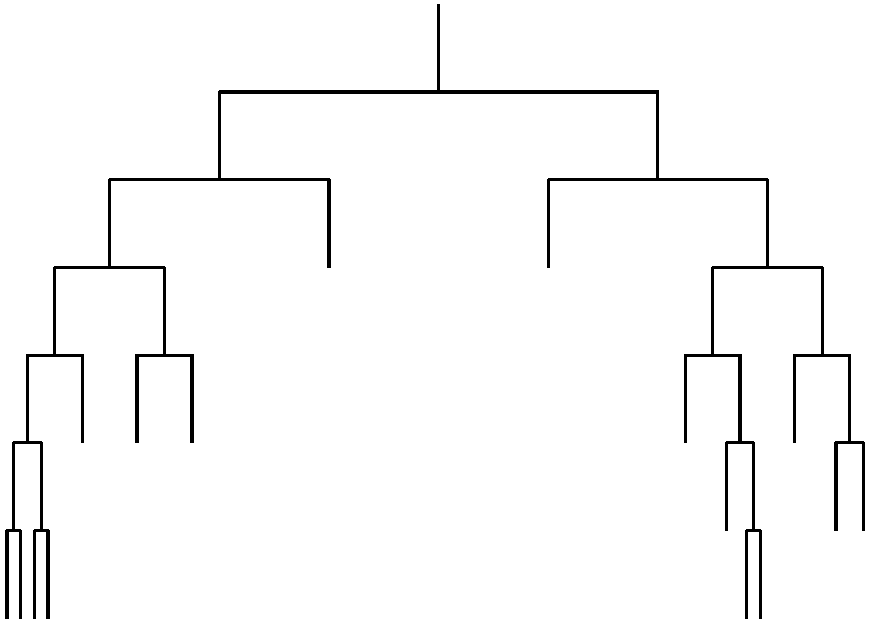

Fig. 3.4. A wavelet packet signal decomposition presented by an optimized tree structure.

The entropy can be obtained by many approaches, for example, the Shannon entropy (Coifman & Wickerhauser 1992) is defined as $\mathcal{E}(x) = -\sum_t x^2(t) \cdot \log(x^2(t))$. In Figure 3.4, the optimized wavelet packet decomposition tree is shown, which schematically presents the idea of this procedure.

3.5.7. "De-noising" the signal

A possible application of the discrete wavelet analysis is to remove undesired components (noise) from the signal through a de-noising approach (paper III). Basically the procedure includes decomposing the signal into the detail components described above, identifying the noise components and reconstructing the signal without those components. This is called the linear denoising approach. The linear denoising approach assumes that the noise can be found within certain scales, for example, at the finest scales when the coarsest scales are assumed to be noise free. More sophisticated de-noising can be done by applying the non-linear thresholding approach, which involves discarding the details exceeding a certain limit. This approach assumes that every wavelet coefficient contain noise and it is distributed over all scales.

The non-linear de-noising by both soft- and hard-thresholding methods can be

performed (Donoho 1995). The soft thresholded wavelet coefficients will be

$$\eta(d_j(k)) = \begin{cases} \text{sign}(d_j(k)) \cdot (|d_j(k)| - p), & \text{if } |d_j(k)| > p \\ 0, & \text{if } |d_j(k)| \leq p \end{cases} \quad , \tag{3.41}$$

where p is the applied threshold. The wavelet coefficients whose absolute values are lower than the threshold, are first set to zero, and then the remaining nonzero coefficients are shrunk towards zero. With hard thresholding, the thresholded coefficients will be

$$\eta(d_j(k)) = \begin{cases} d_j(k), & \text{if } |d_j(k)| > p \\ 0, & \text{if } |d_j(k)| \leq p \end{cases} \quad , \tag{3.42}$$

which simply means setting to zero the absolute coefficients lower than the threshold p.

In paper III, the assumed model for a noisy signal was $x(t) = f(t) + e(t)$, where $f(t)$ is the noise free signal and $e(t)$ is the white or non-white noise of variance δ^2. The performance of the methods was evaluated from the simulations with L_2-norm given by the equation

$$||f_o - \hat{x}_i||_2 = (\sum_t |f_o(t) - \hat{x}_i(t)|^2)^{1/2} \quad , \tag{3.43}$$

where f_o denotes the original ECG signal being the same for all simulations, and $\hat{x}_i$ denotes the ECG signal with added noise after noise removal.

3.5.8. Selection of the threshold

In paper III, the threshold p was selected for each signal using four threshold estimation procedures: SURE, HEURISTIC SURE, FIXTHRES and MINIMAX principles. The aim was to compare the performance obtained by different methods in the noise removal of ECG signal. Stein's Unbiased Risk Estimate (SURE) (Donoho 1993, Donoho & Johnstone 1995) is an adaptive threshold selection rule defined as $p = \sqrt{2 \cdot \log_e(n \cdot \log_2(n))}$, where n is the number of samples in the signal vector. With this approach obtaining risks and minimizing them with respect to p values gives a threshold selection. The method is adaptive through searching a threshold level for each wavelet decomposition level. A fixed threshold approach FIXTHRES calculates the threshold with respect to the length of the signal and the estimated threshold is given by $p = \sqrt{2 \cdot \log_e(n)}$ (Donoho & Johnstone 1994). The HEURISTIC SURE approach being a variant of the first, replaces in very noisy conditions the SURE with FIXTHRES estimate (Misiti *et al.* 1996). Further, the MINIMAX procedure applies a fixed threshold $p = 0.3936 + 0.1829 \cdot \log(n)$ (Misiti *et al.* 1996) to produce the so called minimax performance for mean square error against an ideal case (Bruce & Gao 1996, Donoho & Johnstone 1994).

The underlying signal model in paper III assumes the noise being normally distributed with zero mean and variance of 1, which means that we have to rescale the

threshold values when dealing with unscaled and nonwhite noise. When normally and uniformly distributed noises were studied, calculated thresholds were rescaled by the standard deviation of noise estimated from the finest level of the decomposition of each signal so that $\hat{p} = p \cdot \hat{\delta}$. Further, with AR(4)-noise the noise level was estimated scale by scale to take account the obviously strong high-frequency content. In wavelet approach, this was done by calculating $\hat{\delta}$ for all scales. In wavelet packet case, $\hat{\delta}$ was estimated from the first node at each subdecomposition band which gave the best statistics for the noise level estimation. As a robust estimate of the standard deviation $\hat{\delta} = \text{Median}(|d_j(k)|)/.6745$ was used (Donoho & Johnstone 1994).

3.6. Chaotic modelling

There are numerous investigations into fractal properties (Yamamoto & Hughson 1993, Yamamoto *et al.* 1995, Yeragani *et al.* 1993) and chaos (Babloyantz & Destexhe 1988, Signorini *et al.* 1994, Yamamoto *et al.* 1993) in HRV. The parameters used to assess the latter have included spectral analysis, correlation dimensions, Kolmogorov entropy and Lyapunov exponents. The most recent discussions have concerned chaotic modelling as applied to RR interval time series (Cohen *et al.* 1996, Karrakchou *et al.* 1996) and especially to non-stationary time series (Karrakchou *et al.* 1996).

Cohen *et al.* (1996) studied the logistic equation (*Poincaré equation*)

$$x(t) = A\, x(t-1)(1 - x(t-1)) \quad , \qquad 2 \leq A \leq 4 \tag{3.44}$$

and some of its solutions as an example of a chaotic system. Here the first order Poincaré plot (first order difference plot) was introduced by presenting $x(t+1)$ vs. $x(t)$, and given as a measure of the degree of chaos in a system. In Huikuri *et al.* (1996) an ellipse was fitted to the plot, and the centroid of this ellipse and the lengths of both axes were determined. In some earlier studies the first order Poincaré plot called a "scattergram", was shown to be capable of detecting large, abrupt deviations in heart rate (Baevskij *et al.* 1984, Baselli & Cerutti 1985, Stinton *et al.* 1972). The second-order difference, obtained by presenting ($x(t+2)$ - $x(t+1)$) vs. ($x(t+1)$ - $x(t)$), would show the degree of theoretical chaos (Cohen *et al.* 1996). The first order and second order difference plots are shown in Figure 3.5.

A quantitative measure of the degree of variability in the second-order difference plot, the measure of central tendency (CTM), takes the form

$$\text{CTM} = \frac{\sum_{t=1}^{N-2} \delta(d(t))}{N-2} \quad , \tag{3.45}$$

where

$$\delta(d(t)) = \begin{cases} 1 & , \text{ if } \sqrt{(x(t+2) - x(t+1))^2 + (x(t+1) - x(t))^2} < r \\ 0 & , \text{ otherwise} \end{cases}$$

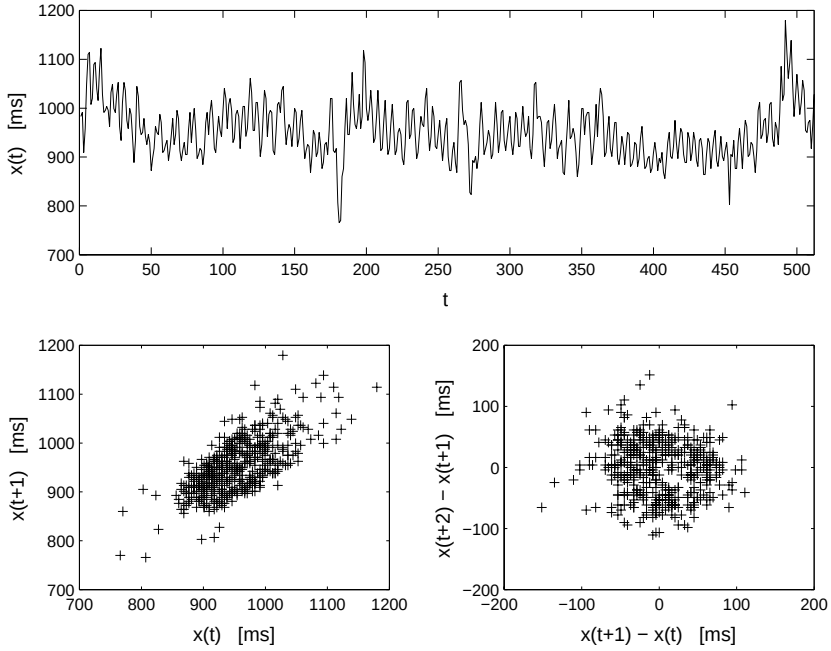

Fig. 3.5. First-order difference (bottom left) and second-order difference (bottom right) plots derived from the RR intervals obtained from a healthy young subject under resting conditions (top).

and N is total number of time series values and r the radius of the central area (dependent on the data).

Cohen *et al.* (1996) suggest that both the normal and diseased heart show chaotic RR interval series when recorded using Holter devices, but that data acquired from patients with congestive heart failure (CHF) and analysed by the above methods show more chaotic behaviour than for normal patients. They also suggest that the approach could serve as a classification method for classifying subjects into normal cases and CHF patients.

A statistical test for chaos in time series used in real-time monitoring is presented in Karrakchou *et al.* (1996), the objective being to test non-linearity and fractality separately, since both are unavoidable conditions in chaotic time series. The fractality of RR interval time series was tested by studying long-term correlations in time series. The mean-square fluctuation of a difference function $d_l(t) = x(t+l) - x(t)$, $l = 1, \ldots, N$, was calculated as follows

$$F^2(l) = \overline{[d_l(t)]^2} - [\overline{d_l(t)}]^2 \quad , \tag{3.46}$$

and if $F(l) \sim l^a$, $a \neq 0.5$, there exist "infinite-range" correlations and the time series is fractal. The authors also pointed out that this expression corresponds to a calculation of the standard deviation of the difference between consecutive

R peaks for different interval lengths. Non-linearities in RR intervals were tested using Keenan's test (Keenan 1985) with the hypothesis of linearity vs. second-order Volterra expansion. If any multiplicative term was found in the expansion, the time series was non-linear. A similar procedure for analysing correlations with the mean fluctuation function was performed by Peng *et al.* (1993).

Several popular methods exist for studying chaos in cardiovascular time series, but the indices proposed for measuring it should be applied cautiously and results obtained should be interpreted with care. The basic condition is the need for large amounts of data which make these methods not well-suitable for real-time analysis (Karrakchou *et al.* 1996). The problem also lies in discriminating a chaotic system from a random one, calculation of the correlation dimension, for example, can give incorrect results in a random time series (Osborne & Provenzale 1989). A random signal having a power spectrum like $1/f^{\lambda}$, $\lambda > 0$, for example, can erroneously be concluded as chaotic when estimating the correlation dimension (Theiler *et al.* 1992). This point should be taken into account because HRV, in particular with long data sets, has a power spectrum inversely related to frequency. A recent development has occured in developing statistical tests for chaos identification in HRV (Kanters *et al.* 1994, Karrakchou *et al.* 1996, Khadra *et al.* 1997). Kanters *et al.* (1994) showed the lack of low-dimensional chaos in RR interval time series acquired from healthy subjects and demonstrated the remarkably non-linear nature of RR interval time series. In Khadra *et al.* (1997), HRV signals obtained from the transplant patients were first detected random, but changed to chaotic as time passed after the operation. It was concluded by Kanters *et al.* (1994) and Karrakchou *et al.* (1996), alongside the adoption of a certain critical point of view, that chaotic modelling could be applied to the monitoring of RR interval time series whether these were chaotic or not.

4. Experimental settings

4.1. RR interval data

RR inteval recordings shown in paper I were made using an ambulatory heart rate recorder, which has recently been developed and stores timed occurences of heart beats and sequences including numerous samples of ECG signals (Ruha *et al.* 1997). The timing accuracy of the device is reported to be 1 ms, and it can store the RR interval data over 24 hours. Examples on the RR interval analyses were produced using Matlab software (The Mathworks, Inc., Natick, MA, USA).

4.2. Dynamics of the ventricular repolarization duration

4.2.1. Measurement equipment and software

The ECG was acquired in paper II by Medilog EXCEL-2 ver. 7.5 Holter Management System (Oxford Medical, Ltd., UK) using a two-channel tape recorder (model MR-45), which contains a C60 cassette as a recording medium. The data were replayed from the recorder by the Holter software and stored on the hard disk of a PC computer with 128 Hz sampling rate and 8 bits resolution. The raw ECG data on the channel 2 (lead II) was read from a file by a program designed specifically for the beat-to-beat measurement of RR and QT intervals.

The program was designed to operate within the Windows environment on a standard PC. The program code was written using Borlands Turbo C++ -compiler (Borland 1991) (Borland International, Inc., USA). The aim was to develop a modular program structure, which is easy to maintain and can be flexibly expanded with new features. Therefore, the program was divided into separate modules. Options for loading the digitized ECG data and displaying data with detection of waveforms are included. The preprocessing and waveform detection procedures perform the analysis based on the theory described in the particular paragraphs in this thesis. The ECG signal can be optionally interpolated in order to increase the

precision of the waveform measurement. The resulting time series (RR and QT intervals) can be shown on a beat-to-beat basis as a function of the beat number. In a scatterdiagram each QT interval value is drawn as a function of the previous RR interval value, i.e. $QT(t)$ vs. $RR(t-1)$, and a regression line is fitted to the data by minimizing the least square error. The program also offers options for exporting the resulting time series and the analyzed ECG as well as for modifying several program parameters.

4.2.2. Testing of the automatic waveform measurement

4.2.2.1. Real ECG signals

Ambulatory ECG was acquired from six healthy subjects to test the automatic waveform analysis procedure. A ten minute section of ECG was selected from each recording and analyzed by using the different options of the program. ECGs had upward R peaks and clear T wave shapes.

The effect of the interpolation of the ECG on the interval variability measurement as well as the effect of different QT interval onset and T wave end position definitions were tested. The "QT interval" onset definitions were true QRS onset (Q), R wave maximum (R), ascending (R_a) or descending (R_d) maximal slopes of R wave. The "T wave end" position definitions were the peak (maximum, T_{max}) and end of T wave (T_e). Combinating these definitions produced a set of "QT interval" time series: QT_e, QT_{max}, R_aT_e, R_aT_{max}, RT_e, RT_{max}, R_dT_e and R_dT_{max}.

4.2.2.2. Simulated ECG signals

Simulated ECGs were generated by obtaining a cardiac cycle from each above mentioned ECG strips and repeating the cycle 600 times. Simulated noise free ECGs were then corrupted with six types of noises at different noise levels, see Table 4.1. Simulations 1-5 were additive noise and summed with the ECG. A sine wave with a frequency varying at 0 - 0.5 Hz (simulation 1) was constructed as

$$x(t) = \sin(2 \cdot \pi \cdot 0.25 \cdot t - 7.645 \cdot \pi \cdot \sin(2 \cdot \pi \cdot t/96)) \tag{4.1}$$

and a sine wave with a frequency varying at 3 - 5 Hz (simulation 2) was generated as

$$x(t) = \sin(2 \cdot \pi \cdot 5 \cdot t - 12.944 \cdot \pi \cdot \sin(2 \cdot \pi \cdot t/20)) \tag{4.2}$$

with $t = 1, \ldots, N$.

Amplitude modulation (AM) in simulation 6 was constructed as follows (Ziemer & Tranter 1990)

$$x(t) = [1 + a \cdot m_n(t)] \cdot y(t) \quad , \tag{4.3}$$

where $x(t)$ is the modulated signal and $y(t)$ is the ECG signal. $m_n(t)$ is a uniformly distributed noise normalized such as the minimum value of $m_n(t)$ is -1. The parameter a is called as the modulation index ($0 \leq a \leq 1$).

The objective was to measure the sensitivity of the automatic measurement of the repolarization duration using commonly-occurring noise types. This type of analysis is especially necessary, because the variability of the repolarization duration is very low, thus, the various disturbances on ECG can produce inaccuracies in this time period measurement. Typically, QT interval variability is SD = 4-5 ms as RR interval variability can be SD = 60-70 ms. The noise level was defined with the signal-to-noise ratio (SNR) in decibels (dB) as

$$\mathrm{SNR} = 20 \log(\frac{\sigma_{\mathrm{cycle}}}{\sigma_{\mathrm{noise}}}) \quad , \tag{4.4}$$

where σ_{cycle} is the root-mean-square (rms) value of the ECG signal obtained from the whole cardiac cycle and σ_{noise} is the rms value of the additive noise signal, respectively. For instance, 10 % relative rms value of the noise signal gives 20 dB SNR value. The effects of different noise types were measured at noise levels of 5 - 50 dB.

Table 4.1. Simulated noise types used in the noise sensitivity measurement.

Simulation	Noise type	Simulated effect
1	0 - 0.5 Hz sine wave	Baseline wander due to breathing
2	3 - 5 Hz sine wave	Motion artefacts
3	50 Hz sine wave	Mains noise
4	Gaussian white noise	EMG, motion artefacts
5	Sum of the noise realizations 1 - 4	Mixed effect
6	Uniformly distributed amplitude modulation	Amplitude modulation due to breathing

4.3. Denoising of an ECG signal

In paper III, fifty independent simulations were used to evaluate the performance of the applied denoising methods. Simulations were created by adding three types of the noise on a noise free ECG: gaussian and uniformly distributed white noise, and non-white noise generated by an autoregressive (AR) model of order 4. The noise amplitudes were scaled so that the signal-to-noise ratio was 5 dB for all signals. The performances of the methods were studied by obtaining errors within an ECG including 2600 samples and more specifically obtaining errors within six QRS-complexes extracted manually from the whole ECG. The latter approach allowed the investigation of the performance of the denoising methods to handle the high frequency parts of the ECG. Matlab software was utilized with Wavelet Toolbox to perform wavelet analysis for the digitized ECG signal obtained from an anesthesized monkey. A 512 Hz sampling frequency was used with a resolution of 12 bits.

When considering the compactly supported orthogonal wavelet families (Daubechies, Symlets, Coiflets) with discrete transform, the Coiflet wavelet basis was found most suitable. The denoising performances were very near between these families, however, Coiflets showing slightly the best performance. The Coiflet wavelet (*Coif5*) of order $N = 5$ was used which had lowest denoising error among Coiflet functions. The error performance was measured with L_2-norm given by Equation 3.43. The *Coif5* function is a near symmetrical wavelet, which is compactly supported with maximum number of vanishing moments for a given support width $(6N - 1)$, Figure 4.1a. The analysis done by *Coif5* wavelet is orthogonal. Wavelet packet analysis was made by Coiflet wavelet packet function $W_{j,m,n}(t)$ with $m = 5$, see Figure 4.1b. The wavelet packet decomposition was optimized by minimizing the Shannon entropy (section 3.5.6).

4.4. Analysis of APD time series

4.4.1. Patients

In paper IV, 12 ordinary cardiology patients (six males and six females), undergoing routine electrophysiological testing for symptomatic cardiac arrhythmias, were included in the study. However, the intended study was not the reason these patients were tested. None of the patients had clinical or echocardiographic evidence of structural heart disease. The clinical indication for the studies was symptomatic supraventricular tachycardia in all patients. All cardiac medications had been stopped at least four days before the studies.

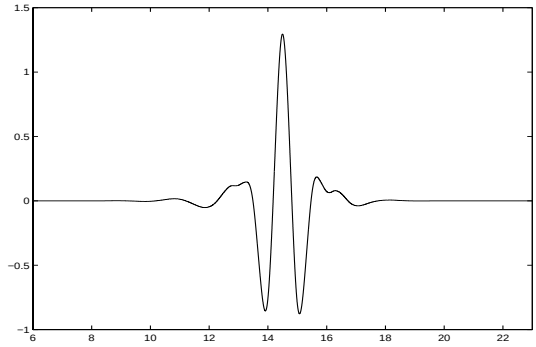

(a)

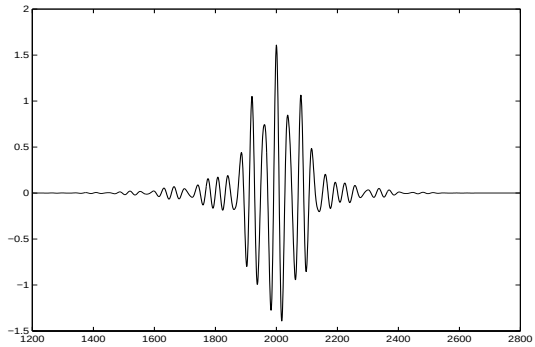

(b)

Fig. 4.1. **(a) A Coiflet wavelet used for a discrete wavelet analysis. (b) A Coiflet wavelet packet used for a discrete wavelet packet analysis.**

4.4.2. Study protocol

The recordings of MAP signals in sinus rhythm and during constant rate pacing were performed after the diagnostic electrophysiological study. Quadripolar electrode catheter was introduced into the high right atrium and a bipolar Ag/AgCl electrode catheter was introduced (USCI, Division of C.R. Bard, Billerica, MA, USA) into the right ventricle. MAPs were obtained by gently pressing the tip of the catheter against the endocardial surface of the right ventricular apex. The signals were recorded on a CardioLab (Prucka Engineering, Inc., Houston, TX, USA) using 1024 Hz sampling rate with a resolution of 0.1 mV of the amplitude of the signal. The MAP signals were amplified and filtered at frequencies of 0.05 - 500 Hz. The amplitude (>10 mV) and stability of the signals were assessed before recordings.

The MAP signals were recorded in sinus rhythm during quiet normal respiration

for ten minutes. After baseline recordings in sinus rhythm, the high right atrium was paced at the cycle length of 600 ms for ten minutes. Only those patients with 1:1 atrioventricular (AV) conduction without significant fluctuation in the atriohisian conduction time with the atrial pacing at the cycle length of 500 ms were included.

4.4.3. Analysis of MAP signals

The CardioLab software was used to acquire the MAP data from patients. The MAP Analysis program was written in Pascal 7.0 language (Borland International, Scotts Valley, CA, USA) to be used with CardioLab equipment on a standard PC under a DOS or a Windows environment. The program processes MAPs and calculates the amplitude, RR interval, and the 15 %, 30 %, 50 % and 90 % repolarization times producing a series of results calculated from successive waveforms, see Figure 1 in paper IV. There is a possibility to edit manually the automatic analysis. Changing the baseline updates all the calculated results. It is also possible to discard a waveform distorted by noise and exclude it from the final results.

4.4.4. Analyses of variability of RR intervals and action potential duration

Two-dimensional vector analyses of variability of RR interval and action potential duration (APD) time series were performed by a method described previously (Huikuri *et al.* 1996). Poincaré plots were generated where each time series value is plotted as a function of the previous value for a predetermined length of time series. Quantitative analysis of the plots involves fitting an ellipse to the plot and estimating the long and short term time series variability from the lengths of the axes of the ellipse. The Poincaré plots of RR intervals and APD at the 90 % (APD_{90}) and 50 % (APD_{50}) of repolarization were generated for the two segments of five minute periods in sinus rhythm and one segment of five minute period at the end of the pacing (i.e., five minutes after the onset of constant rate pacing) at which point the APD had reached its steady-state level. The segments with ectopic beats, artifacts, and distortion of the MAP signals were edited both manually and automatically and deleted before analyses.

Paired t-test was used to compare the measures of variability of APD and RR intervals in sinus rhythm during pacing. Pearson correlation coefficient was used to assess the univariate correlations between the measures of variability. $p < 0.05$ was concidered significant.

4.5. Wavelet analysis of HRV

RR inteval recordings analyzed in section 5.4 were made using Medilog EXCEL-2 ver. 7.5 Holter Management System (Oxford Medical, Ltd., UK). RR interval data was further processed using HEARTS software (Heart Signal Oy, Oulu, Finland) to exclude inappropriate intervals. Time series were then resampled using 2.4 Hz sampling frequency to obtain an equidistantly sampled data. Analyses were performed using Matlab software with Wavelet Toolbox (The Mathworks, Inc., Natick, MA, USA) at the Center for Scientific Computing, CSC (Espoo, Finland).

The Coiflet wavelet and wavelet packet functions of order 5 were used to obtain the corresponding spectra (Figure 4.1). The optimization of the wavelet packet decomposition was performed by minimizing the Shannon entropy (section 3.5.6).

RR interval recordings after noradrenaline injections were analyzed from eight healthy subjects. Recordings included a baseline period before drug administration, which was continuously increased using 50, 100 and 150 ng injections. A second set of RR interval data was collected from ordinary cardiology patients during several hours prior to ventricular fibrillation. The wavelet analysis was done within one hour before the event for 11 patients.

5. Results

5.1. Dynamics of the ventricular repolarization duration

5.1.1. Interpolation of the ECG

A standard Holter recording frequency of 128 Hz is not sufficiently robust to capture the low level of QT interval variability found in most patients. Therefore, a higher sampling rate is needed to obtain precise measurements. An important aim of this study was to test the feasibility of interpolation as a means of increasing the fidelity of an ECG initially digitized at the low Holter sampling rate. However, the disadvantage of the interpolation is that the features of the ECG cannot be better resolved than the original digitized ECG allows. Interpolation of the ECG allows a better time resolution for time interval variability measurement.

In the present study the ECG recordings were interpolated to 256, 512, 768 and 1024 Hz to illustrate the changes in the resolution of QT interval variability. For example, in a RT_{max} time series obtained from an original ECG signal sampled at 128 Hz, the natural variability can not be seen (Figure 2, top, in paper II). In contrast, the same recording interpolated to 1024 Hz shows the existing variability more clearly (Figure 2, bottom, in paper II). This method also provides a means to obtain a proper time series distribution for analysis.

5.1.2. RMSSD of QT interval time series

The RMSSD value is a simple and traditional measurement of the variation in a cardiovascular variability signal. The absolute RMSSD values (ms) of a QT time series with different T wave end definitions (T_{max} and T_e) as a function of sampling frequency for one patient are presented in Figure 5.1. The variability decreases in all QT time series as ECG is interpolated, reaching a maximal efficiency at about 1 kHz. At 1024 Hz, the RMSSD values are 25-30 % and 40-60 % lower compared to 128 Hz for T_e and T_{max}, respectively.

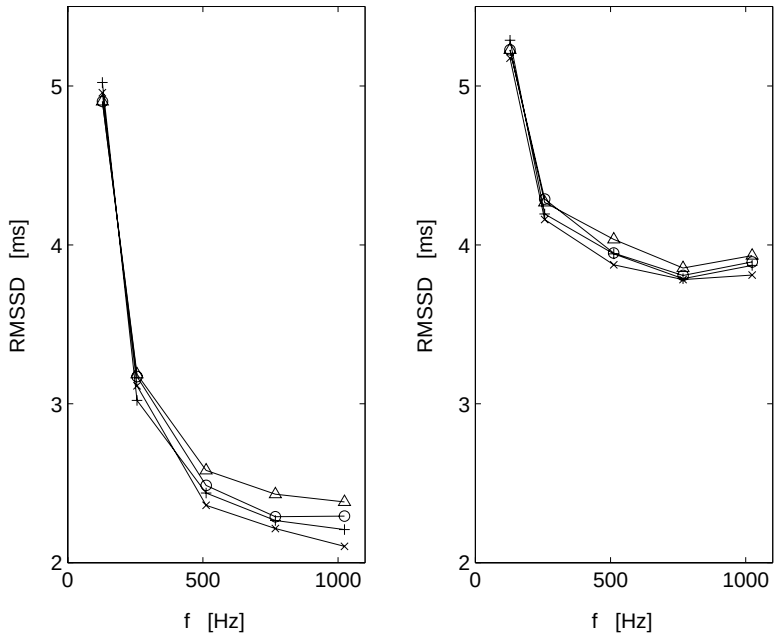

Fig. 5.1. **The absolute RMSSD values of QT interval time series using (a) T_{max} and (b) T_e definition. Abbreviations for the QT interval onset definition: true QRS onset, Q (△); ascending maximal slope of R wave, R_a (○); R wave maximum, R (+); and descending maximal slope of R wave, R_d (×).**

Furthermore, at 1024 Hz sampling frequency the variability observed in time series with T_{max} definition is about 40 % lower than the variability with T_e definition. Remarkable differences in variabilities do not typically exist due to the definition of the start of the repolarization duration. Defining the start of repolarization duration at the maximum or at the descending maximal slope of the R wave, gives slightly smaller variability than the other choices. Looking for the onset of Q wave produces the largest variability in time series. The 40% difference between T_{max} and T_e observed in the RMSSD interpolated at 1024 Hz, may be due to the increase in noise at T_e resulting in an increase in the signal variability at that end-point. The start-point for the measurement of QT can be defined as Q, R_a, R or R_d. For the T_{max} end-point, differences among these starting points were observed with Q displaying the greatest variability and R_d the least.

The RMSSD values of RT_{max} and RT_e time series for the six patients measured is shown in Figure 5.2. This example demonstrates the reproducibility of the variability measurement when interpolating the ECG signal. Defining the onset of the QT interval at the maximum of the R wave and the offset of the T wave at the maximum of T wave, seems to give a reproducible variability measurement.

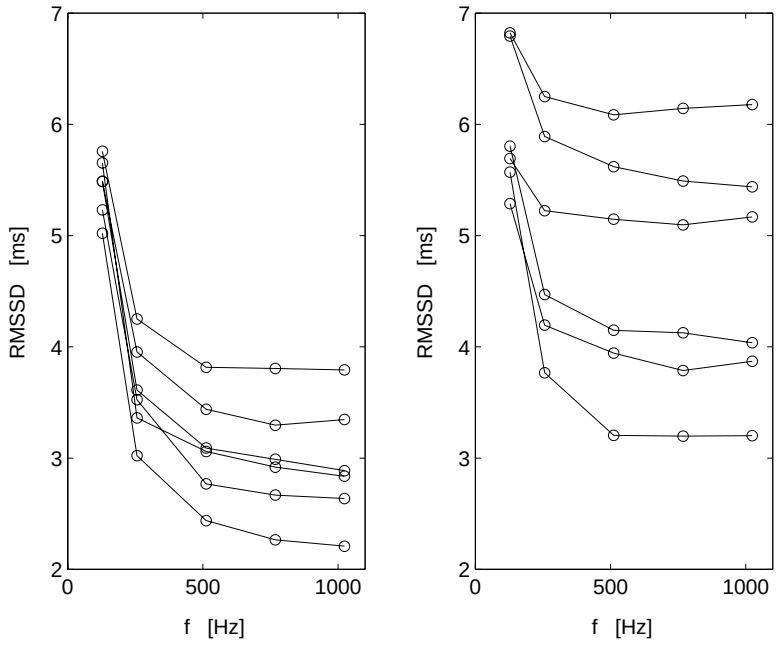

Fig. 5.2. RMSSD **values of (a) RT_{max} and (b) RT_e interval time series obtained from six patients.**

5.1.3. Power spectrum estimates

In order to evaluate further the applicability of our algorithm, we also used power spectrum estimates to quantify the QT interval variability. RR, RT_{max} and RT_e interval time series from one patient was obtained by an ECG interpolated to 1024 Hz (Figure 5.3). The power spectrum estimates are presented in Figure 5.4. All power spectra show a clear peak at $f = 0.32$ Hz which is probably due to breathing. In addition to the sum spectrum the spectra of the separate components are estimated.

The power estimates of the main component observed at $f = 0.32$ Hz in the RT_{max} and RT_e spectra were plotted as a function of the sampling rate (Figure 8 in paper II). As was demonstrated with RMSSD, the power estimates decrease as the sampling rate increases. At sampling frequency of 1024 Hz, the estimated power of the main peak for the power spectrum of the RT_{max} time series was 56 % of that estimated for RT_e time series in terms of ms^2. In this case, the total powers in the time series were 5.7 ms^2 and 9.4 ms^2 for RT_{max} and RT_e, respectively.

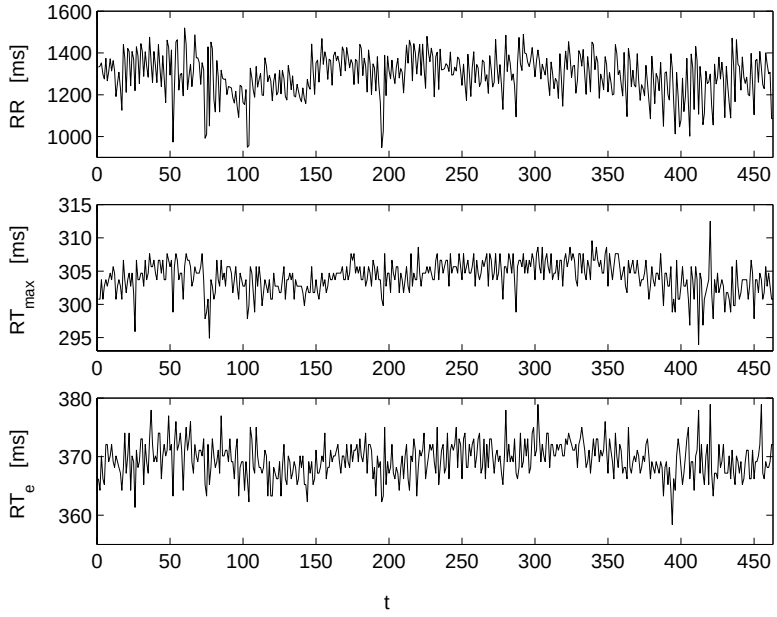

Fig. 5.3. **RR (top), $\mathbf{RT}_{\max}$ (middle) and $\mathbf{RT}_{\mathrm{e}}$ (bottom) interval time series obtained from patient 6.**

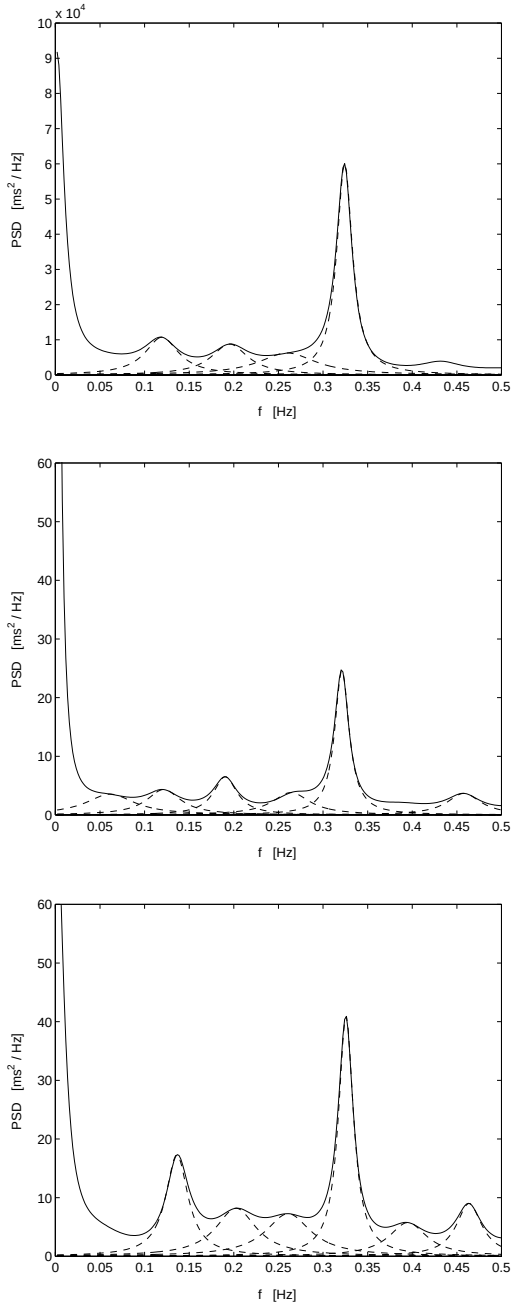

Fig. 5.4. Power spectrum estimates of RR (top), $\mathbf{RT}_{\max}$ (middle) and $\mathbf{RT}_{\mathrm{e}}$ (bottom) interval time series obtained from patient 6. The estimates represent the sum spectrum (solid line) and the spectra of the separate components (dashed lines).

5.1.4. Simulated ECG signals

A critical step in the development of any QT algorithm is to determine the best start and end points for ventricular repolarization to obtain an accurate estimate of QT interval. To achieve this goal we compared the variability in the QT time series using different start and end points. Simulations of six commonly-encountered types of noise (Table 4.1) were used to ascertain which of eight possible intervals produced the least degree of variability for each noise type. These results are presented in Tables 2 - 7 in paper II. The lower the SD value, the greater the precision of the measurement. Overall, the intervals using RT_{max} and R_dT_{max} provided the most reliable results in most situations.

The first type of noise was at 0-0.5 Hz, simulating baseline drift due to breathing (Table 2, paper II). At low SNRs using T_e as the endpoint of the QT interval gives the most precise results. At levels of 25 dB and higher, it is better to use T_{max}. For the simulation of motion artefacts (3-5 Hz), electrical line noise (50 Hz) and Gaussian white noise (Tables 3 - 5, paper II), T_{max} was consistently more precise. Summing the noise simulations 1-4 and adding them to the ECG signal produced similar results, i.e. T_{max} is the most precise endpoint (Table 6, paper II). Using Q as a start point showed greater variability and was therefore less precise than using R in most cases.

Noise due to breathing also contains an amplitude component and can be simulated by amplitude modulation (Table 7, paper II). The mean SD values of all analyzed time series are given as a function of the modulation index a, see section 4.2.2.2. At values $a \leq 0.3$, defining the end of the QT interval as T_e, produced the lowest variability. The results also indicate that choosing the onset of the QT interval at the descending slope of R wave is the most insensitive to this kind of the simulated noise. It is interesting to note that measuring RR interval in cases of amplitude modulation produces lower variability than QT. In fact, measuring RR interval for each type of noise (Tables 7 and 8, paper II) overall showed less variability compared to measurements of QT interval.

The variability of RT_{max} as a measurement of QT interval among six different patients is shown in Table 9 in paper II. In each case the sum of each type of simulated noise was added to the signal. Coefficients of variation (CV) were calculated to study the amount of variability with respect to the mean value of the analyzed time series. According to the obtained CV values, the variability of all QT time series were less than 11 % of the mean of each time series at all noise levels. For example, at SNR of 30 dB, the percentage amounts of variability were between 0.24 - 0.47 % compared to the mean CV of 0.32 %.

The simulated noises were also added to the real ECG data in order to study the effect on the real variability. As an example, SD values of RT_{max} time series of patient number 6 with different simulated noises are shown in Table 5.1. The SNR refer here to the same noise amplitude as used with simulated ECGs above. SD value of the original time series was 2.35 ms^2. The signal variability with all noise types reached this level at SNR of at least 20-25 dB. With amplitude modulation (simulation 6), SD values were 9.63, 6.55, 3.12, 2.63 and 2.45 ms^2 as a function of decreasing modulation index.

Table 5.1. SD *values of the RT_{max} time series measured from patient n:o 6 with different simulated noises.*

SNR	0 - 0.5 Hz sine wave	3 - 5 Hz sine wave	50 Hz sine wave	Gaussian white noise	Sum of the noise realizations 1-4
dB	ms	ms	ms	ms	ms
5	2.59	80.01	4.03	83.12	72.77
10	2.46	38.45	3.24	29.45	17.68
15	2.39	9.27	2.64	4.19	3.80
20	2.37	3.41	2.48	3.04	2.88
25	2.37	2.75	2.40	2.58	2.55
30	2.37	2.54	2.42	2.42	2.41
40	2.36	2.39	2.36	2.38	2.38
50	2.35	2.36	2.36	2.36	2.37

5.1.5. Discussion

The analysis of the dynamics of RR or QT time series can only be performed by observing the beat-to-beat variability in a time series. There is no "absolute" unbiased measurement of ventricular repolarization duration because even a manual measurement done by an experienced cardiologist is limited by the precision of the tool used. There also exists a natural variability between manual measurements done by different persons. All automatic measurement systems and algorithms produce some error in interval measurement as well. An automatic algorithm, however, rapidly analyses an ECG and the results can be reproducible. The performance and reproducibility can be compared between different measurement algorithms and against manual measurement.

In previous studies, the ventricular duration variability has been reported to be very low compared to RR interval variability. For instance, a study by Nollo *et al.* (1992) showed SD values of 2-6 ms depending on the definition of the measured time interval. Ambulatory ECGs are commonly acquired at a low sampling rate due to lack of the data storage capacity of the equipment. As it was shown in this study, an ECG sampled at 128 Hz can not be used to obtain the beat-to-beat variability in QT time series. Variability decreased as the sampling frequency of the ECG increased, which is produced by the improved time resolution in the waveform analysis. Due to these factors, an interpolation procedure was included in the analysis scheme to obtain improved precision. The interpolation can significantly improve the resolution of the ventricular repolarization duration measurement, and the procedure can cause a minor distortion only in the QRS complex, but not in the T wave (Speranza *et al.* 1993).

The noise sensitivity of the implemented algorithm was tested with several types

of simulated noise. In this context, the testing was important, because QT interval variability is low, and therefore a significant part of the observed variability can be due to noise. Until now, there have been only a few publications dealing with noise sensitivity of QRS detection (Barbaro *et al.* (1991), Friesen *et al.* (1990), Koeleman *et al.* (1984) and Ruha *et al.* (1997)). Furthermore, there are only a few references, where the noise sensitivity of QT interval measurement is actually considered (Nollo *et al.* (1990), Nollo *et al.* (1992), Porta *et al.* (1996) and Speranza *et al.* (1993)). The algorithm used in this work has not previously been systemically tested with simulated noise.

Our noise simulations present the most common disturbances observed in ambulatory electrocardiogram with precision reported as SD values. Six simulated test signals were constructed by adding noise to an "ideal" ECG. In addition, the effect of the amplitude modulation of respiration were modelled as the uniformly distributed amplitude modulation of the ECG. It should be noted that there may exist different definitions of signal-to-noise ratio and the noise distribution should be known.

Our simulations showed that, in most of the cases, defining the end of QT interval at the maximum of the T wave gave most precise measurement of the ventricular repolarization duration. However, when the shape of the T wave was altered by amplitude modulation (simulation 6) choosing the end of T wave produced the lowest variability in a time series. This observation has also been made by Porta *et al.* (1996). Adding a 0-0.5 Hz sine wave, using T_{max} definition produced larger variability in time series at lowest signal-to-noise ratios (SNR $\leq$ 20 dB). These findings may suggest that the apex of the T wave is especially sensitive to the noise due to breathing.

The definition of the onset of the ventricular repolarization duration is most precisely made on the maximum or descending maximal slope of the R wave. The choice between R and R_d definition in this waveform analysis algorithm may depend on the quality of the measured signal. For example, if a particular R wave has two peaks with variable amplitudes located very near to each other, the algorithm may produce noise in a time series due to jitter when looking for the maximum of the R wave. The Q wave was often missing in the patient ECGs, which produced a lot of the noise in the QT_e and QT_{max} time series.

In a previous study (Speranza *et al.* 1993) an ECG was sampled at 250 Hz and interpolated to 1024 Hz sampling rate. The algorithm was tested only with Gaussian noise added at different noise levels. The coefficient of variation (CV) was about 1 % for RT_{max} and less than 4 % for the RT_e time series at SNR = 40 dB. As a comparison, the mean CV values in our work, were 0.16 % and 0.20 %, with mean SD values of 0.42 ms and 0.70 ms, respectively (Table 5, paper II). These results clearly show a better precision in the QT estimate. The SNR definition is assumed to be the same in both studies.

The analysis of dynamics of RR or QT time series can only be quantified by observing beat-to-beat variability in time series. Furthermore, the periodic variability in RR and QT time series can be observed by using power spectrum estimation. The results show that the estimated powers in QT time series are very low compared to powers estimated in RR interval spectrum, as demonstrated in

earlier studies (Nollo *et al.* 1992, Speranza *et al.* 1993). However, power spectrum estimation by AR modelling seems to be capable of showing clear components also in time series with low variability.

In this study, differences were found in the noise sensitivity of the computer analysis of ventricular repolarization when various definitions of QT interval were used. In most cases, RT_{max} or R_dT_{max} time series can be regarded as the most precise QT interval estimate. The results suggest that low amplitude variability may be hidden by noise due to inadequate time resolution of the signal, breathing, muscle activity and motion artefacts. These factors may require a more critical assessment of data obtained by either manual or automated analysis of QT interval dynamics.

5.2. Wavelet transform based noise removal of ECG

Denoising performances of the four threshold selection methods are reported in Tables 5.2 and 5.3 with optimal decomposition depths. Generally, denoising error first decreased as the decomposition depth increased. The results were optimized in respect of the minimum value of the error averages giving an optimal downsampling depth, which varied between denoising approaches. Methods are compared in wavelet and wavelet packet analyses applying both soft and hard thresholding. First the performance within the whole ECG strip including six cardiac cycles was measured. The results show that wavelet denoising approaches had better overall denoising performances than wavelet packet approaches in all cases except with the HEURISTIC SURE rule when using hard thresholding for white noises. The wavelet methods were preferable in removing especially the AR(4)-noise, when the errors were generally 2-5 times greater with wavelet packets (Tables 5.2 and 5.3). With other noise types the difference varied from a few to a few tens of percents for wavelet methods.

Table 5.2. Denoising performance of wavelet denoising approach. Values are means and standard deviations of $||f_o - \hat{x}_i||_2$. N(0,δ^2) is normally distributed and zero mean noise with variance δ^2, U[a,b] stands for a uniformly distributed noise and AR(4) is the non-white noise generated by an autoregressive model of order 4. d_{opt} is the optimal decomposition depth minimizing the denoising error.

Noise type	Thresholding nonlinearity	Thresholding selection rule			
		SURE	HEURISTIC SURE	FIXTHRES	MINIMAX
		d_{opt}	d_{opt}	d_{opt}	d_{opt}
N(0,δ^2)	soft	449.3±16.25	445.7±12.75	573.0±11.62	538.1±16.24
	hard	660.8±74.04	539.9±19.84	444.5±12.04	531.9±24.84
U[a,b]	soft	445.3±13.65	444.6±13.45	576.2±10.72	532.5±17.74
	hard	646.4±64.64	543.5±19.44	446.3±17.04	526.0±25.64
AR(4)	soft	363.5±20.74	363.3±14.14	394.2±13.32	390.2±13.52
	hard	526.4±93.04	382.6±15.74	365.4±15.84	481.9±25.24

5.2.1. Overall performances

In the wavelet based approach, the most efficient noise removing method with soft thresholding was the HEURISTIC SURE, which gave the lowest error averages (Table 5.2). The FIXTHRES rule showed the best performance with hard thresholding. When comparing soft and hard thresholding, the result depended upon the threshold selection rule and the added noise. The highest errors for all noise types with soft thresholding were produced by the FIXTHRES and MINIMAX methods and with hard thresholding by the SURE and HEURISTIC SURE methods.

In the wavelet packet based approach, the HEURISTIC SURE and FIXTHRES rules produced the lowest denoising errors (Table 5.3). FIXTHRES and MINIMAX approaches gave the largest errors when soft thresholding was used. Furthermore, with hard thresholding, the SURE and MINIMAX methods had the highest error averages except the AR(4)-noise when the FIXTHRES and MINIMAX indicated the poorest performance. When comparing the soft and hard thresholding methods, in all cases but FIXTHRES with all noise types and MINIMAX with AR(4)-noise, the soft thresholding was better in denoising the ECG.

Table 5.3. Denoising performance of wavelet packet denoising approach. Values are means and standard deviations of $||f_o - \hat{x}_i||_2$. See Table 5.2 for abbreviations.

Noise type	Thresholding non-linearity	Thresholding selection rule			
		SURE	HEURISTIC SURE	FIXTHRES	MINIMAX
		d_{opt}	d_{opt}	d_{opt}	d_{opt}
N(0,δ^2)	soft	466.1±22.75	447.8±20.95	866.3±27.37	594.1±20.46
	hard	705.4±66.13	526.8±21.05	505.7±19.55	699.1±27.63
U[a,b]	soft	462.2±19.75	448.7±20.25	859.1±25.77	591.1±17.76
	hard	685.3±61.53	526.8±20.14	507.7±18.95	695.5±31.43
AR(4)	soft	745.6±38.76	600.9±222.16	2074.5±114.67	1371.2±101.47
	hard	903.3±23.06	650.5±144.66	1416.1±117.57	1020.5±45.36

5.2.2. Performances within QRS-complex

The ability of denoising methods to remove noise from the high frequency parts of ECG was studied by determing the error values within QRS-complexes, see Tables 5.4 and 5.5. The wavelet methods were more efficient to remove the AR(4)-noise, when the errors were upto 4 times greater with wavelet packets. However, wavelet packet approaches showed better performances than wavelet approaches in removing normally or uniformly distributed noise within QRS-area especially as hard thresholding was used. The SURE method produced the lowest proportional error for the wavelet denoising using hard thresholding method for all noise types. With soft thresholding, except the AR(4)-noise, the FIXTHRES had the lowest proportional error within QRS-area. In the wavelet packet approach, the lowest proportional error was indicated most often by SURE or HEURISTIC SURE rules. Generally, denoising errors seem to concentrate on the QRS-area when the pure wavelet approach is employed. The QRS-complex area included proportionally less error when hard thresholding was used, except the FIXTHRES rule as the wavelet decomposition was used.

Table 5.4. Denoising performance of wavelet denoising approach measured within QRS-complexes. Values presented are means and standard deviations of $||f_o - \hat{x}_i||_2$. *The decomposition depths are the same as in Table 5.2. See Table 5.2 for abbreviations.*

Noise type	Thresholding nonlinearity	Thresholding selection rule			
		SURE	HEURISTIC SURE	FIXTHRES	MINIMAX
N(0,δ^2)	soft	286.2±21.4	300.5±18.5	258.5±10.6	445.8±18.4
	hard	274.6±25.4	259.9±12.2	319.7±16.7	287.9±17.9
U[a,b]	soft	283.6±19.6	297.3±19.0	259.1±11.9	439.5±19.2
	hard	269.5±20.0	262.1±12.3	321.7±18.1	289.1±17.5
AR(4)	soft	208.6±13.9	230.0±9.9	214.3±7.7	200.7±8.4
	hard	221.9±28.2	209.7±10.0	224.4±10.1	226.2±22.6

When comparing the performance within QRS-complexes using absolute error measurement, HEURISTIC SURE or FIXTHRES gave most often the lowest error values for the wavelet approach. In the wavelet packet approach, the best performances were found by SURE and HEURISTIC SURE rules. Further, hard thresholding method gave lower absolute errors with all variations of denoising methods, when the wavelet packet approach was used. With pure wavelet denoising, results were the same except with FIXTHRES, when soft thresholding gave lower error. SURE

Table 5.5. Denoising performance of wavelet packet denoising approach measured within QRS-complexes. Values presented are means and standard deviations of $||f_o - \hat{x}_i||_2$. The decomposition depths are the same as in Table 5.3. See Table 5.2 for abbreviations.

Noise type	Thresholding nonlinearity	Thresholding selection rule			
		SURE	HEURISTIC SURE	FIXTHRES	MINIMAX
N(0,δ^2)	soft	271.2±19.1	301.8±28.7	607.1±22.4	381.3±19.4
	hard	270.9±27.6	253.9±17.0	272.4±16.6	287.6±23.4
U[a,b]	soft	267.1±18.0	300.5±27.7	602.7±23.2	377.5±18.6
	hard	264.9±24.8	264.4±16.4	276.5±16.1	286.6±18.2
AR(4)	soft	324.0±34.1	308.8±39.9	866.2±61.6	562.5±32.2
	hard	320.8±23.2	258.3±42.7	493.8±36.9	391.4±33.7

and MINIMAX showed also better denoising performance for the AR(4)-noise with soft thresholding.

5.2.3. Checking the error signals

Because numerical error measures do not necessarily tell everything about noise removal, it is useful to check the denoised signals visually. There probably exist such strange signal patterns which can not be predicted from error values. It is important to see the error signal between the noisy and the denoised signal, because then one can observe how the error is localized within the cardiac cycle. In Figure 5.5, the successful result of denoising ECG with normally distributed noise by wavelet approach using the MINIMAX method is shown. The error between the original and denoised ECG is mainly concentrated within the QRS-complexes.

Sometimes performing the signal denoising does not mean that only the added noise has been removed. ECG can be very clean after denoising and the error signal has a large amplitude, which means that the denoising method has not only been robust in removing added noise but also has seriously altered the ECG signal (Figure 4, paper III). This result was observed particularly with wavelet packet approach when the FIXTHRES approach was applied. With the wavelet based denoising hard thresholding showed spiky patterns in the error signal which are seen also in the denoised ECG, which was typical with all noise types when the SURE and MINIMAX rules were used (Figure 5, paper III). The wavelet packet based approaches had difficulties in removing the noise as can be seen in Figure

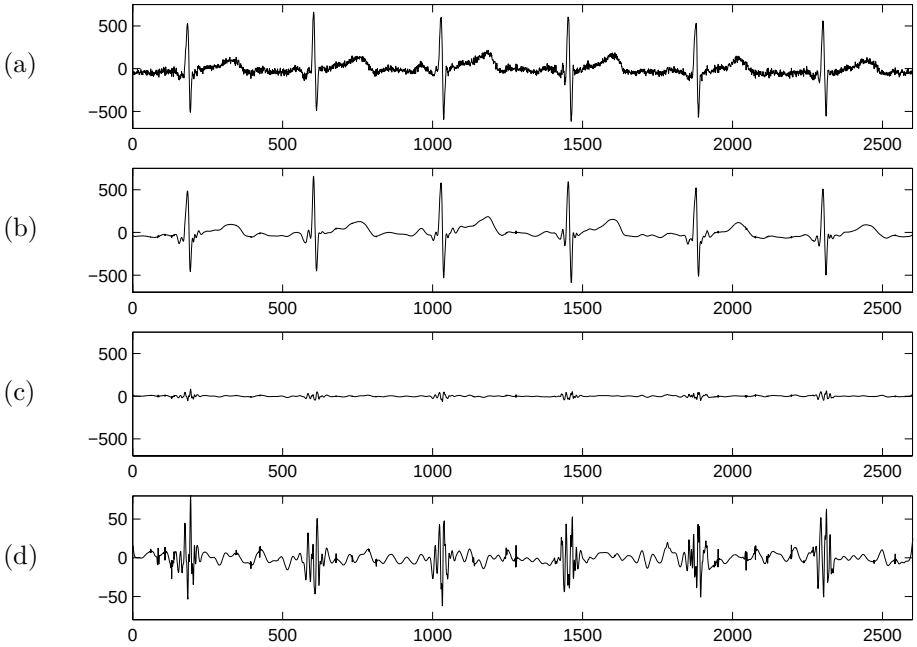

Fig. 5.5. **(a) ECG with added normally distributed white noise. (b) The result of the noise removal performed by wavelet based approach using** MINIMAX **thresholding selection rule with soft thresholding nonlinearity. (c) The error signal between the original and denoised ECG. (d) The error signal in an enlarged scale.**

5.6, where the error signal includes a large random component due to non-white noise. This was common particularly when SURE and MINIMAX were applied, and also often with other rules with hard thresholding.

5.2.4. Discussion

In this work new wavelet and wavelet packet based noise removal schemes were studied using ECG with simulated noises. The performances of several variations of denoising including thresholding rules and the type of non-linearity were compared. A level dependent scaling of the thresholds was used for adjusting to the non-white noise structure.

Wavelet and wavelet packets showed different results which is mainly due to the different division strategies of the signal decomposition structures. Furthermore, these analyzing functions also differ in shape. The wavelet-based approach produces the dyadic decomposition structure constant for all signals. Correspond-

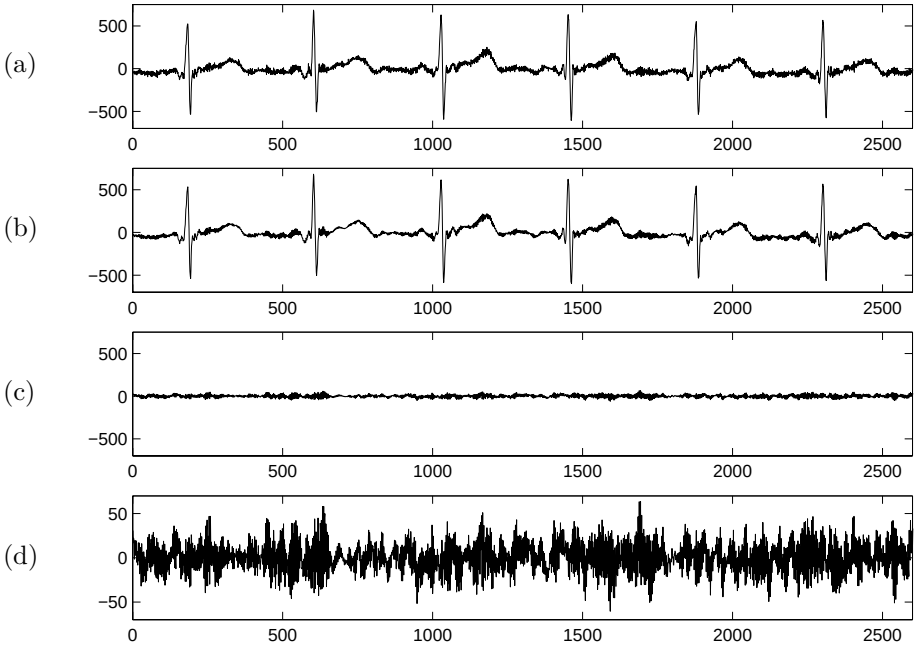

Fig. 5.6. (a) ECG with added noise generated by an autoregressive model of order 4. (b) The result of the noise removal performed by wavelet packet based approach using SURE thresholding selection rule with hard thresholding nonlinearity. (c) The error signal between the original and denoised ECG. (d) The error signal in an enlarged scale.

ingly, the wavelet packet approach is an adaptive method using an optimization of the best tree decomposition structure independently for every signal, which can be quite irregular and reach very fine features. Generally, this kind of adaptivity did not offer an improved overall denoising performance compared to a more simple wavelet approach. Only HEURISTIC SURE rule with soft thresholding produced a superior result. Inside the high-frequency parts of the ECG the situation varied more. The visual examination of the error signal was remarkable showing the localization of the error within the cardiac cycle as well as its nature. The obtained error values can not directly indicate the improvement for the ECG waveform detection. However, a large error within a certain area suggest an impaired accuracy of the waveform measurement, which can only be quantified by the appropriate tests.

The performance of the wavelet packet based noise removal may be improved by adapting the signal decomposition structure to the changing signal characteristics as presented by Xiong *et al.* (1997), where the signal was divided into segments of variable lengths using dynamic programming setting. The approach involves calculating optimized wavelet packet decompositions independently for each seg-

ment. This procedure would probably be useful for ECGs, which are corrupted by different types of noises with time varying magnitudes.

Bruce & Gao (1996) studied soft and hard non-linearities and derived a theoretical result that soft thresholding has higher bias, but lower variance than hard thresholding. This was also supported by their experiments. This is probably due to the basic properties of these two approaches: the hard thresholding function has a discontinuity, and the soft thresholding function shrinks all big coefficients towards zero. Their results were obtained for FIXTHRES and MINIMAX rules as wavelet denoising approach was applied.

The observations found in this work support those findings partly, as with these two threshold selection rules soft thresholding tend to give higher overall error values. Nevertheless, hard thresholding gave constantly bigger errors within QRS-area as FIXTHRES rule was used. The wavelet packet approach showed different results indicating larger error rates in all cases for soft than hard thresholding within QRS-complexes. With SURE and HEURISTIC SURE rules, the soft thresholding non-linearity tends to give a more acceptable overall denoising result compared to hard thresholding. However, it should be noted that with using soft non-linearity, the error between the original and denoised ECG was concentrated within the QRS-complexes. In that case, the absolute error values were generally bigger than using hard non-linearity. Only FIXTHRES rule with hard non-linearity showed with wavelet approach proportionally higher error within QRS-area than soft non-linearity. It is apparent that soft and hard thresholding cause different high-frequency balances. This is due to fact that the soft thresholding in general produces proportionally a larger error within QRS-area by rounding off towards zero the coefficients bigger than the threshold, which obviously touches the coefficients including a remarkable amount of information about the original ECG.

5.3. Analysis of APD variability

Examples of Poincaré plots of RR interval and APD_{90} time series in sinus rhythm and during steady-state pacing are shown in Figure 2 in paper IV. The plots of RR intervals and APD_{90} typically showed similar comet shaped plots characterized by increased next interval differences of long R intervals and APD_{90}, respectively, relative to short ones in sinus rhythm. Only minimal fluctuations of RR intervals were observed during steady-state pacing due to subtle fluctuation in AV nodal conduction, but the plots of APD_{90} showed clear long-term fluctuations.

Results of quantitative analyses of Poincaré plots of RR intervals, APD_{90} and APD_{50} in sinus rhythm and the end of constant rate pacing are presented in Table 5.6. In sinus rhythm, the ratio between instantaneous and long-term variability (SD1/SD2 ratio) of RR intervals and APD did not differ, but the standard deviation of all APD intervals was only 8 % of the standard deviation of all RR intervals. Both SD1 and SD2 of APD_{90} and APD_{50} were significantly smaller than SD1 and SD2 of RR intervals in sinus rhythm ($p < 0.001$ for both). A correlation was observed between the SD1 of RR intervals and SD1 of APD in sinus rhythm ($r = 0.64$, $p < 0.05$), but the SD2 of RR intervals and SD2 of APD did not correlate with each other (r=0.32, NS). During constant rate atrial pacing, quantitative analysis revealed only minimal variability of RR intervals. Similarly, no clear instantaneous beat-to-beat variability was observed in APD, but the long-term variability (SD2) of APD_{90} and APD_{50} were larger than the SD2 of RR intervals ($p < 0.001$ for both) (Table 5.6, Figure 2 in paper IV).

Table 5.6. Quantitative analysis of Poincaré plots of RR intervals and action potential durations in sinus rhythm and during steady-state pacing. Values are means and standard deviations. SD_{tot} *is standard deviation of all intervals;* SD1 *is standard deviation of short term variability;* SD2 *is standard deviation of long-term variability;* SD1/SD2 *is ratio between short-term and long-term standard deviation.*

	Mean	SD_{tot}	SD1	SD2	SD1/SD2
	ms	ms	ms	ms	
Sinus rhythm					
RR intervals	785 ± 89	35 ± 13	15 ± 9	46 ± 17	0.30 ± 0.11
APD_{90}	270 ± 17	2.8 ± 0.8	1.2 ± 0.3	3.9 ± 1.5	0.33 ± 0.16
APD_{50}	229 ± 12	3.8 ± 2.4	1.1 ± 0.3	4.3 ± 2.0	0.33 ± 0.23
Steady-state pacing					
RR intervals	600 ± 0	1.4 ± 0.7	1.3 ± 0.8	1.6 ± 0.8	0.79 ± 0.21
APD_{90}	227 ± 14	1.7 ± 0.5	0.9 ± 0.3	2.2 ± 0.7	0.45 ± 0.16
APD_{50}	194 ± 11	1.9 ± 0.9	0.8 ± 0.3	2.4 ± 1.0	0.39 ± 0.16

5.3.1. Discussion

Duration of the ventricular repolarization depends on the complex interaction between the HR and fluctuation of autonomic tone. There is an immediate cycle length dependency of the duration of repolarization and there is also a hysteresis effect of previous cycle lengths on the duration of subsequent repolarization (Lau & Ward 1989). In addition to rate-dependent effects, autonomic tone has direct influences on ventricular repolarization phase. All these influences have different temporal feedback loops, which control the duration of repolarization. A two-dimensional vector analysis described here is able to quantify the temporal dynamics of repolarization time by separating the instantaneous and long-term variability from each other without a requirement of stationarity of the data or periodicity of variability, which are essential requirement in spectral analysis methods. In sinus rhythm, the shape of the plots of repolarization time resembled the plots of successive RR intervals showing that the dynamics of HR and APD have similar temporal characteristics.

The SD of all APD intervals was only 8 % of the SD of all RR intervals, when analyzed from the 5-minute segments in sinus rhythm. These results suggest that due to a small overall variability, an accurate measurement with a high sampling frequency and a high quality of the signal are essential for reliable quantitative analysis of variability of the repolarization time. These requirements may be difficult to achieve by analyzing the QT interval dynamics from ambulatory ECG recordings. It should be noted, however, that there are potential technical errors in the measurement of MAPs caused by poor electrode contact and the effects of fluctuations in blood pressure and contractility of the ventricle on the signal. The sampling frequency and filtering may also influence the analysis of signal characteristics. Careful automatic and manual editing of the questionable portions of the signals performed here should, however, minimize the effects of artifacts on results.

Instantaneous beat-to-beat variability of the APD was related to the short-term fluctuations of RR intervals in sinus rhythm, indicating that respiratory vagal modulation of HR has significant indirect effects on the dynamics of ventricular repolarization. In addition to subtle instantaneous beat-to-beat fluctuations, there were clear long-term oscillations in the duration of ventricular repolarization. These fluctuations were not strongly related to HR variability, suggesting that there are intrinsic low frequency fluctuations in repolarization time. This was confirmed by observation of clear long-term fluctuation of APD during constant rate pacing. The observation of clear long-term repolarization variability reduced significantly during constant rate pacing, suggesting that long-term HR fluctuation still has a major influence on repolarization variability in sinus rhythm. This concept is also supported by results of Merri *et al.* (1993), who demonstrated a significant coherence between spectral measures of HR variability and QT interval variability measured from Holter recordings.

5.4. Spectral estimation using wavelet transforms

This section presents the spectral estimation of the RR interval time series using wavelet and wavelet packet transforms. These results are not given in any of the original papers enclosed in the thesis. An objective was to look spectral changes linked to some cardiac events. The analyzed signals last approximately an hour, when the purpose was to quantify the short term variation in RR intervals. As it was suggested in a theoretical section above, wavelet transforms are presented by the squared magnitudes of the transform coefficients.

In discrete wavelet transform a signal decomposition was made on six levels using the Coiflet function of order 5. The decomposition conforms to dyadic splitting of the frequency spectrum to the wavelet scales. For example, in Figure 5.7, the discrete wavelet transform of RR intervals obtained from a healthy young person during a noradrenaline administration is shown. The transform clearly shows the spectral evolution in HRV due to continuous and increasing drug injection. Levels 2 and 3, which contain information from respiratory related HRV, indicate a variability augmenting as the dose of the drug administration increases. Level 4, which mostly includes variability linked to blood pressure regulation, shows less variability in the course of the injection than the level 3. The amplitudes on the levels 3 and 4 diminish notably toward the end of the recording. Overall, HRV responses varied largely between the persons, and time series were nonstationary. The discrete wavelet transform using other wavelet functions, such as Daubechies function of order 12, gave very similar results. This suggests that choosing between the wavelet functions of the same kind is not a critical task.

Further examples are given from the analysis of RR intervals obtained from patients with ventricular fibrillation (Figure 5.8). The analysis was made for signals recorded one hour before this serious event in order to monitor the spectral changes possibly predicting the event. The discrete wavelet transform is capable to show the spectral changes also in these recordings. Some transient events in a time series altered the wavelet spectrum practically on all levels (Figure 5.8a). However, these changes disappear rapidly which support an idea of monitoring the time evolution of the wavelet spectrum.

As a comparison, RR intervals were analyzed using the wavelet packet transform with an optimized division of the frequency spectrum to wavelet packet scales. The decomposition was made on six levels using the Coiflet wavelet packet function of order 5. In Figures 5.9 and 5.10 the wavelet packet transforms of RR intervals are shown. The presentations show integrated wavelet packet spectra matching the low frequency (LF) and high frequency (HF) bands in RR interval time series. The wavelet packet spectrum is slightly smoother than the above discrete wavelet spectrum, but it can also show similar spectral changes. Also with this approach replacing the wavelet packet function with a nearly similar one did not alter the results.

Due to preliminary stage of the study it was not possible to point out figures which might regularly predict ventricular fibrillation using either wavelet or wavelet packet transform. However, in some cases RR interval variability recognizably diminished at the end of the analysis period (Figure 5.8b, Figure 5.10b) and thus

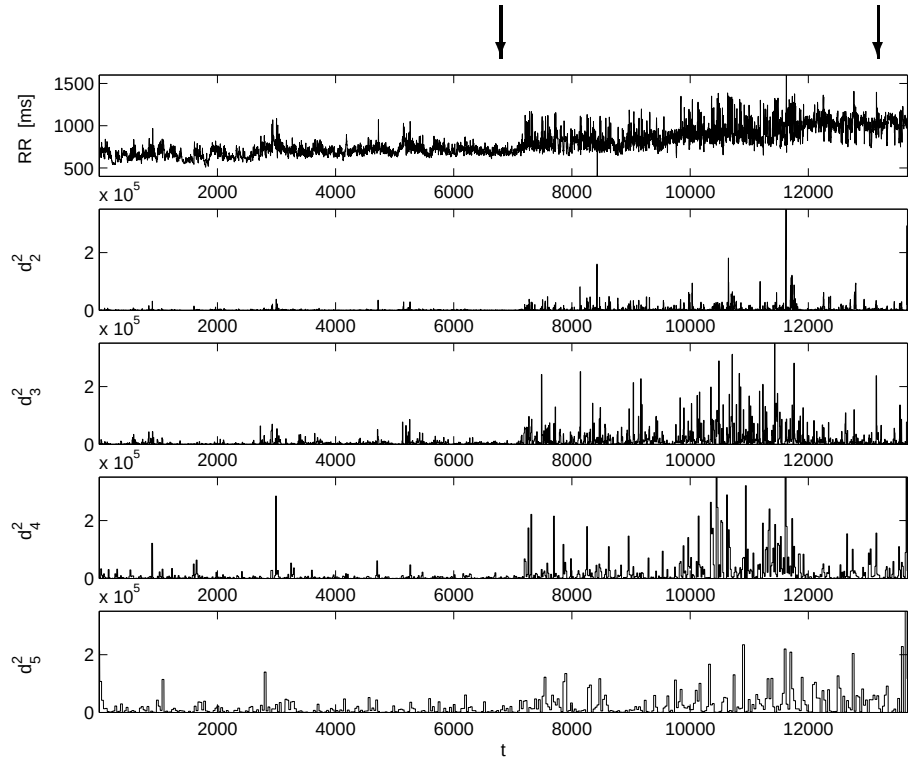

Fig. 5.7. **RR intervals recorded during a noradrenaline administration (top). The squared wavelet coefficients on levels 2-5 (lower panels). The start and end of the injection is marked by arrows.**

prior to the onset of ventricular fibrillation. Burst-like patterns were observed in many cases, which result mainly on levels 2 and 3 in the wavelet transform (Figures 5.8a,b) and is also visible on the HF band in the wavelet packet transform (Figures 5.10a,b).

5.4.1. Discussion

The study of RR interval spectrum was presented by means of wavelet and wavelet packet transforms. The analysis involved a time-dependent estimation of short-term fluctuations of RR intervals. In analogy with Fourier analysis the aim was to present the signal as a linear superposition of basis functions called wavelet and wavelet packet functions. The basis functions differ from complex exponentials connected to Fourier analysis so that they do not oscillate infinitely. Many signals obviously correlate better with a finite waveform which make wavelets and wavelet

packets more capable for the analysis of nonstationary signals. In this approach the analyzing functions are as well often properly localized in time.

The wavelet approach made a dyadic division of the frequency spectrum of the signal. The wavelet packet scheme utilized an optimized division. The wavelet packet analysis is a flexible approach, because the division of the frequency spectrum can be regular, performed using optimized schemes or it can be made also manually. In pure wavelet method the division need not be dyadic with a dilation factor $a = 2$, but values $a > 2$ are also possible. A noninteger rational value, for example $a = \frac{3}{2}$, can provide a sharper frequency localization for the wavelet base (Daubechies 1992). However, choosing the value $a = 2$ provides the simplest construction of wavelet bases, and multiresolution scheme can work only with rational dilation factors (Daubechies 1992). Wavelet packet transform has been made to adapt to the signal characteristics by calculating an optimized decomposition for the whole RR interval time series (Wiklund *et al.* 1997). Further, it might be useful to adapt the decomposition continuously by obtaining a new decomposition as signal properties change significantly (Xiong *et al.* 1997).

Time-frequency analysis was discussed earlier in this thesis. Wavelet methods have improved resolution properties compared to short time Fourier transform (STFT). Wavelet methods differ from AR spectral estimation methods so that the model order need not be estimated, which can sometimes be a difficult task. Matching pursuit (MP) approach was suggested superior to wavelet method in Akay & Mulder (1996), where MP method was applied to fetal heart rate variability (FHRV) analysis demonstrating its advantages for time-frequency analysis of nonstationary signals. Overall, wavelet and wavelet packet approaches have been introduced for interpretation of nonstationary signals (Akay 1995, Priestley 1996). According to theory these methods monitor and detect signal properties in time-scale domain instead of time-frequency domain.

The discrete wavelet transform has been applied to HRV analysis during a simulated stress test (Tsuji & Mori 1994) and during carotid surgery (Akay *et al.* 1993). The wavelet packet transform with an optimized decomposition was used to analyze HRV during a set of consecutive autonomic function tests and compared to discrete cosine transform and short-time Fourier transform by Wiklund *et al.* (1997). A wavelet filtering scheme may be used to eliminate very slowly oscillating components (detrending) from RR interval time series (Wiklund *et al.* 1997). Yang & Liao (1997) used a wavelet approach to simulate RR interval time series and to construct a decomposition scheme. In this study, the emphasis was on monitoring HRV along with noradrenaline injection and predicting ventricular fibrillation. The results demonstrate that both discrete wavelet and wavelet packet transform can successfully analyze the RR interval spectrum. The advantages of wavelet and wavelet packet methods for the analysis of nonstationary signals were also shown.

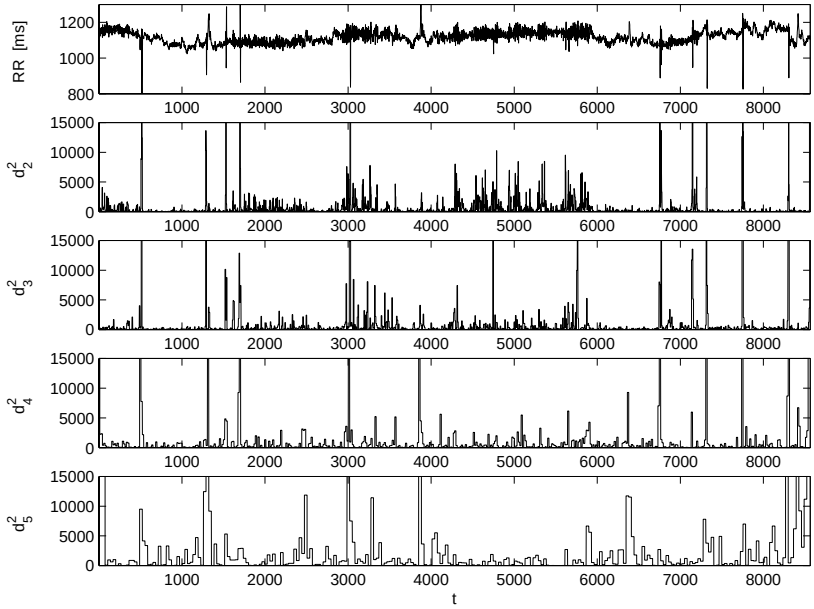

(a)

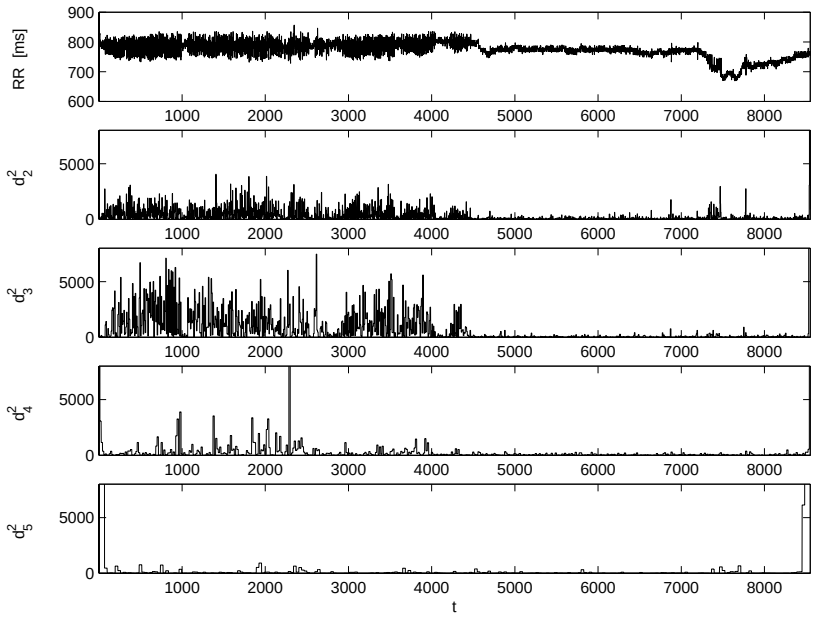

(b)

Fig. 5.8. Two RR interval time series recorded during one hour prior to the onset of ventricular fibrillation (top panels). The squared wavelet coefficients on levels 2-5 (lower panels).

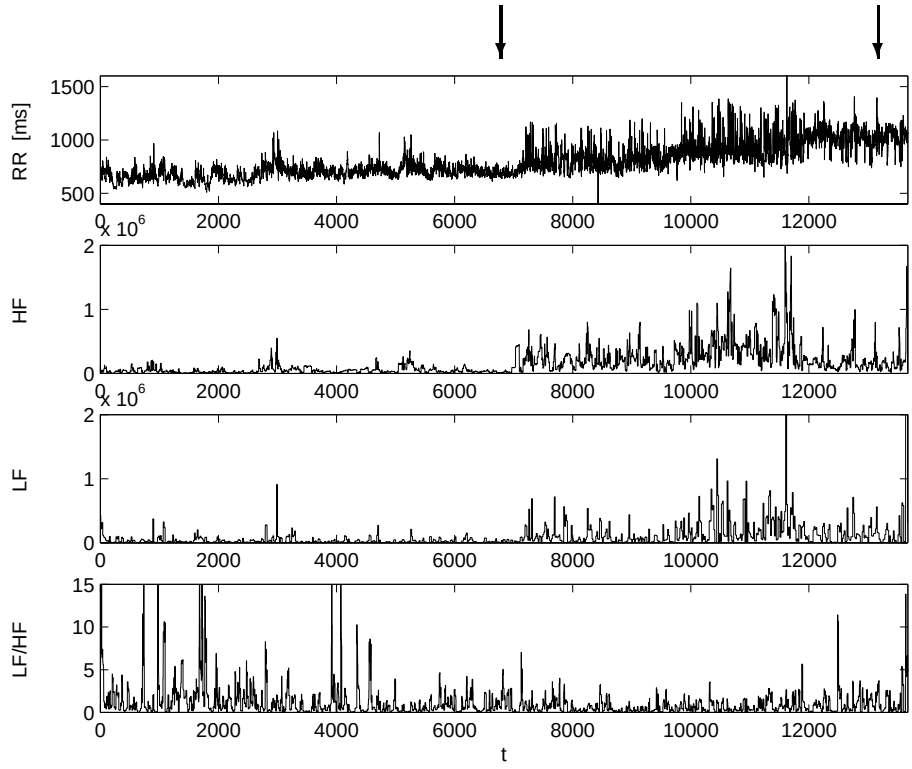

Fig. 5.9. RR intervals recorded during a noradrenaline administration (top). The wavelet packet spectra matching the high frequency (HF) and low frequency (LF) bands (middle), and the LF/HF-ratio (bottom). The start and end of the injection is shown by arrows.

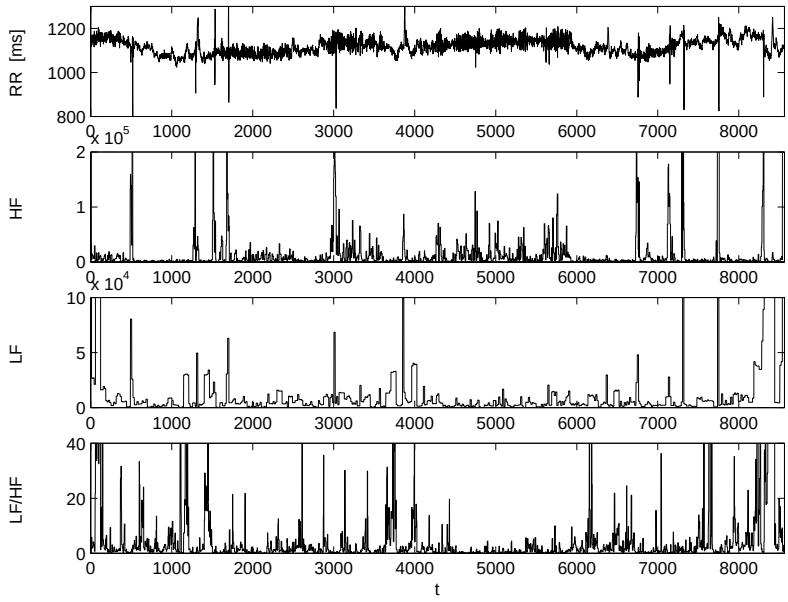

(a)

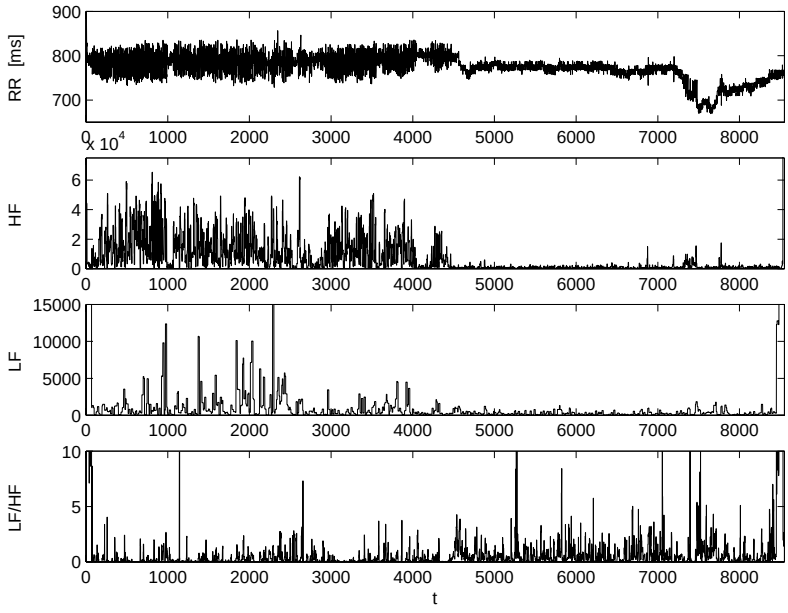

(b)

Fig. 5.10. Two RR interval time series recorded during one hour prior to the onset of ventricular fibrillation (top panels). The wavelet packet spectra matching the high frequency (HF) and low frequency (LF) bands (middle panels), and the LF/HF-ratio (bottom panels).

6. Summary and conclusion

Quantifying the variability in cardiovascular signals provides information about autonomic neural regulation of the heart and the circulatory system. Neural regulation due to the sympathetic and parasympathetic divisions of the autonomic nervous system involve responses to respiration, blood pressure regulation and thermoregulation. Many cardiovascular diseases, medication and physical and mental stress alter the degree of neural regulation. It is the amount and balance of the sympathetic and parasympathetic regulations which is often being quantified. Several factors thus have an indirect effect on these signals. Artifacts and several types of noise are also contamined together with a useful information. All these data can be observed in the dynamics of both heart rate and ventricular repolarization duration.

The ambulatory measurement setting produces a further demand on the recording and analysis of signals. However, there is an increasing need for extending the ambulatory recording and increasing the duration of data acquisition. This trend naturally leads to a greater mass of data and a need for the development of more sophisticated and robust signal analysis schemes.

RR interval recording, which is used to describe heart rate variability (HRV), involves a noninvasive and easy approach to gain information on cardiovascular function. Accurate recording equipment has been developed for this technique. The variability in RR intervals is often so large that most of the analysis methods may be resolved fairly well in noticeably noisy conditions. Nevertheless, there are important factors which should be taken into account when RR interval measurement is used. The accuracy of HRV measurement is a consequence of the sampling accuracy of an ECG and the properties of the method quantifying the signal variability. For example, spectral analysis methods may not fit conditions where some time domain methods can be used. The reproducibility of the measurement is affected by the lack of precisely controlled conditions and variation of the results thus appear among repeated recordings. This kind of variation is characteristic for an indirect acquisition of information from a biological system. Overall, the variation is an unavoidable condition and has to be kept in mind when interpreting the results between repeated recordings made for a single person as well as comparing the results obtained from different patient sets. RR interval recordings often

include abnormal intervals, which may be due to heart rhythm disturbances or errors in signal detection of a technical or physiological origin. Time series including data points differing from a normal sinus rhythm sometimes carry important information, but may not be, as such, suitable for an analysis performed by all HRV indices. Furthermore, non-periodic changes in RR intervals due to physiological responses can also impair the stationarity of the signal. Several approaches for correcting artifacts from time series and eliminating their effect on HRV indices have been developed.

The above points also concern ventricular repolarization duration (VRD) measurement, which has additional requirements. The detection of the onset of Q wave and the offset of T wave has turned out to be a difficult task due to poor signal-to-noise ratio. To solve this problem and, when the interest actually lies on the measurement of the ventricular repolarization duration, $\mathrm{RT}_{\mathrm{max}}$ interval has been chosen for a QT interval estimate. In addition, VRD time series has a much lower variability than RR intervals, which places higher requirements on the sampling frequency of the ECG. The variability of VRD time series has been more frequently extracted from an ambulatory ECG with an interpolation procedure to obtain an adequate time resolution for time interval measurement. There is thus a need for data acquisition equipment, which can collect and store ambulatory ECG with a higher sampling frequency than ordinary Holter devices do. It was shown by the experiments in this study that VRD variability measurement involve potential noise sources and errors, which should be kept in mind during the analysis phase.

An improved accuracy of VRD variability estimation can be attained by the measurement of action potential duration (APD) variability, which is an invasive procedure. However, there may exist technical problems in monophasic action potential (MAP) measurements mainly due to poor electrode contact and the effects of fluctuations in blood pressure and contractility of the ventricle. APD intervals showed a low variability compared to RR intervals, which further support the requirements given for the VRD variability estimation. The study of the instantaneous APD variability related to the short-term RR interval variability in sinus rhythm, indicated that the respiratory vagal modulation of heart rate modify indirectly the ventricular repolarization duration. Intrinsic long term fluctuations were observed in APD variability, but the constant rate pacing experiment showed that the long-term heart rate fluctuation is still the most essential factor determining the VRD dynamics in sinus rhythm.

The most simple parameters describing the variability in a time series are statistical indices in time domain, which has traditionally been widely used. The indices referred in this study as time domain methods contain scarcely any information on periodic fluctuations, but rather measure the average or maximum amplitude of the variability. On the other hand, when the information content of these indices may be limited, they suffer less from nonstationarities in a time series.

The periodic fluctuations in cardiovascular variability signals have been analyzed using spectral estimation performed by Fourier and parametric (autoregressive, AR) techniques. The main objective has been to decompose the periodic fluctuations due to various sources into well separated components in the power

spectrum. Furthermore, some emphasis has been placed on the estimate of variability (power) included in a single component and of the central frequency of the component. The main components in the power spectrum have been linked to the neural regulation of the heart due to autonomic nervous system through its sympathetic and parasympathetic parts. In this thesis, the stress was on the estimation of the power spectrum using an AR model of a time series. An approach for estimating the powers and the spectra related to components using residue calculation was also presented.

Observing the evolution of the spectral properties of the signal is of more current interest. The temporal location of the spectral components has often been shown to give more information than a single "average" spectrum. Time-frequency methods include short-time Fourier transform and Wigner distribution, when approaches based on the parametric time series modelling are referred to time-variant spectral analysis methods. The objective has also been to take account existing nonstationarities in time series.

Wavelet transforms are fairly novel approaches in cardiovascular signal analysis, where they may be suitable for processing of nonstationary signals. In this study the basic theory of wavelet methods was briefly introduced including multiresolution, subband filtering and wavelet packet analysis schemes. The theory related to signal denoising with several principles for the threshold selection was presented. The methods were then applied to remove simulated noise from ECG. The experiments showed that wavelet packet approaches with adaptation by means of the optimization of the best tree decomposition structure were not generally more efficient than the basic wavelet approach. Denoising errors seemed to concentrate on the high-frequency parts of the ECG when the pure wavelet approach was employed. Furthermore, the soft thresholding nonlinearity tend to produce proportionally a larger error than the hard thresholding nonlinearity within the QRS-complex.

The motivation of estimating the spectrum of RR interval time series using wavelet transforms was based on the idea of a more suitable basis function compared to Fourier transforms and that any assumptions concerning signal stationarity was not made. In addition, wavelet transforms have flexible resolution properties which means, for example, that they can detect high frequency components with a good time resolution. The results show that wavelet transforms were capable to estimate the evolution of the spectrum of RR interval time series obtained by an ambulatory recording in conjunction with a drug injection and prior to the onset of ventricular fibrillation. In this application wavelet transforms are closely related to time-frequency and time-variant spectral analysis methods.

There is an obvious need of standardization and definition of the measurement and analysis schemes of the cardiovascular variability signals. The meaning of some variability measures is more complicated than often regarded which sometimes result in variable and erroneous conclusions. The Task Force report (Task Force of ESC & NASPE 1996) can be seen as a step along this way, although it contains chiefly a report of performed investigations without deeper arguments for methods and their application.

The development of analysis procedures for cardiovascular variability signals

will continue and novel methods will be applied in this field. It is probable that approaches for the analysis of nonstationary signals will be more extensively used in the future. As these signals can only be assumed stationary within some period, there is also an interest to analyze data obtained under varying conditions like autonomic function tests. Detecting nonlinearities is also of growing interest as some approaches were reviewed in this thesis. Novel analysis schemes may offer additional and valuable information when the characteristics of methods are sufficiently described.

References

Adamson P, Huang M, Vanoli E, Foreman R, Schwartz P & Hull S (1994) Unexpected interaction between β-adrenergic blockade and heart rate variability before and after myocardial infarction: a longitudinal study in dogs at high and low risk for sudden cardiac death. Circulation 90: 976–982.

Akay M (1995) Wavelets in biomedical engineering. Ann Biomed Eng 23: 531–542.

Akay M, Landesberg G, Welkowitz W, Akay YM & Sapoznikov D (1993) Carotid-cardiac interaction: Heart rate variability during the unblocking of the carotid artery. In: Sideman S & Beyar R (eds) Interactive Phenomena in the Cardiac System. Plenum Press, New York, p 365–372.

Akay M & Mulder E (1996) Examining fetal heart-rate variability using matching pursuits. IEEE Eng Med Biol 15(5): 64–67.

Akselrod S, Gordon D, Madved J, Snidman N, Shannon D & Cohen R (1985) Hemodynamic regulation: investigation by spectral analysis. Am J Physiol 249: H867–H875.

Babloyantz A & Destexhe A (1988) Is the normal heart a periodic oscillator. Biol Cybern 58: 203–211.

Baevskij R, Kirillov O & Kletskin S (1984) Mathematical Analysis of the Changes in Cardiac Rhythm During Stress. Nauka, Moscow.

Barbaro V, Bartolini P & Fierli M (1991) New algorithm for the detection of the ECG fiducial point in the averaging technique. Med Biol Eng Comput 29: 129–135.

Basano L, Ottonello P, Poggi A, Adezati L, Semino S, Ubaldi P & Viviani G (1995) An instrument for real-time spectral estimation of heart rate variability signal. Comput Methods Programs in Biomed 47: 229–236.

Baselli G & Cerutti S (1985) Identification techniques applied to processing of signals from cardiovascular systems. Med Inf 10(3): 223–235.

Baselli G, Cerutti S, Civardi S, Lombardi F, Malliani A, Merri M, Pagani M & Rizzo G (1987) Heart rate variability signal processing: A quantitative approach as an aid to diagnosis in cardiovascular pathologies. Int J Bio Med Comput 20: 51–70.

Bellavere F (1995) Heart rate variability in patients with diabetes and other noncardiological diseases. In: Malik M & Camm A (eds) Heart rate variability. Futura Publishing Company, Armonk, p 507–516.

Bernardi L, Ricordi L, Lazzari P, Soldá P, Calciati A, Ferrari M, Vandea I, Finardi G & Frantino P (1992) Impaired circulation modulation of sympathovagal modulation of sympathovagal activity in diabetes. Circulation 86: 1443–1452.

Berntson G, Quigley J, Jaye F & Boysen S (1990) An approach to artifact identification: Application to heart period data. Psychophysiology 27(5): 586–598.

Bianchi A, Mainardi L, Petrucci E, Signorini M, Mainardi M & Cerutti S (1993) Time-variant power spectrum analysis for the detection of transient episodes in HRV signal. IEEE Trans Biomed Eng BME-40(2): 136–144.

Bigger J, Rolnitzky L, Steinman R & Fleiss J (1994) Predicting mortality after myocardial infarction from the response of RR variability to antiarrhythmic drug therapy. J Am Coll Cardiol 23: 733–740.

Borland (1991) Turbo C++ 3.0 for Windows. Programmer's Guide. Borland International, Inc., Scotts Valley.

Bruce AG & Gao HY (1996) Understanding WaveShrink: Variance and bias estimation. Biometrika 83(4): 727–745.

Calcagnini G, Censi F, Camera A, Lino S & Cerutti S (1996) Interference and phase locking patterns between low and high frequency rhythms of cardiovascular signals in normal subjects. Proc 18th Annual International Conference of IEEE–EMBS, Amsterdam.

Casolo G, Balli E, Taddei T, Amuhasi J & Gori C (1989) Decreased spontaneous heart rate variability in congestive heart failure. Am J Cardiol 64: 1162–1167.

Casolo G, Stroder P, Signorini C, Calzolari F, Zucchini M & Balli E (1992) Heart rate varibility during the acute phase of myocardial infarction. Circulation 85: 2073–2079.

Cerutti S, Bianchi A, Baselli G, Civardi S, Guzzetti S, Malliani A, Pagani A & Pagani M (1989) Compressed spectral arrays for the analysis 24-hr heart rate variability signal. Enhancement of parameters and data reduction. Comput Biomed Res 22: 424–441.

Choi B (1992) ARMA Model Identification. Springer-Verlag, New York.

Clouet J, Fouque J & Postel M (1995) Estimation of local power spectral densities for non-stationary signals using wavelet transform. Math Comput Simulat 38: 183–188.

Cohen A & Kovacević J (1996) Wavelets: The mathematical background. Proc IEEE 84(4): 514–522.

Cohen L (1989) Time-frequency distributions - a review. Proc IEEE 77(7): 941–981.

Cohen M, Hudson D & Deedwania P (1996) Applying continuous chaotic modeling to cardiac signal analysis. IEEE Eng Med Biol 15(5): 97–102.

Coifman R & Wickerhauser M (1992) Entropy-based algorithms for best basis selection. IEEE Trans Inform Theory 38(2): 713–718.

Coumel P, Fayn J, Maison-Blanche P & Rubel P (1994) Clinical relevance of assessing QT dynamicity in Holter recordings. J Electrocardiology 27S: 62–66.

Daubechies I (1992) Ten Lectures on Wavelets. SIAM, Philadelphia.

Decker J, Schouten E, Klootwijk P, Pool J & Kromhout D (1994) Association between QT interval and coronary heart disease in middle-aged and elderly men - The Zutphen Study. Circulation 90: 779–785.

Dimier-David L, Billon N, Costagliola D, Jaillon P & Funck-Brentano C (1994) Reproducibility of non-invasive measurement and of short-term variability of blood pressure and heart rate in healthy volunteers. Br J Clin Pharmacol 38: 109–115.

Donoho D (1993) Nonlinear wavelet methods for recovery of signals, densities, and spectra from indirect and noisy data. Proc Symp Appl Math 47: 173–205.

Donoho D (1995) De-noising by soft-thresholding. IEEE Trans Inform Theory 41(3): 612–627.

Donoho D & Johnstone I (1994) Ideal spatial adaptation by wavelet shrinkage. Biometrika 81(3): 425–455.

Donoho D & Johnstone I (1995) Adapting to unknown smoothness via wavelet shrinkage. J Am Statist Assoc 90: 1200–1224.

Eckberg D (1983) Human sinus arrhythmia as an index of vagal cardiac outflow. Respirat Environ Exercise Physiol 54(4): 961–966.

Extramiana F, Huikuri H, Neyroud N, Koistinen J, Coumel P & Maison-Blanche P (1997) QT rate adaptation: A new index to discriminate patients with and without ventricular arrhythmias following myocardial infarction (abstract). Circulation 96(8): 4014.

Farrell T, Bashir Y, Cripps T, Malik M, Poloniecki J, Bennett E, Ward D & Camm A (1991) Risk stratification for arrhythmic events in postinfarction patients based on heart rate variability, ambulatory electrocardiographic variables and the signal averaged electrocardiogram. J Am Coll Cardiol 18: 687–697.

Ferrari GD, Mantica M, Vanoli E, Hull S & Schwartz P (1993) Scopolamine increases vagal tone and vagal reflexes in patients after myocardial infarction. J Am Coll Cardiol 22: 1327–1334.

Franz G (1991) Method and theory of monophasic action potential recording. Prog Cardiovasc Dis 33: 347–368.

Freeman R, Saul J, Roberts M, Berger R, Broadbridge C & Cohen R (1991) Spectral analysis of heart rate in diabetic neuropathy. Arch Neurol 48: 185–190.

Friesen G, Jannett T, Jadallah M, Yates S, Quint S & Nagle H (1990) A comparison of the noise sensitivity of nine QRS detection algorithms. IEEE Trans Biomed Eng 37: 85–98.

Furlan R, Guzzetti S, Crivellaro W, Dassi S, Tinelli M, Baselli G, Cerutti S, Lombardi F, Pagani M & Malliani A (1990) Continuous 24-hour assessment of neural regulation of systemic arterial pressure and RR variabilities in ambulant subjects. Circulation 81: 537–547.

Furlan R, Piazza S, Dell'Orto S, Gentile E, Cerutti S, Pagani M & Malliani A (1993) Early and late effects of exercise and athletic training on neural mechanisms controlling heart rate. Cardiovascular Research 27: 482–488.

Guzzetti S, Dassi S, Pecis M, Casati R, Masu A, Longoni P, Tinelli M, Cerutti S, Pagani M & Malliani A (1991) Altered pattern of circadian neural control of heart period in mild hypertension. J Hypertens 9: 831–838.

Hainsworth R (1995) The control and physiological importance of heart rate. In: Malik M & Camm A (eds) Heart rate variability. Futura Publishing Company Inc., Armonk, p 3–19.

Hamilton P & Tompkins W (1986) Quantitative investigation of QRS detection rules using the MIT/BIH arrhythmia database. IEEE Trans Biomed Eng 33(12): 1157–1165.

Hess-Nielsen N & Wickerhauser M (1996) Wavelets and time-frequency analysis. Proc IEEE 84(4): 523–540.

Hlawatsch F & Boudreaux-Bartels G (1992) Linear and quadratic time-frequency signal representations. IEEE Signal Process Mag 9(2): 21–67.

Hoopen MT & Bongaarts J (1969) Probabilistic characterization of R-R intervals. Cardiovasc Res 3: 218–236.

Huikuri H (1997) Abnormal dynamics of ventricular repolarization - a new insight into the mechanisms of life-threatening ventricular arrhythmias. Eur Heart J 18: 893–895.

Huikuri H, Linnaluoto M, Seppänen T, Airaksinen K, Kessler K, Takkunen J & Myerburg R (1992) Circadian rhythm of heart rate variability in survivors of cardiac arrest. Am J Cardiol 70: 610–615.

Huikuri H, Seppänen T, Koistinen M, Airaksinen K, Ikäheimo M, Castellanos A & Myerburg R (1996) Abnormalities in beat-to-beat dynamics of heart rate before the spontaneous onset of life-threatening ventricular tachyarrhythmias in patients with prior myocardial infarction. Circulation 93: 1836–1844.

Jaffe R, Fung D & Behrman K (1993) Optimal frequency ranges for extracting information on automatic activity from the heart rate spectrogram. J Auton Nerv Syst 46: 37–46.

Janssen M, Swenne C, de Bie J, Rompelman O & van Bemmel J (1993) Methods in heart rate variability analysis: Which tachogram should we choose? Comput Methods Programs Biomed 41: 1–8.

Johnsen S & Andersen N (1978) On power estimation in maximum entropy spectral analysis. Geophysics 43(4): 681–690.

Kamalesh M, Burger A, Kumar S, & Nesto R (1995) Reproducibility of time and frequency domain analysis of heart rate variability in patients with chronic stable angina. PACE 18: 1991–1994.

Kamath M & Fallen E (1993) Power spectral analysis of heart rate variability: a noninvasive signature of cardiac autonomic function. Crit Rev Biomed Eng 21(3): 245–311.

Kanters J, Holstein-Rathlou NH & Agner E (1994) Lack of evidence for low-dimensional chaos in heart rate variability. J Cardiovasc Electrophysiol 5: 591–601.

Karrakchou M, Vibe-Rheymer K, Vesin JM, Pruvot E & Kunt M (1996) Improving cardiovascular monitoring through modern techniques. IEEE Eng Med Biol 15(5): 68–78.

Katona P & Jih F (1975) Respiratory sinus arrhythmia: noninvasive measure of parasympathetic cardiac control. J Appl Physiol 39(5): 801–805.

Kay S (1988) Modern Spectral Estimation. Theory & Application. Prentice Hall, Englewood Cliffs.

Keenan DM (1985) A Tukey nonadditivity-type test for time series nonlinearity. Biometrika 72(1): 39–44.

Keselbrener L & Akselrod S (1996) Selective discrete Fourier transform algorithm for time-frequency analysis: Method and application on simulated and cardiovascular signals. IEEE Trans Biomed Eng 43(8): 789–802.

Khadra L, Maayah T & Dickhaus H (1997) Detecting chaos in HRV signals in human cardiac transplant recipients. Computers and Biomedical Research 30: 188–199.

Kitney R, Fulton T, McDonald A & Linkens D (1985) Transient interactions between blood pressure, respiration and heart rate in man. J Biomed Eng 7: 217–224.

Kitney R & Rompelman O (eds) (1987) The Beat-by-Beat Investigation of Cardiovascular Function. Clarendon Press, Oxford.

Kleiger R, Stein P, Bosner M & Rottman J (1992) Time domain measurements of heart rate variability. Ambulatory Electrocardiography 10(3): 487–498.

Kobayashi M & Musha T (1982) $1/f$ fluctuations of heartbeat period. IEEE Trans Biomed Eng 29(6): 456–457.

Koeleman A, van den Akker T, Ros H, Janssen R & Rompelman O (1984) Estimation accuracy of P wave and QRS complex accurrence times in the ECG: The accuracy for simplified theoretical and computer simulated waveforms. Signal Processing 7: 389–405.

Korhonen I (1997) Methods for the analysis of short-term variability of heart rate and blood pressure in frequency domain. PhD thesis, Tampere University of Technology.

Laguna P, Thakor N, Caminal P, Jane R & Yoon HR (1990) New algorithm for QT interval analysis in 24-hour Holter ECG: Performance and applications. Med Biol Eng Comput 28: 67–73.

Lau C & Ward D (1989) QT hysteresis: The effect of an abrupt change in pacing rate. In: Butrous G & Schwartz P (eds) Clinical Aspects of Ventricular Repolarization. Farrand Press, London, p 175–181.

Lee F & Nehorai A (1992) Adaptive power spectrum estimation algorithm for heart rate variability analysis. Computers in Cardiology, 273–276.

Lippman N, Stein K & Lerman B (1994) Comparison of methods for removal of ectopy in measurement of heart rate variability. Am J Physiol 267(Heart Circ. Physiol. 36): H411 – H418.

Lombardi F, Sandrone G, Mortara A, Rovere ML, Colombo E, Guzzetti S & Malliani A (1992) Circadian variation of spectral indices of heart rate variability after myocardial infarction. Am Heart J 123: 1521–1529.

Loughlin P (1996) Special issue on time-frequency analysis. Proc IEEE 84(9).

Mainardi L, Bianchi A, Baselli G & Cerutti S (1995) Pole-tracking algorithms for the extraction of time-variant heart rate variability spectral parameters. IEEE Trans Biomed Eng 42(3): 250–259.

Mainardi L, Bianchi A & Cerutti S (1994) On-line beat-to-beat monitoring of spectral parameters of heart rate variability signal using a pole-tracking algorithm. Methods Inf Med 33: 85–88.

Malik M, Cripps T, Farrell T & Camm J (1989a) Long-term spectral analysis of heart rate variability - an algorithm based on segmental frequency distributions of beat-to-beat intervals. Int J Biomed Comput 24: 89–110.

Malik M, Farrell T & Camm A (1990) Circadian rhythm of heart rate variability with clinical and angiographic variables and late mortality after coronary angiography. Am J Cardiol 66(12): 1049–1054.

Malik M, Farrell T, Cripps T & Camm A (1989b) Heart rate variability in relation to prognosis after myocardial infarction: Selection of optimal processing techniques. Eur Heart J 10(12): 1060–1074.

Malik M, Xia R, Odemuyiwa O, Staunton A, Poloniecki J & Camm A (1993) Influence of the recognition artefact in automatic analysis of long-term electrocardiograms on time-domain measurement of heart rate variability. Med Biol Eng Comput 31(5): 539–544.

Malliani A, Pagani M, Lombardi F & Cerutti S (1991) Cardiovascular neural regulation explored in the frequency domain. Circulation 84(2): 482–492.

Malmivuo J & Plonsey R (1995) Bioelectromagnetism. Oxford University Press, New York.

Marple S (1987) Digital Spectral Analysis with Applications. Prentice Hall, Englewood Cliffs.

Merri M (1989) Static and dynamic analyses of ventricular repolarization duration. PhD thesis, University of Rochester, Rochester, New York.

Merri M, Alberti M, Benhorin J & Moss A (1991) Preprocessing of Holter ECGs for analysis of the dynamic interrelations between heart rate and repolarization duration variabilities. J Electrocardiology 23S: 157–162.

Merri M, Alberti M & Moss A (1993) Dynamic analysis of ventricular repolarization duration from 24-hour Holter recordings. IEEE Trans Biomed Eng 40(12): 1219–1225.

Merri M, Benhorin J, Alberti M, Locati E & Moss A (1989) Electrocardiographic quantitation of ventricular repolarization. Circulation 80: 1301–1308.

Merri M, Farden D, Mottley J & Titlebaum E (1990) Sampling frequency of the electrocardiogram for spectral analysis of the heart rate variability. IEEE Trans Biomed Eng 37(1): 99–106.

Merri M, Moss A, Benhorin J, Locati E, Alberti M & Badini F (1992) Relation between ventricular repolarization duration and cardiac cycle length during 24-hour Holter recordings. Circulation 85: 1816–1821.

Misiti M, Misiti Y, Oppenheim G & Poggi JM (1996) Wavelet Toolbox. For Use with MATLAB. Wavelet Toolbox User's Guide. The MathWorks, Inc., Natick.

Molgaard H, Mickley H, Pless P, Bjerregaard P & Moller M (1993) Effects of metoprolol on heart rate variability in survivors of acute myocardial infarction. Am J Cardiol 71: 1357–1359.

Moser M, Lehofer M, Sedminek A, Lux M, Zapotoczky HG, Kenner T & Noordegraf A (1994) Heart rate variability as a prognostic tool in cardiology - a contribution to the problem from the theoretical point of view. Circulation 90(2): 1078–1082.

Mulder L (1992) Measurement and analysis methods of heart rate and respiration for use in applied environments. Biol Psychol 34: 205–236.

Nikias C & Petropulu A (1993) Higher-Order Spectra Analysis: A Nonlinear Signal Processing Framework. PTR Prentice Hall, Englewood Cliffs.

Nollo G, Speranza G, Grasso R, Bonamini R & Antolini R (1990) Dynamic measurement of the QT interval. Computers in Cardiology, 463–466.

Nollo G, Speranza G, Grasso R, Bonamini R, Mangiardi L & Antolini R (1992) Spontaneous beat-to-beat variability of the ventricular repolarization duration. J Electrocardiol 25(1): 9–17.

Novak P & Novak V (1993) Time/frequency mapping of the heart rate, blood pressure and respiratory signals. Med Biol Eng Comput 31: 103–110.

Novak V, Novak P, Champlain JD, Blanc AL, Martin R & Nadeau R (1993) Influence of respiration on heart rate and blood pressure fluctuations. J Appl Physiol 74(2): 617–626.

Odemuyiwa O, Malik M, Farrell T, Bashir Y, Poloniecki J & Camm J (1991) Comparison of the predictive characteristics of heart rate variability index and left ventricular ejection fraction for all-cause mortality, arrhythmic events and sudden death after acute myocardial infarction. Am J Cardiol 68: 434–439.

Oetken G, Parks T & Schuessler H (1979) A computer program for digital interpolator design. In: the Digital Signal Processing Committee (ed) Programs for Digital Signal Processing. IEEE Press, New York, p 8.1.1–8.1.6.

Osborne A & Provenzale A (1989) Finite correlation dimension for stochastic systems with power-law spectra. Physica D 35: 357–381.

Pagani M, Lombardi F, Guzzetti S, Rimoldi O, Furlan R, Pizzinelli P, Sandrone G, Malfatto G, Dell'Orto S, Piccaluga E, Turiel M, Baselli G, Cerutti S & Malliani A (1986) Power spectral analysis of heart rate and arterial pressure as a marker of sympatho-vagal interaction in man and concious dog. Circ Res 59: 178–193.

Pagani M, Lombardi F, Guzzetti S, Rimoldi O, Malfatto G, Cerutti S & Malliani A (1984) Power spectral density of heart rate variability as an index of sympatho-vagal interaction in normal and hypertensive subjects. J Hypertens 2(suppl. 3): 383–385.

Pagani M, Lucini D, Rimoldi O, Furlan R, Piazza S & Biancardi L (1995) Effects of physical and mental exercise on heart rate variability. In: Malik M & Camm A (eds) Heart rate variability. Futura Publishing Company Inc., Armonk, p 245–266.

Pagani M, Malfatto G, Pierini S, Casati R, Masu A, Poli M, Guzzetti F, Lombardi F, Cerutti S & Malliani A (1988a) Spectral analysis of heart rate varibility in the assessment of autonomic diabetic neuropathy. J Auton Nerv Syst 23: 143–153.

Pagani M, Somers V, Furlan R, Dell'Orto S, Conway J, Baselli G, Cerutti S, Sleight P & Malliani M (1988b) Changes in autonomic regulation induced by physical training in mild hypertension. Hypertension 12: 600–610.

Pahlm O & Sörnmo L (1984) Software QRS detection in ambulatory monitoring - a review. Med Biol Eng Comput 22: 289–297.

Peng CK, Mietus J, Hausdorff J, Havlin S, Stanley H & Goldberger A (1993) Long-range anticorrelations and non-gaussian behavior of the heartbeat. Phys Rev Lett 70(9): 1343–1346.

Pinna G, Maestri R, Cesare AD, Colombo R & Minuco G (1994) The accuracy of power-spectrum analysis of heart-rate variability from annotated RR lists generated by Holter systems. Physiol Meas 15: 163–179.

Pinna G, Maestri R & Sanarico M (1996) Effects of record length selection on the accuracy of spectral estimates of heart rate variability: A simulation study. IEEE Trans Biomed Eng 43(7): 754–757.

Pitzalis M, Mastropasqua F, Massari F, Forleo C, Maggio MD, Passantino A, Colombo R, Biase MD & Rizzon P (1996) Short- and long-term reproducibility of time and frequency domain heart rate variability measurements in normal subjects. Cardiovasc Res 32: 226–233.

Pola S, Macerata A, Emdin M & Marchesi C (1996) Estimation of the power spectral density in nonstationary cardiovascular time series: Assessing the role of the time-frequency representations (TFR). IEEE Trans Biomed Eng 43(1): 46–59.

Pomeranz B, Macaulay R, Caudill M, Kutz I, Adam D, Gordon D, Kilborn K, Barger A, Shannon D, Cohen R & Benson H (1985) Assessment of autonomic function in man by heart rate spectral analysis. Am J Physiol 248(Heart Circ. Physiol. 17): H151–H153.

Porta A, Baselli G, Lombardi F, Malliani A, Greco MD, Ravelli F, Antolini R & Nollo G (1996) Performance analysis of the automatic RT_{apex} and RT_{end} measurement. Computers in Cardiology, 533–536.

Priestley M (1981) Spectral Analysis and Time Series. Academic Press Inc., London.

Priestley M (1996) Wavelets and time-dependent spectral analysis. J Time Series Analysis 17(1): 85–103.

Proakis J, Rader C, Ling F & Nikias C (1992) Advanced Digital Signal Processing. Macmillan, New York.

Rienzo MD, Castiglioni P, Mancia G, Parati G & Pedotti A (1989) 24 h sequential spectral analysis of arterial blood pressure and pulse interval in free-moving subjects. IEEE Trans Biomed Eng 36(11): 1066–1075.

Rienzo MD, Mancia G, Parati G, Pedotti A & Zanchetti A (eds) (1993) Blood Pressure and Heart Rate Variability. Computer Analysis and Clinical Applications. IOS Press, Amsterdam.

Rioul O & Vetterli M (1991) Wavelets and signal processing. IEEE Signal Process Mag 8(4): 14–38.

Rovere ML, Specchia G, Mortara A & Schwartz P (1988) Baroreflex sensitivity, clinical correlates, and cardiovascular mortality among patients with a first myocardial infarct. Circulation 78: 816–824.

Ruha A, Sallinen S & Nissilä S (1997) A real-time microprocessor QRS detector system with a 1 ms timing accuracy for the measurement of ambulatory HRV. IEEE Trans Biomed Eng 44(3): 159–167.

Sandrone G, Mortara A, Torzillo D, Rovere ML, Malliani A & Lombardi F (1994) Effects of beta blockers (atenolol or metoprolol) on heart rate variability after acute myocardial infarction. Am J Cardiol 74: 340–345.

Sapoznikov D, Luria M & Gotsman M (1993) Comparison of different methodoligies of heart rate variability analysis. Comput Methods Programs Biomed 41: 69–75.

Sapoznikov D, Luria M & Gotsman M (1994) Differentation of periodic from nonperiodic low-frequency heart rate fluctuations. Comput Biomed Res 27: 199–209.

Sapoznikov D, Luria M, Mahler Y & Gotsman M (1992) Computer processing of artifact and arrhythmias in heart rate variability analysis. Comput Methods Programs Biomed 39: 75–84.

Saul J, Albrecht P, Berger R & Cohen R (1987) Analysis of long term heart rate variability: Methods, $1/f$ scaling and implications. Computers in Cardiology pp. 419–422.

Scott D (1979) On optimal and data-based histograms. Biometrika 66(3): 605–610.

Selman A, McDonald A, Kitney R & Linkens D (1982) The interaction between heart rate and respiration: Part I. Experimental studies in man. Automedica 4: 131–139.

Signorini M, Cerutti S, Guzzetti S & Parola R (1994) Non-linear dynamics of cardiovascular variability signals. Methods Inf Med 33: 81–84.

Speranza G, Nollo G, Ravelli F & Antolini R (1993) Beat-to-beat measurement and analysis of the R-T interval in 24 h ECG Holter recordings. Med Biol Eng Comput 31: 487–494.

Stein P, Bosner M, Kleiger R & Conger B (1994) Heart rate variability: A measure of cardiac autonomic tone. Am Heart J 127(5): 1376–1381.

Stinton P, Tinker J, Vickery J & Vahl S (1972) The scattergram. A new method for continuous electrocardiographic monitoring. Cardiovasc Res 6: 598–604.

Strang G & Nguyen T (1996) Wavelets and Filter Banks. Wellesley-Cambridge Press, Wellesley.

Task Force of ESC & NASPE (1996) Heart rate variability. Standards of measurement, physiological interpretation, and clinical use. Task Force of the European Society of Cardiology and the North American Society of Pacing and Electrophysiology. Circulation 93(5): 1043–1065.

Thakor N & Sherman D (1995) Wavelet (time-scale) analysis in biomedical signal processing. In: Bronzino J (ed) The Biomedical Engineering Handbook. CRC Press, Inc., Boca Raton, p 886–906.

Theiler J, Eubank S, Longtin A, Galdrikian B & Farmer J (1992) Testing for nonlinearity in time series: The method of surrogate data. Physica D 58: 77–94.

Thomas L, Clark K, Mead C, Ripley K & Oliver G (1979) Automated cardiac dysrhythmia analysis. Proc IEEE 67(9): 1322–1337.

Tsuji H & Mori H (1994) New analysis of HRV through wavelet transform. International Journal of Human Computer Interaction 6(2): 205–217.

Tsuji H, Venditi F, Manders E, Evans J, Larson M, Feldman C & Levy D (1994) Reduced heart rate variability and mortality risk in an elderly cohort - The Framingham Heart Study. Circulation 90(2): 878–883.

Unser M & Aldroubi A (1996) A review of wavelets in biomedical application. Proc IEEE 84: 626–638.

VanRavenswaaij-Arts C, Kollée L, Hopman J, Stoelinga G & VanGeijn H (1993) Heart rate variability, review. Ann Intern Med 118(6): 436–447.

Wiklund U, Akay M & Niklasson U (1997) Short-term analysis of heart-rate variability by adapted wavelet transforms. IEEE Eng Med Biol 16(5): 113–138.

Willard K & Connelly D (1992) Nonparametric probability density estimation: Improvements to the histogram for laboratory data. Comput Biomed Res 25: 17–28.

Xiong Z, Ramchandran K, Herley C & Orchard M (1997) Flexible tree-structured signal expansions using time-varying wavelet packets. IEEE Trans Signal Processing 45(2): 333–345.

Yamamoto Y, Fortrat JO & Hughson R (1995) On the fractal nature of heart rate variability in humans: Effects of respiratory sinus arrhythmia. Am J Physiol 269(Heart Circ. Physiol. 38): H480–H486.

Yamamoto Y & Hughson R (1993) Extracting fractal components from time series. Physica D 68: 250–264.

Yamamoto Y, Hughson R, Sutton J, Houston C, Cymerman A, Fallen E & Kamath M (1993) Operation everest II: An indication of deterministic chaos in human heart rate variability at simulated extreme altitude. Biol Cybern 69: 205–212.

Yang F & Liao W (1997) Modeling and decomposition of HRV signals with wavelet transforms. IEEE Eng Med Biol 16(4): 17–22.

Yeragani V, Srinivasan K, Vempati S, Pohl R & Balon R (1993) Fractal dimension of heart rate time series: An effective measure of autonomic function. J Appl Physiol 75(6): 2429–2438.

Ziegler D, Laux G, Dannehl K, Spüler M, Mühlen H, Mayer P & Gries F (1992) Assessment of cardiovascular autonomic function: Age-related normal ranges and reproducibility of spectral analysis, vector analysis, and standard tests of heart rate variation and blood pressure responses. Diabet Med 9: 166–175.

Ziemer R & Tranter W (1990) Principles of Communications. Systems, Modulation and Noise. Houghton Mifflin Company, Boston.

Zuanetti G, Latini R, Neilson J, Schwartz P, Ewing D & the Antiarrhythmic drug evaluation group (ADEG) (1991) Heart rate variability in patients with ventricular arrhythmias: Effect of antiarrhythmic drugs. J Am Coll Cardiol 17: 604–612.

Öri Z, Monir G, Weiss J, Sayhouni X & Singer D (1992) Heart rate variability. Frequency domain analysis. Ambulatory Electrocardiography 10(3): 499–537.